

Supplementary Information

In-depth chemical profiling of tire and artificial turf crumb rubber: aging, transformation products, and transport pathways

Madison H. McMinn^{a,b}, Ximin Hu^c, Katherine Poisson^{a,b}, Phillip Berger^{a,b}, Paola Pimentel^a, Xinwen Zhang^a, Pranali Ashara^a, Ella Greenfield^a, Jessica Eig^a, Zhenyu Tian^{*a,b}

^a Department of Chemistry and Chemical Biology, College of Science, Northeastern University, Boston, MA, USA

^b Barnett Institute for Chemical and Biological Analysis, College of Science, Northeastern University, Boston, MA, USA

^c Department of Civil and Environmental Engineering, University of Washington, Seattle, Washington, USA

* Corresponding author. Zhenyu Tian, z.tian@northeastern.edu

Figure	Page #
Figure S1. Chemical structure of compound classes selected for quantitation	S2
Figure S2. Quantitation in crumb rubber extractables of (a) 2-amino-BTH, (b) 4-phenylazodiphenylamine, and (c) 6PPD-quinone.	S2
Figure S3. Relative concentrations of crumb rubber samples from extractables in (a) PPDs and PPD TPs, (b) plasticizers, (c) cross-linking agents, (d) vulcanizing accelerators, (e) other rubber antioxidants and (f) benzothiazoles and benzotriazoles.	S3
Figure S4. Relationship between total peak area and number of features with crumb rubber age in positive ion mode for (a) leachables, (b) extractables, (c) gastric and (d) gastrointestinal sample.	S4
Figure S5. Relationship between total peak area and number of features with crumb rubber age in negative ion mode for (a) leachables, (b) extractables, (c) gastric and (d) gastrointestinal sample preparation methods.	S5
Figure S6. Relationship between median retention time (RT) and median <i>m/z</i> with crumb rubber age in negative ion mode for (a) leachables, (b) extractables, (c) gastric and (d) gastrointestinal sample preparation methods.	S6
Figure S7. PCA of extractables in negative ion mode.	S7
Figure S8. PCA of leachables in (a) positive and (b) negative ion mode.	S8
Figure S9. Comparison between experimental and mzVault library MS/MS spectra in CD 3.3.	S9
Figure S10. MS/MS Compounds identified from other sources (Level 2a).	S33
Figure S11. Comparison between experimental and in-house standard (Level 1).	S35
Figure S12. MS/MS of PPD transformation products in extractables.	S41
Figure S13. Hierarchical clustering of tire and turf crumb rubber leachables in positive ion mode.	S47

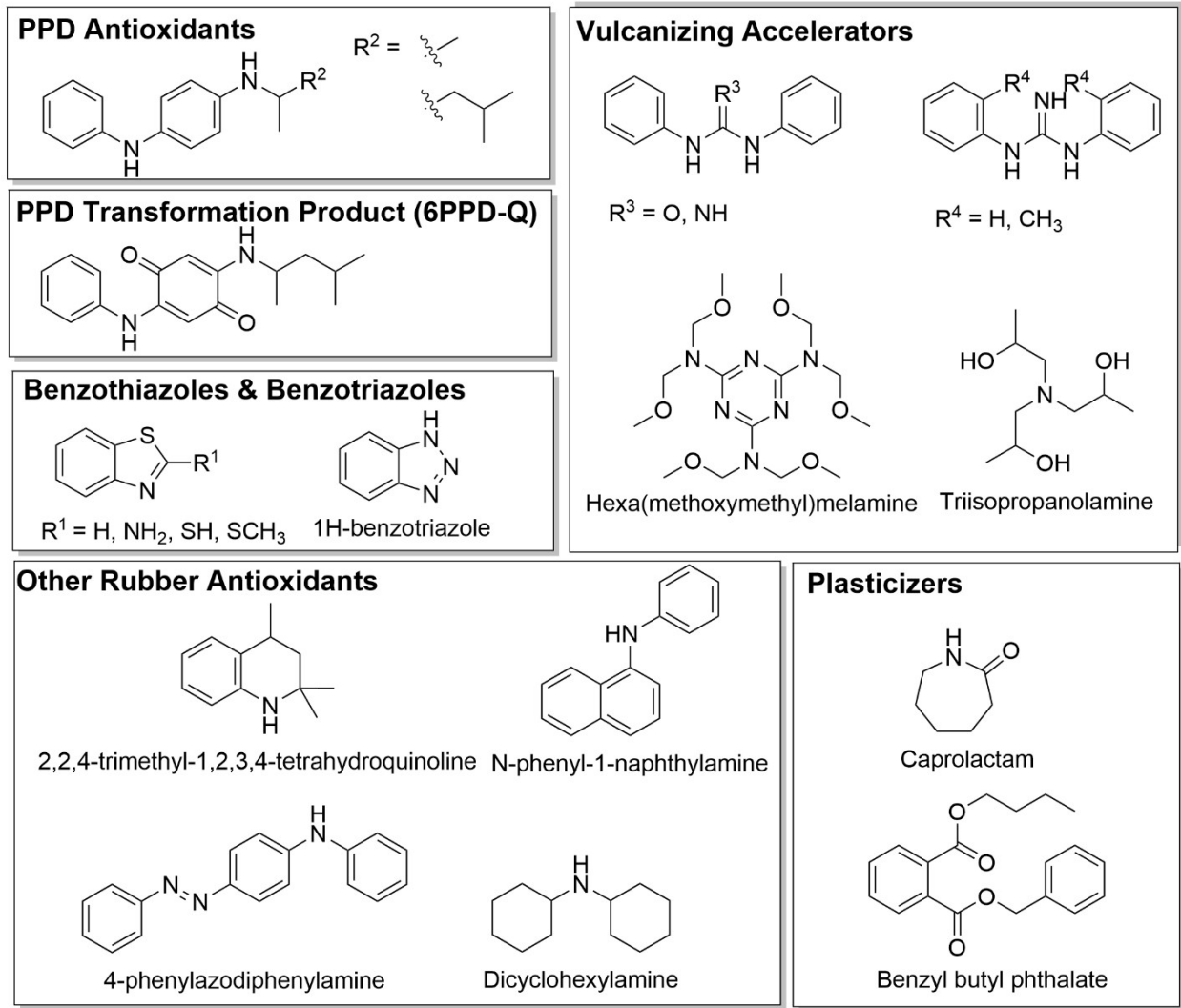


Figure S1. Chemical structure of compound classes selected for quantitation

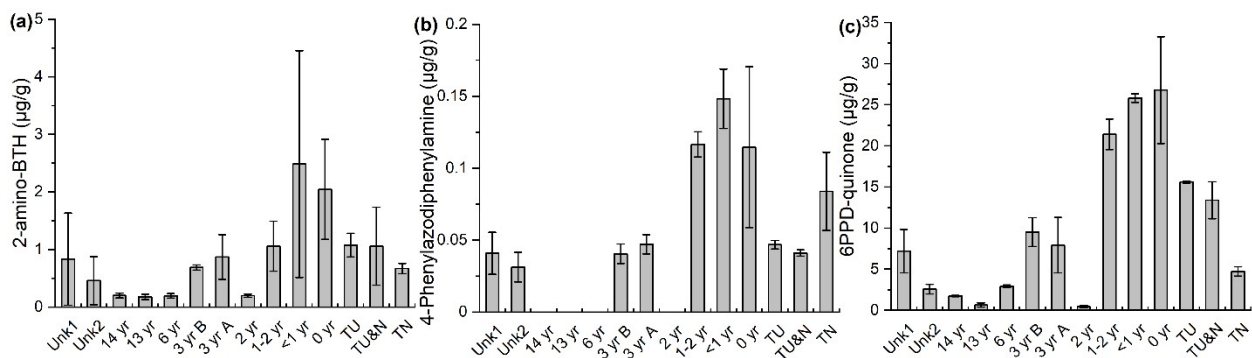


Figure S2. Quantitation in crumb rubber extractables of (a) 2-amino-BTH, (b) 4-phenylazodiphenylamine, and (c) 6PPD-quinone.

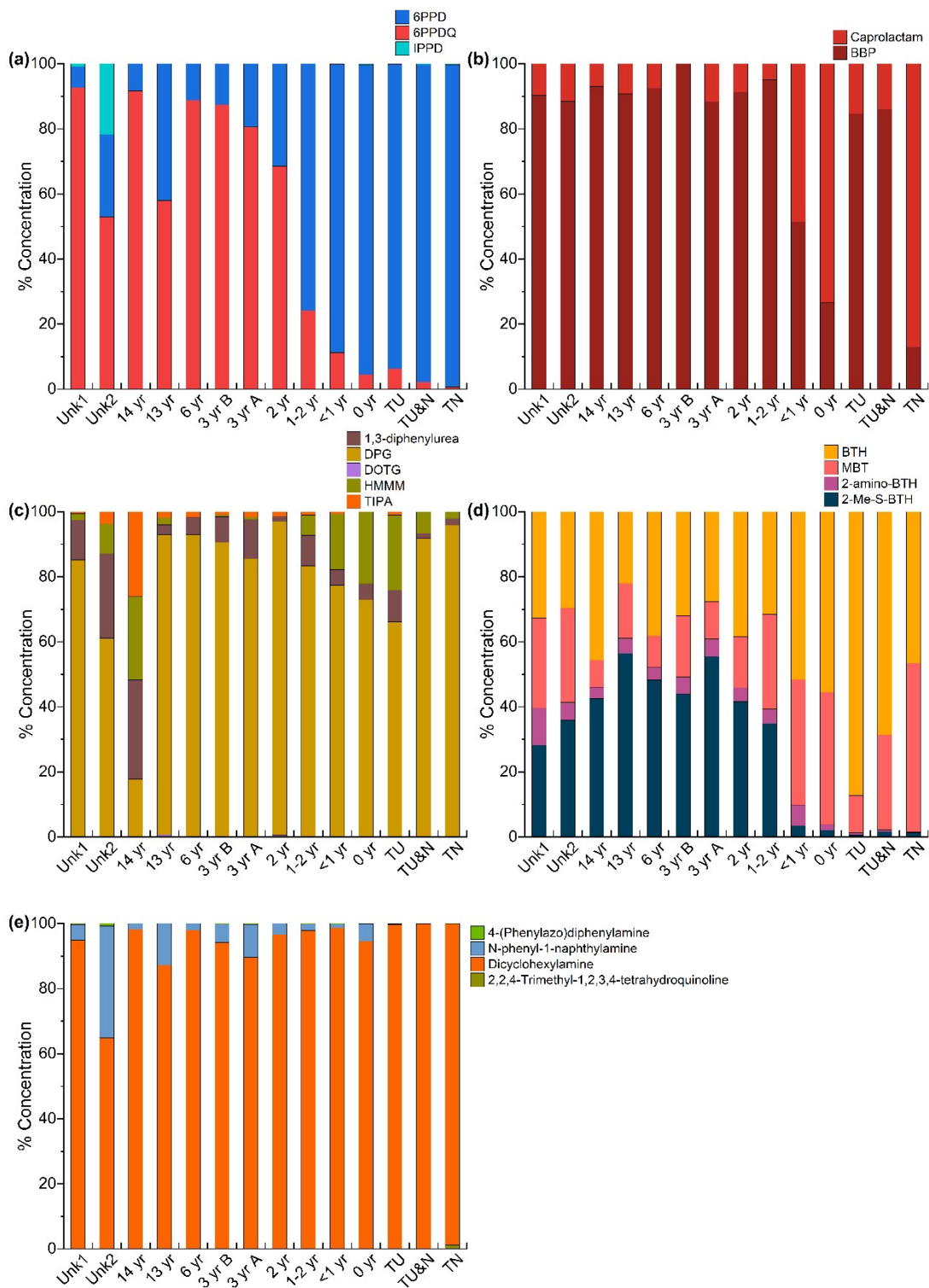


Figure S3. Relative concentrations of crumb rubber samples from extractables in (a) PPDs and PPD TPs, (b) plasticizers, (c) vulcanizing accelerators, (d) benzothiazoles and benzotriazoles and (e) other rubber antioxidants.

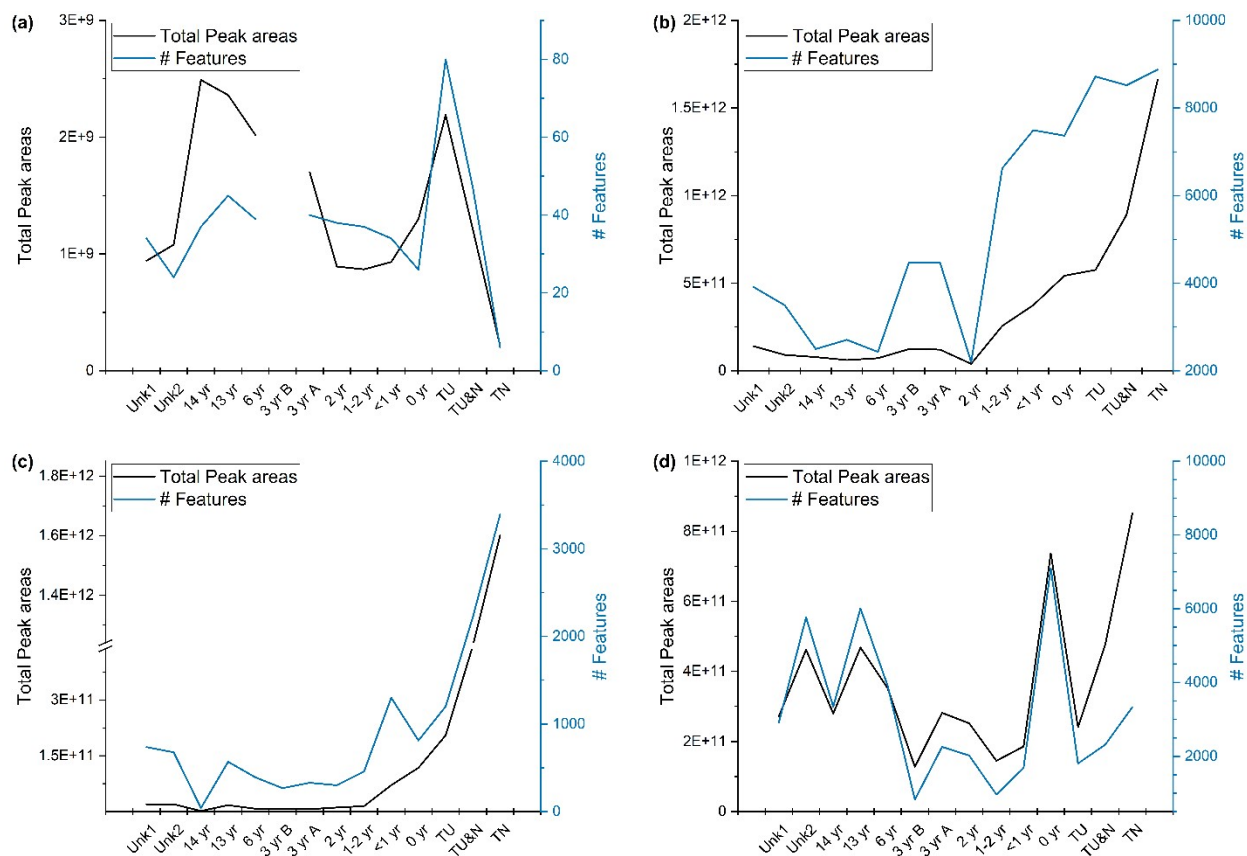


Figure S4. Relationship between total peak area and number of features with crumb rubber age in positive ion mode for (a) leachables, (b) extractables, (c) gastric and (d) gastrointestinal sample preparation methods.

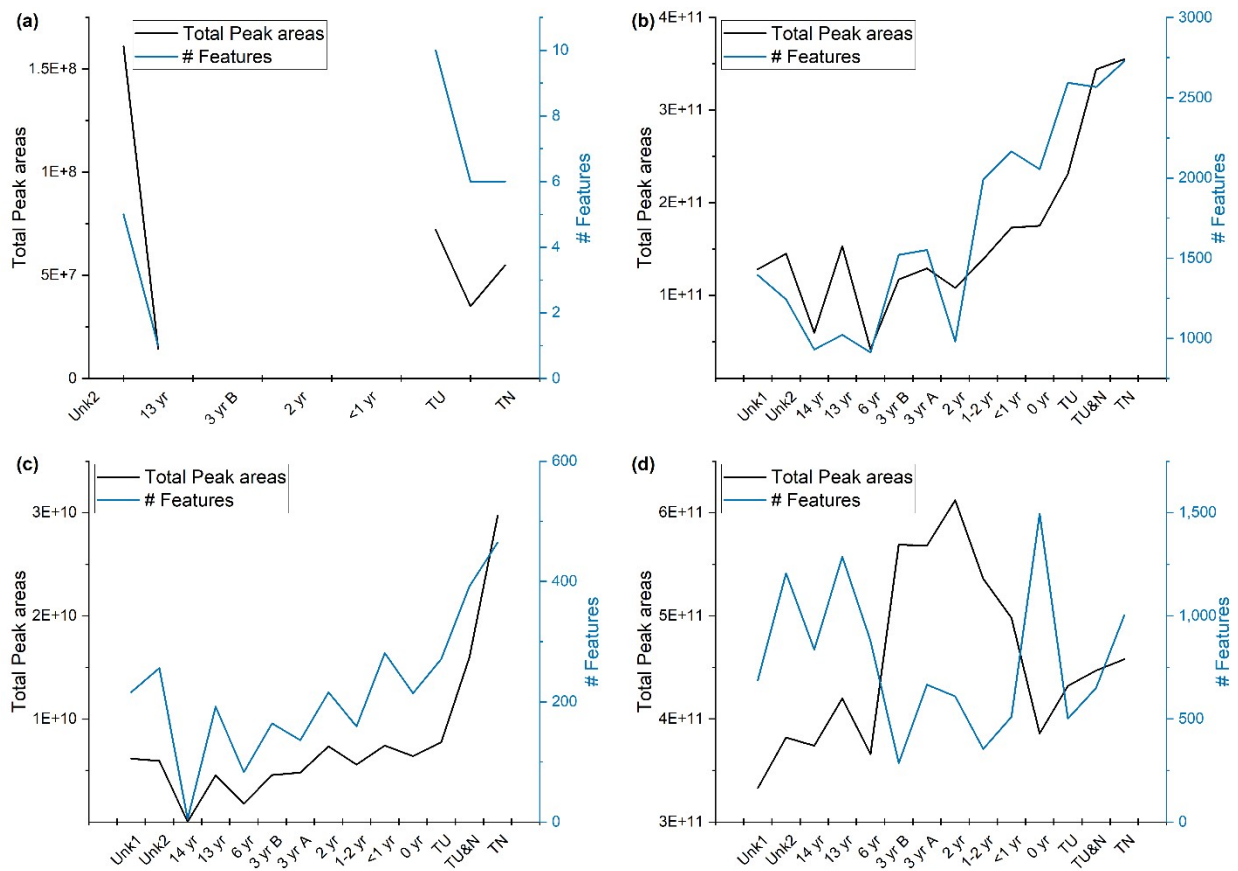


Figure S5. Relationship between total peak area and number of features with crumb rubber age in negative ion mode for (a) leachables, (b) extractables, (c) gastric and (d) gastrointestinal sample preparation methods.

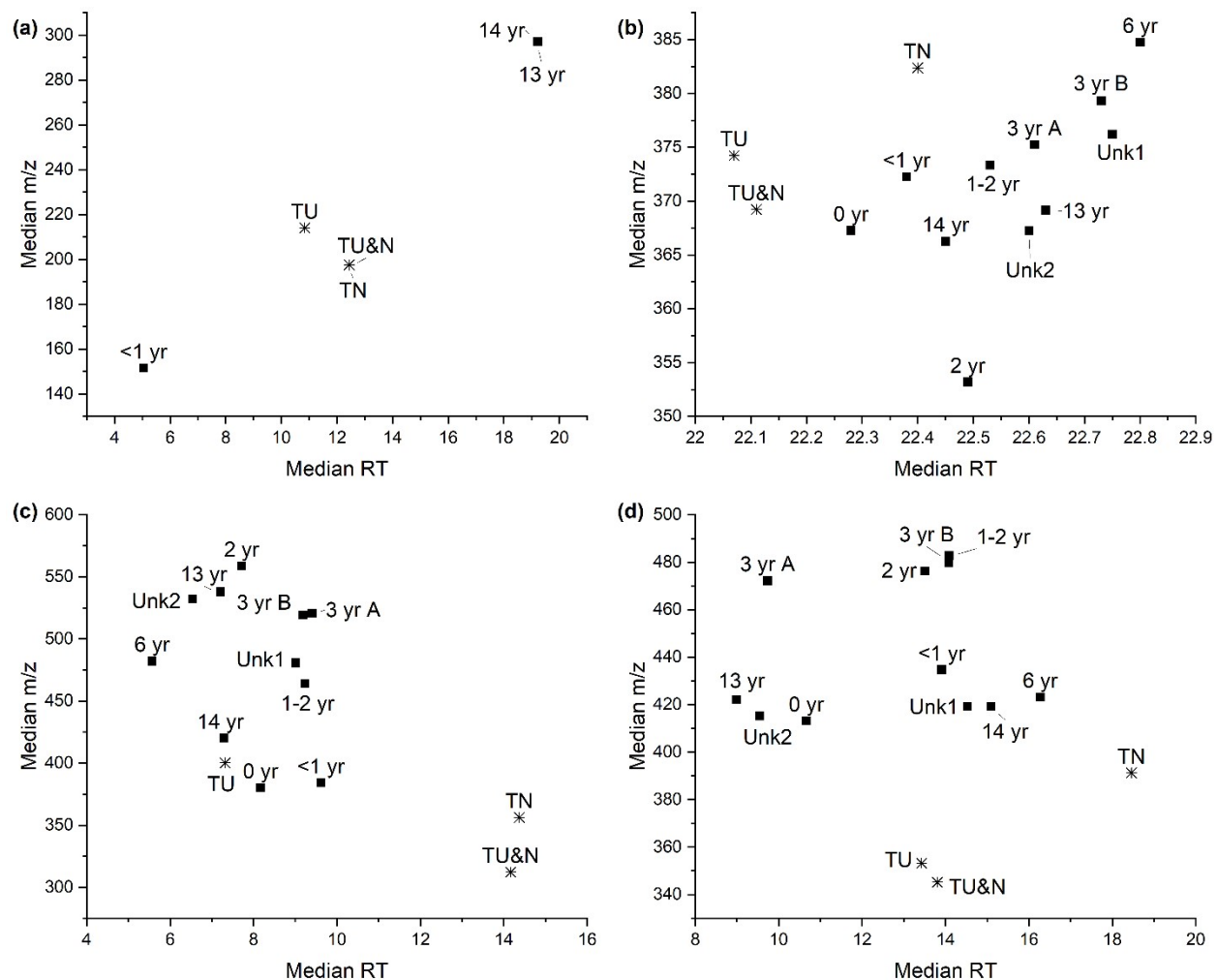


Figure S6. Relationship between median retention time (RT) and median m/z with crumb rubber age in negative ion mode for (a) leachables, (b) extractables, (c) gastric and (d) gastrointestinal sample preparation methods.

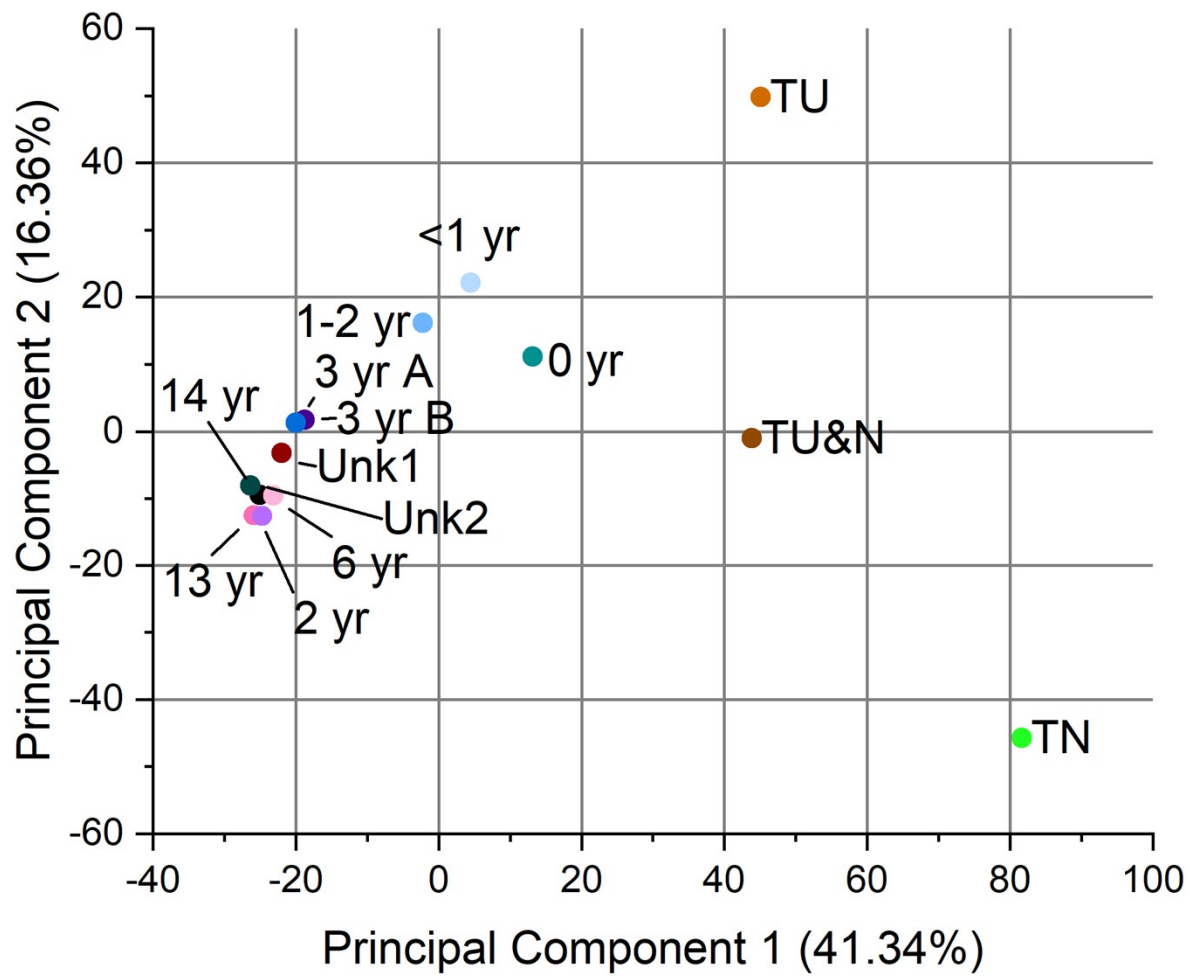


Figure S7. PCA of extractables in negative ion mode.

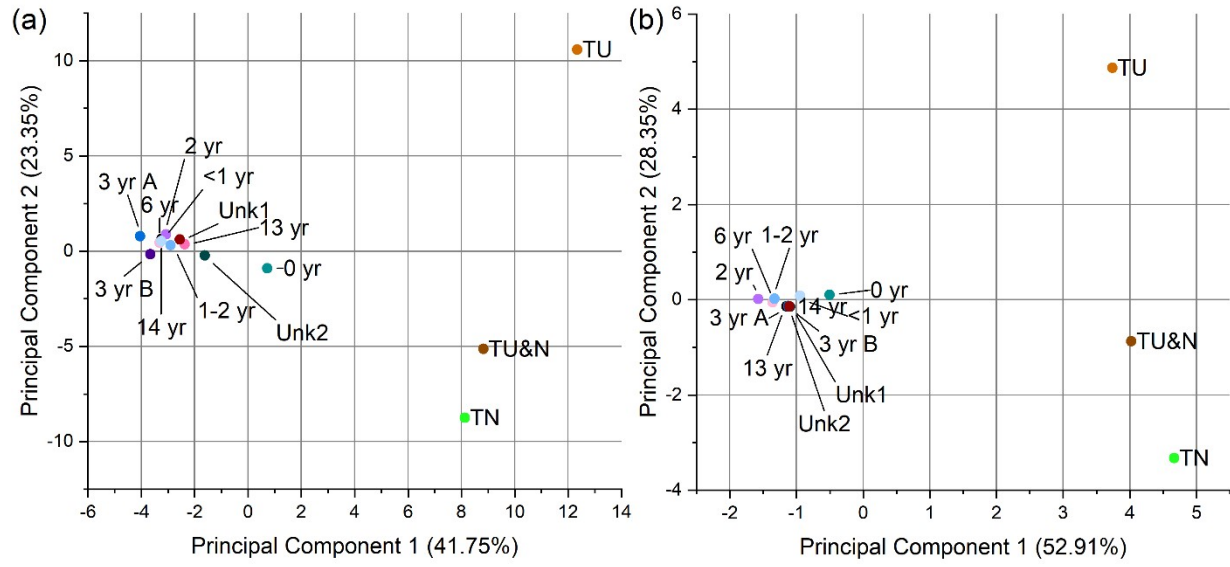
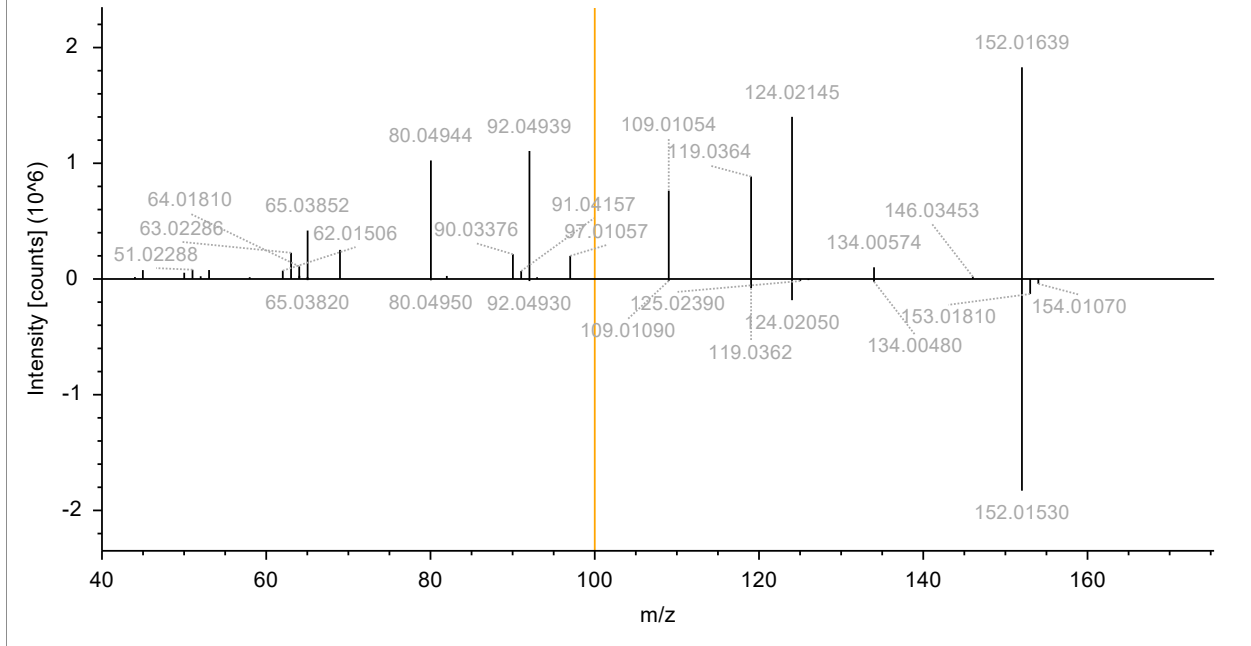


Figure S8. PCA of leachables in (a) positive and (b) negative ion mode.

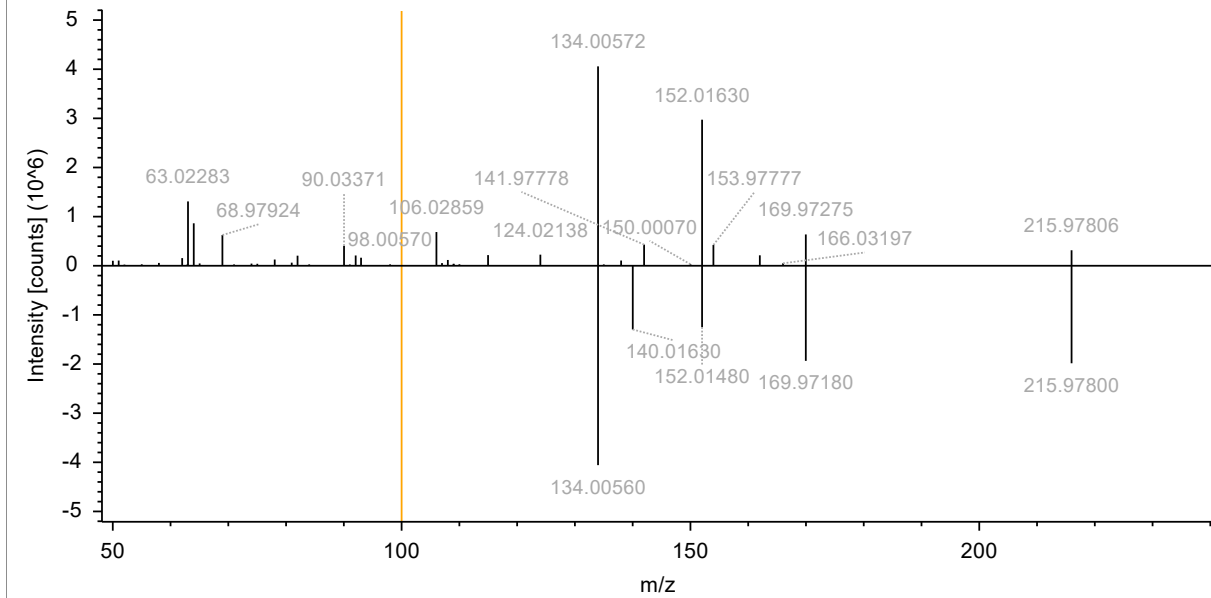
2-Hydroxybenzothiazole (Match 93.8)

RAWFILE(top): 2023_10_26_Quant_Ext_T2_3_20231031035408 (F45) #7247, RT=9.781 min, MS2, FTMS (+), (HCD, DDA, 15+1)



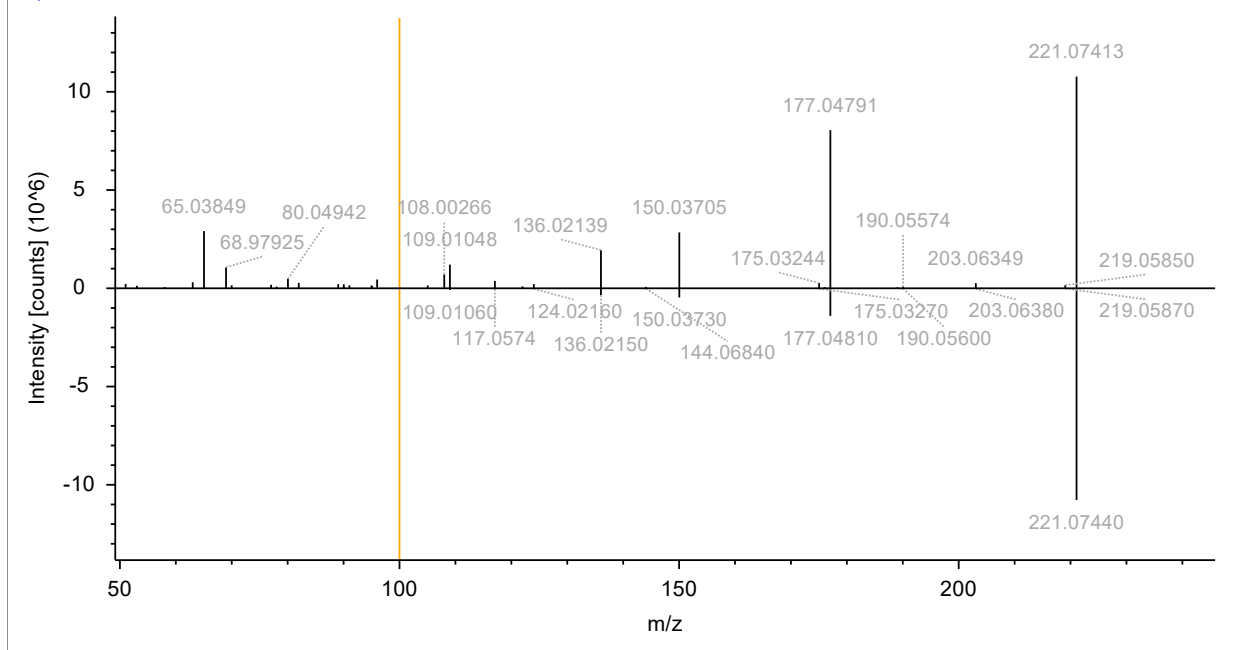
2-Benzothiazolesulfonic acid (Match 85.7)

RAWFILE(top): 2023_10_26_Quant_Ext_T2_3_20231031035408 (F45) #4236, RT=5.736 min, MS2, FTMS (+), (HCD, DDA, 21+1)



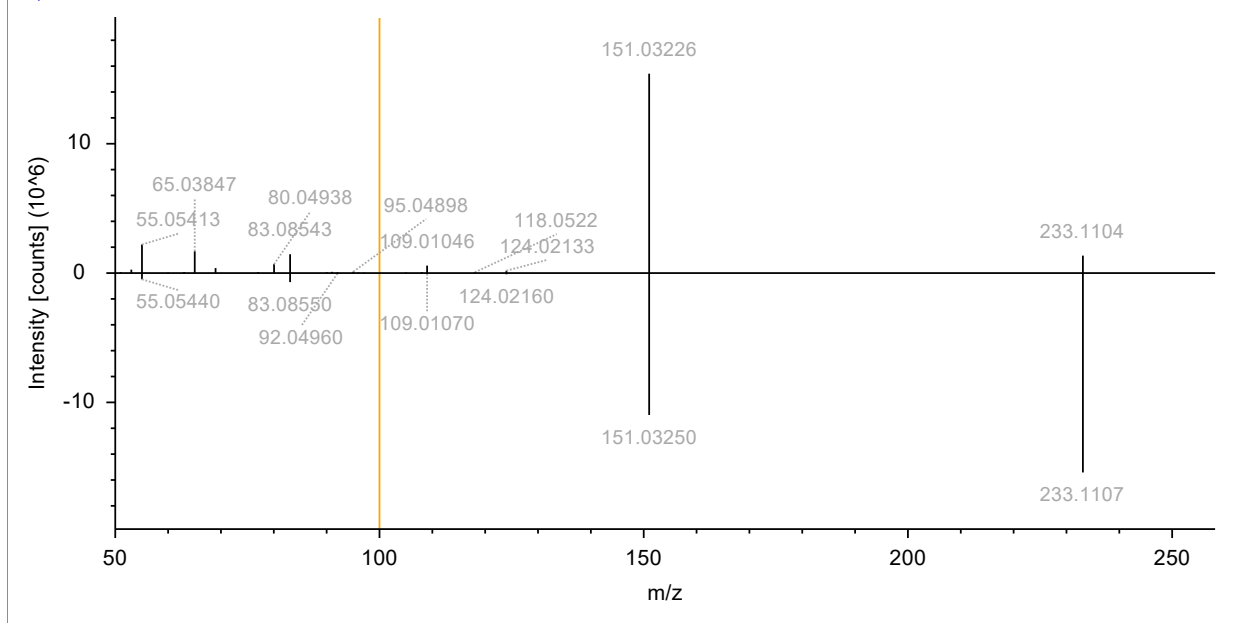
2-(4-morpholinyl)benzothiazole (Match 81.5)

RAWFILE(top): 2023_10_26_Quant_Ext_C11_3_20231030230527 (F33) #9171, RT=12.365 min, MS2, FTMS (+), (HCD, DDA, +1)



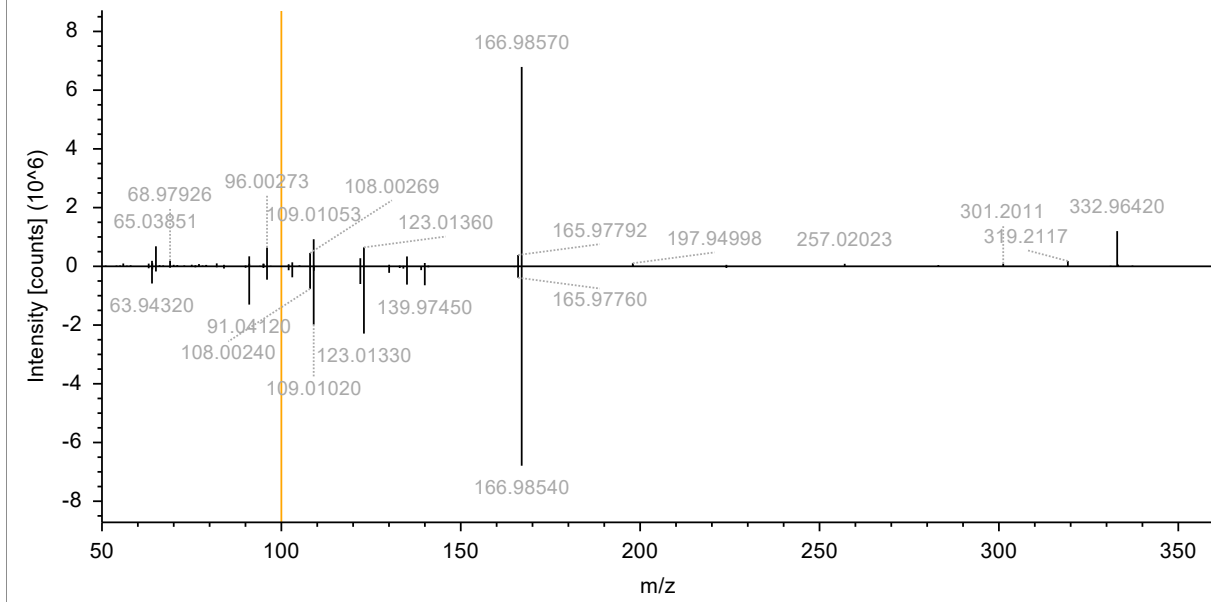
N-cyclohexyl-2-benzothiazol-amine (Match 88.0)

RAWFILE(top): 2023_10_26_Quant_Ext_T2_3_20231031035408 (F45) #9962, RT=13.407 min, MS2, FTMS (+), (HCD, DDA, 2 +1)



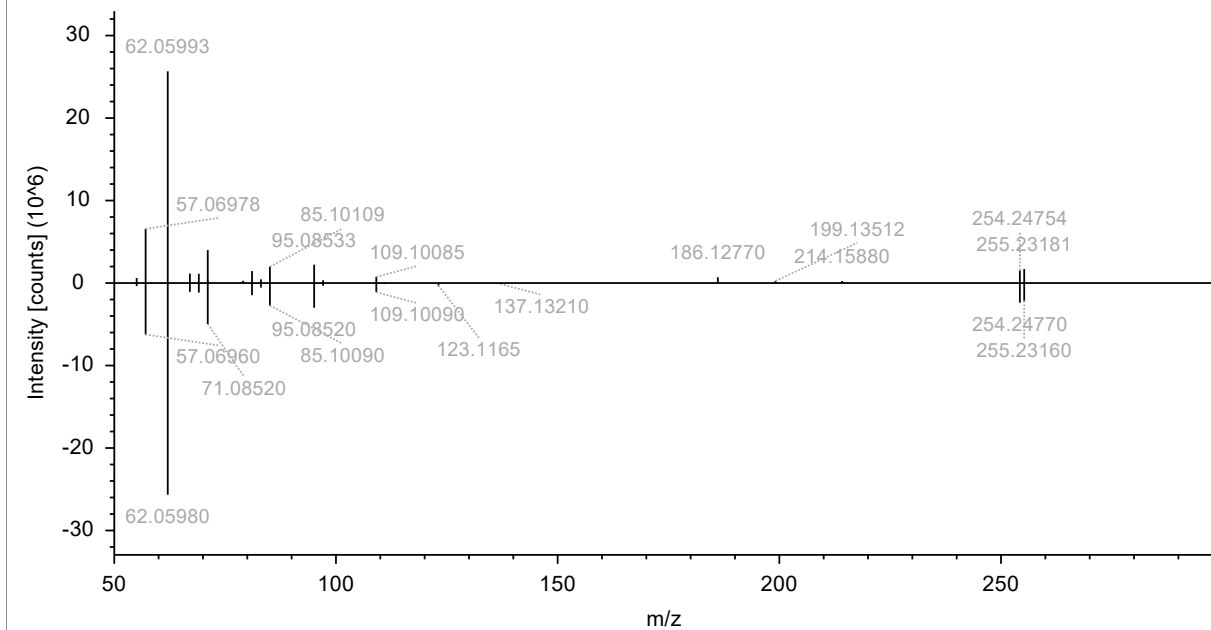
2,2-dithiobis(benzothiazole) (Match 88.9)

RAWFILE(top): 2023_10_26_Quant_Ext_T3_3_20231031053030 (F48) #15239, RT=20.417 min, MS2, FTMS (+), (HCD, DDA, +1)



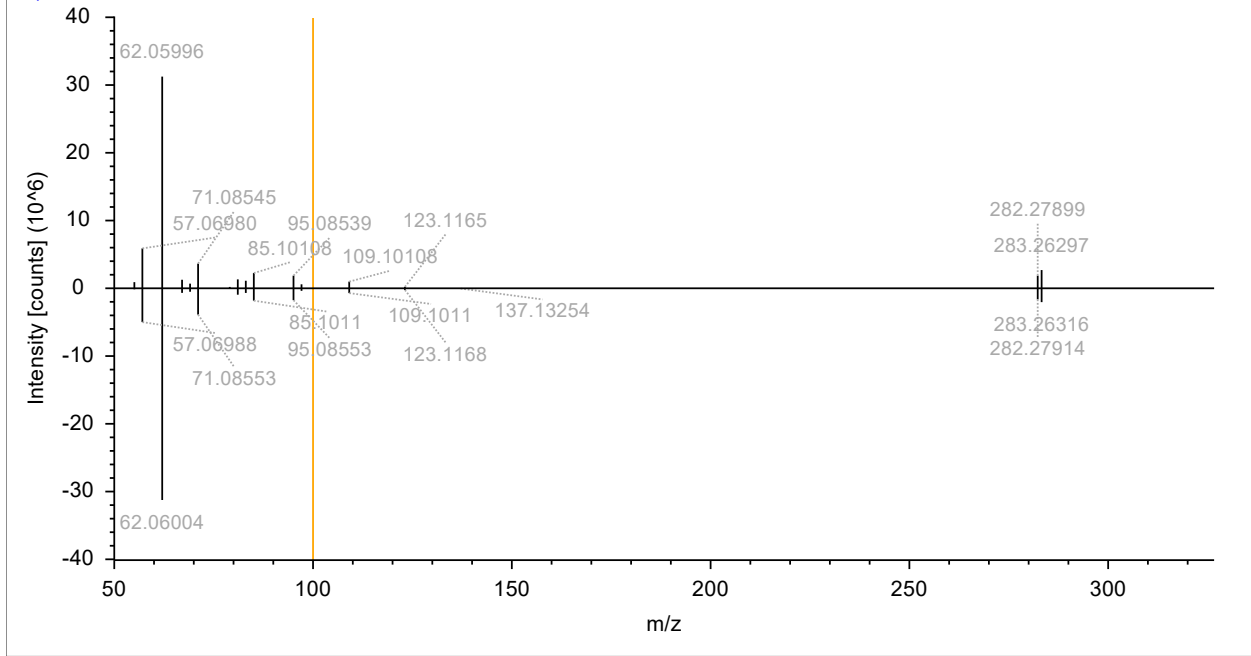
Myristoyl ethanolamide (95.7)

RAWFILE(top): 2023_10_26_Quant_Ext_T3_2_20231031045821 (F47) #15774, RT=21.137 min, MS2, FTMS (+), (HCD, DDA, +1)



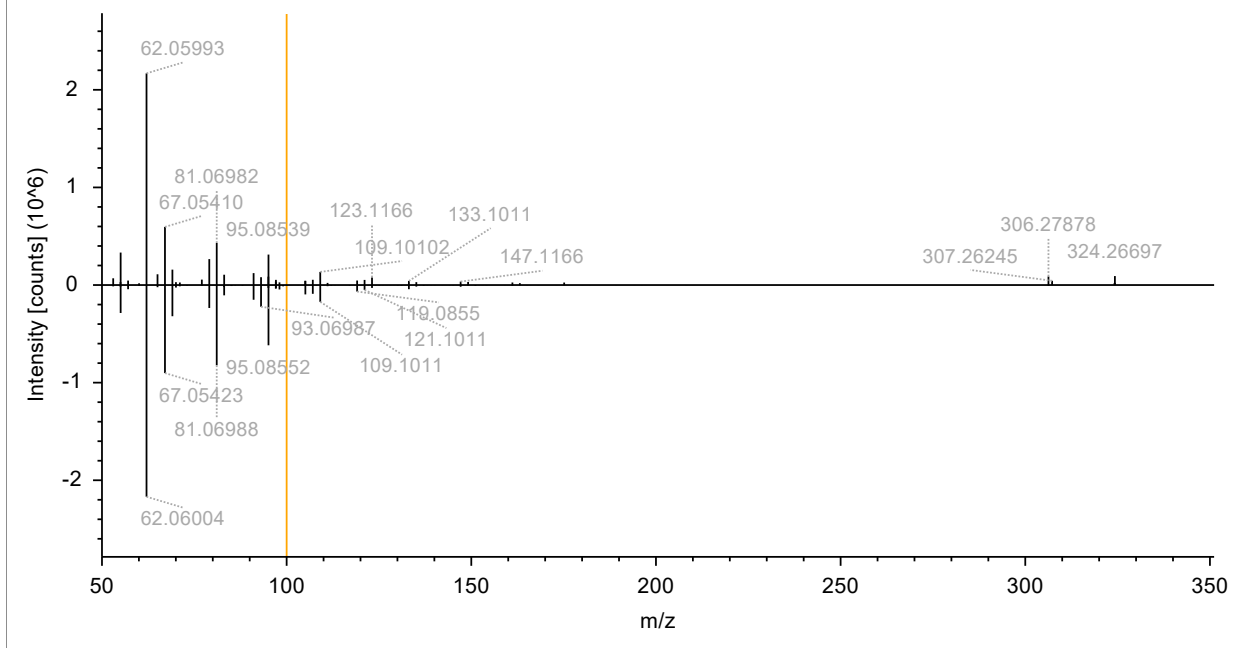
Palmitoyl ethanolamide (Match 99.0)

RAWFILE(top): 2023_10_26_Quant_Ext_T3_2_20231031045821 (F47) #16966, RT=22.718 min, MS2, FTMS (+), (HCD, DDA, +1)



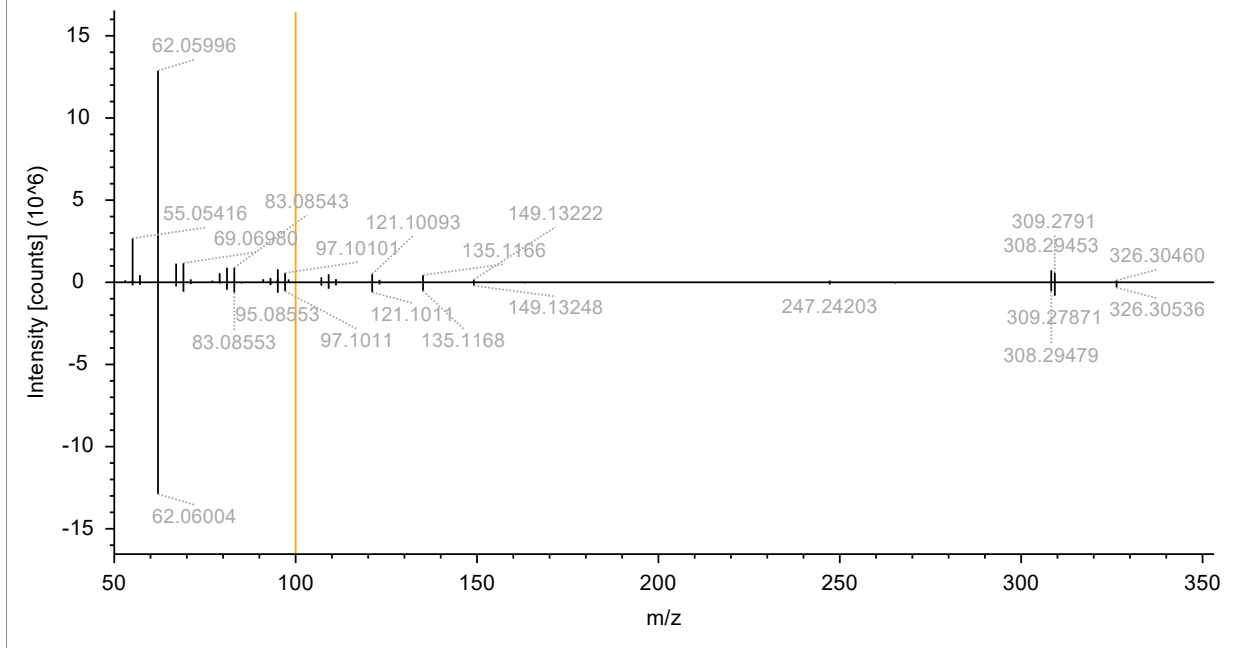
Linoleyl ethanolamide (Match 87.7)

RAWFILE(top): 2023_10_26_Quant_Ext_T3_2_20231031045821 (F47) #16676, RT=22.334 min, MS2, FTMS (+), (HCD, DDA, +1)



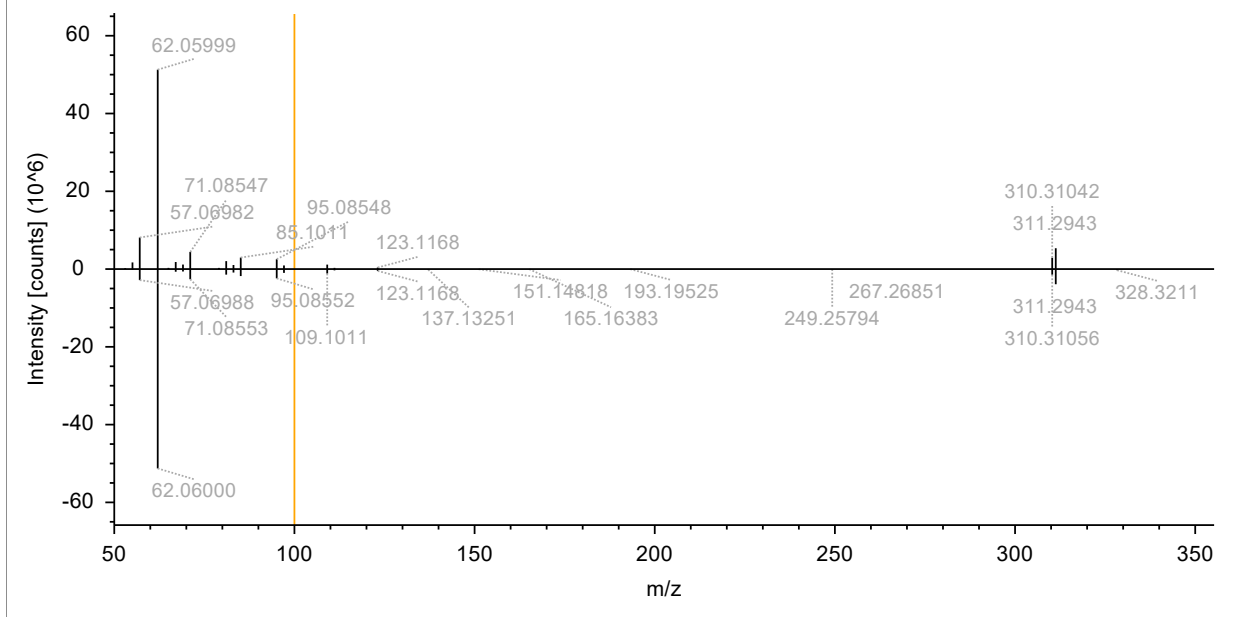
Oleoyl ethanolamide (Match 91.1)

RAWFILE(top): 2023_10_26_Quant_Ext_T3_2_20231031045821 (F47) #17321, RT=23.188 min, MS2, FTMS (+), (HCD, DDA, +1)



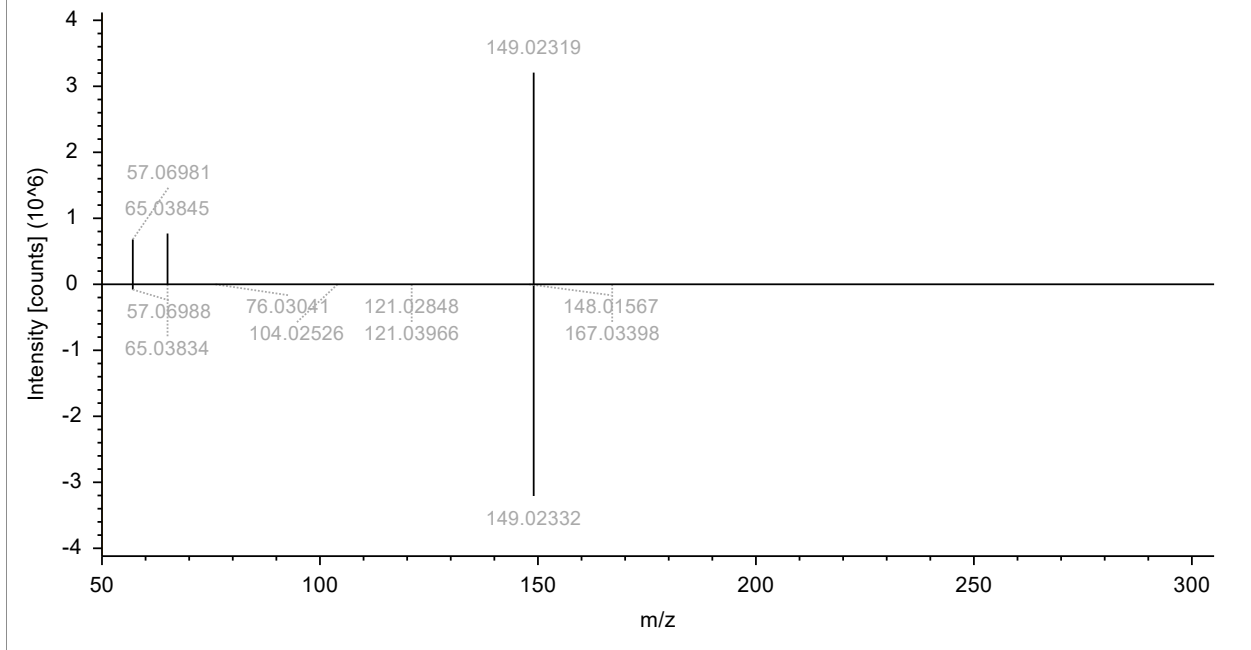
Stearoyl ethanolamide (Match 93.9)

RAWFILE(top): 2023_10_26_Quant_Ext_T3_1_20231031042613 (F46) #17926, RT=23.983 min, MS2, FTMS (+), (HCD, DDA, +1)



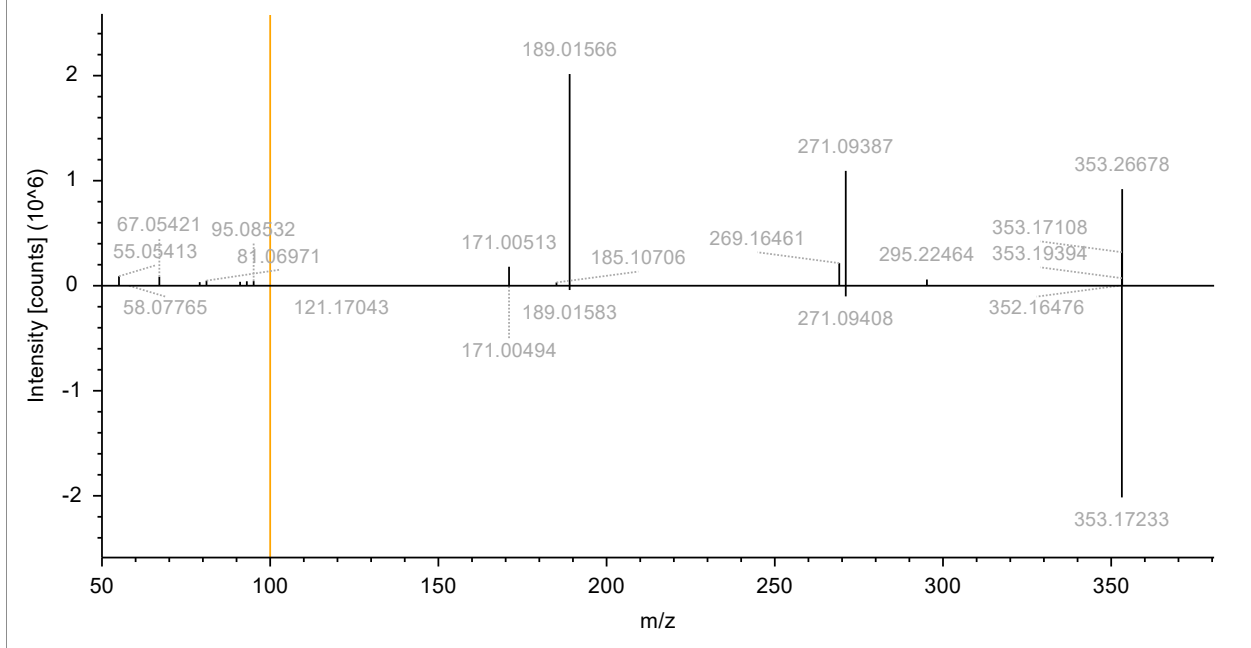
Dibutyl phthalate (Match 93.9)

RAWFILE(top): 2023_10_26_Quant_Ext_T1_3_20231031021754 (F42) #14204, RT=19.076 min, MS2, FTMS (+), (HCD, DDA, +1)



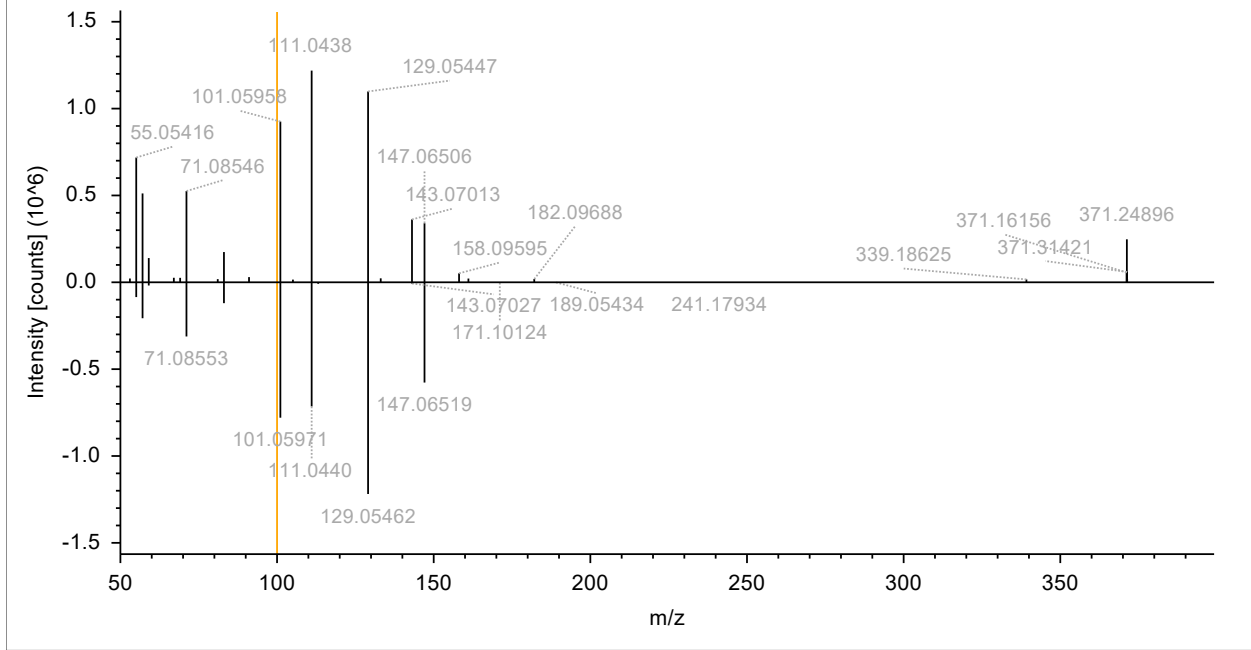
Dicyclohexyl phthalate (Match 86.9)

RAWFILE(top): 2023_10_26_Quant_Ext_C8_2_20231030174441 (F23) #15936, RT=21.404 min, MS2, FTMS (+), (HCD, DDA, +1)



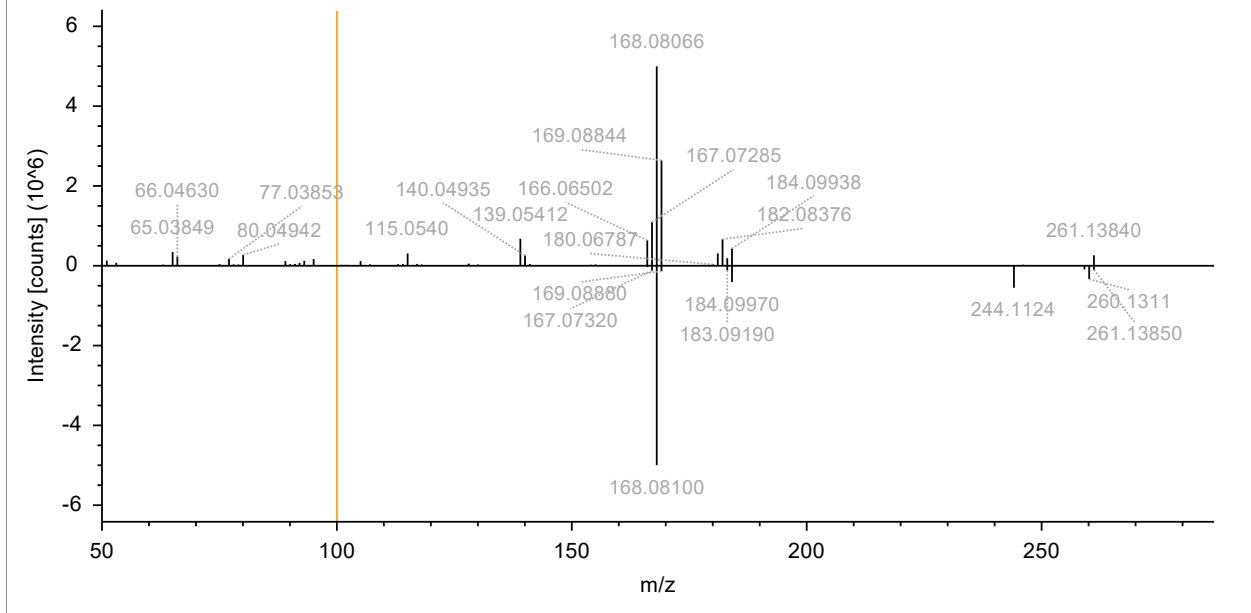
Bis(2-ethylhexyl)adipate (Match 95.4)

RAWFILE(top): 2023_10_26_Quant_Ext_T2_3_20231031035408 (F45) #18510, RT=24.754 min, MS2, FTMS (+), (HCD, DDA, +1)



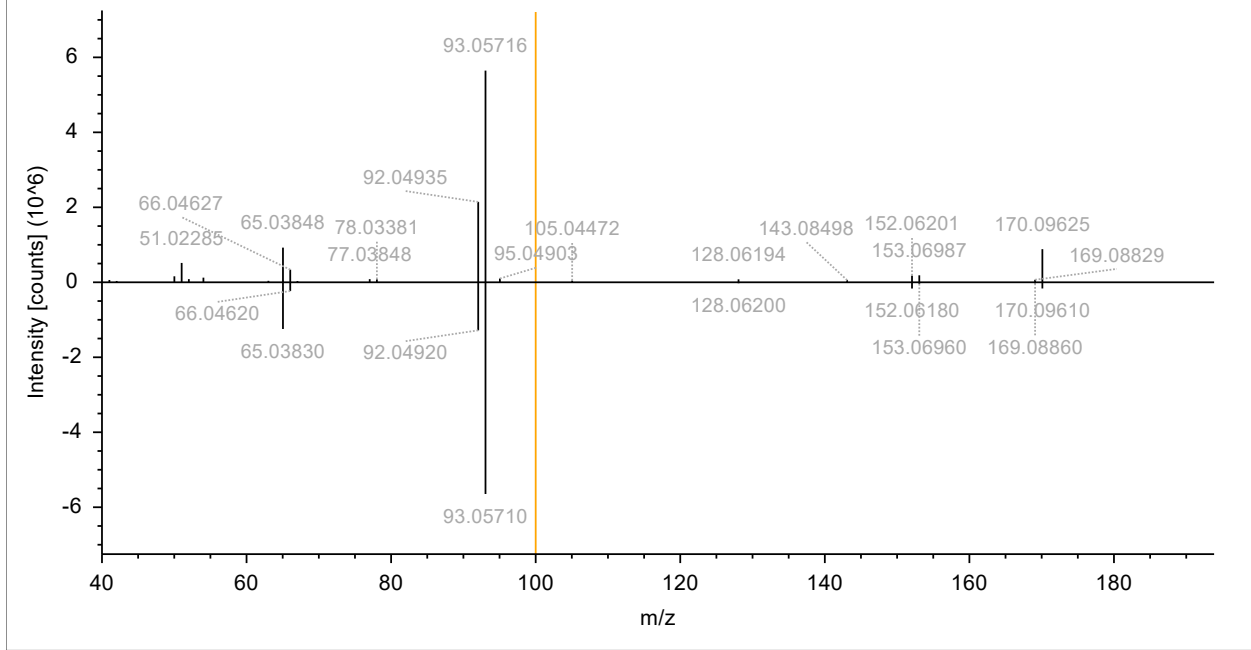
Diphenyl-p-phenylenediamine (Match 79.1)

RAWFILE(top): 2023_10_26_Quant_Ext_T3_3_20231031053030 (F48) #14411, RT=19.319 min, MS2, FTMS (+), (HCD, DDA, +1)



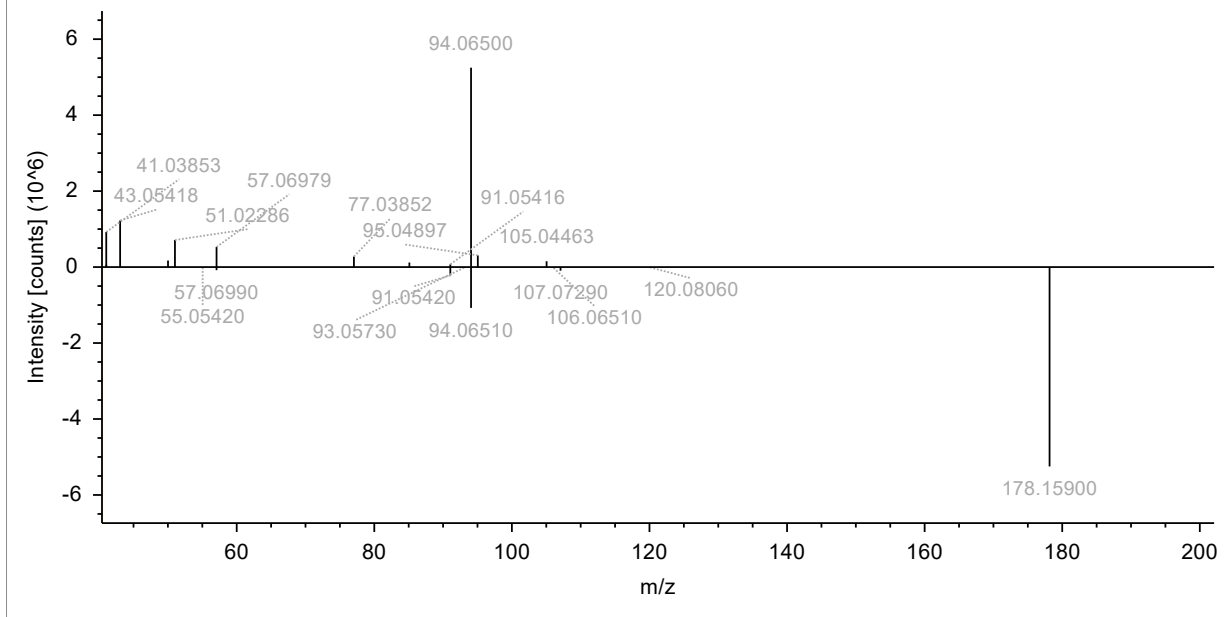
Diphenylamine (Match 94.3)

RAWFILE(top): 2023_10_26_Quant_Ext_T3_2_20231031045821 (F47) #11619, RT=15.624 min, MS2, FTMS (+), (HCD, DDA, +1)



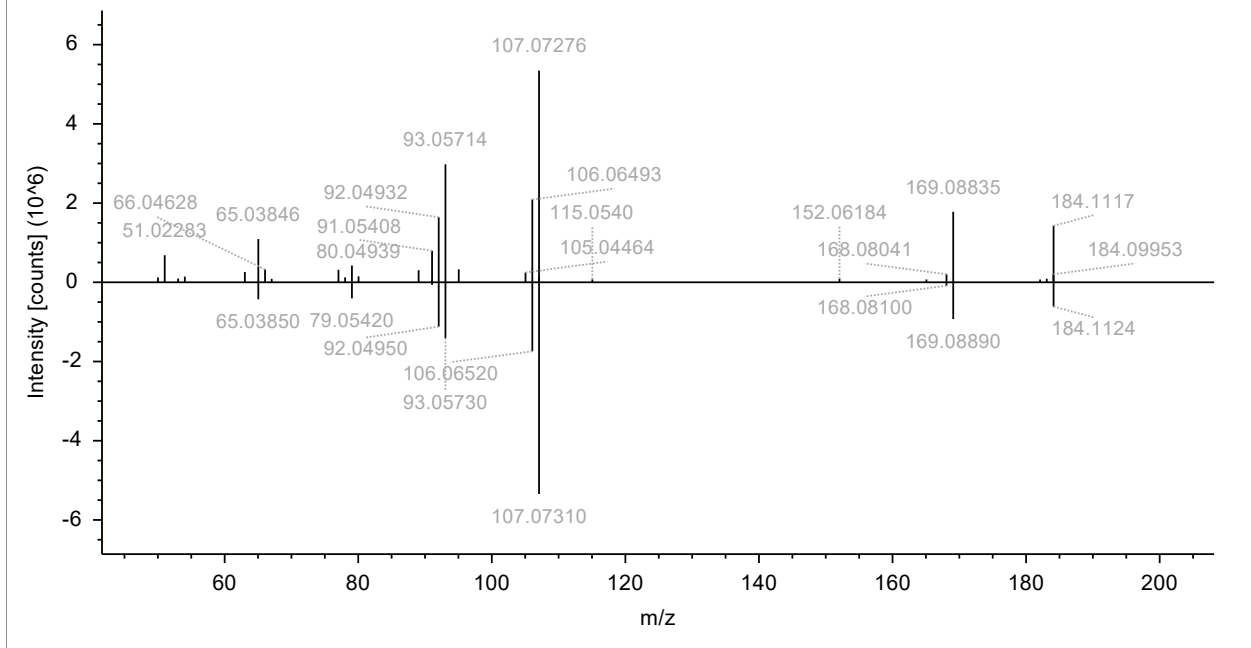
4-hexylaniline (Match 92.0)

RAWFILE(top): 2023_10_26_Quant_Ext_T3_2_20231031045821 (F47) #7899, RT=10.653 min, MS2, FTMS (+), (HCD, DDA, 1 +1)



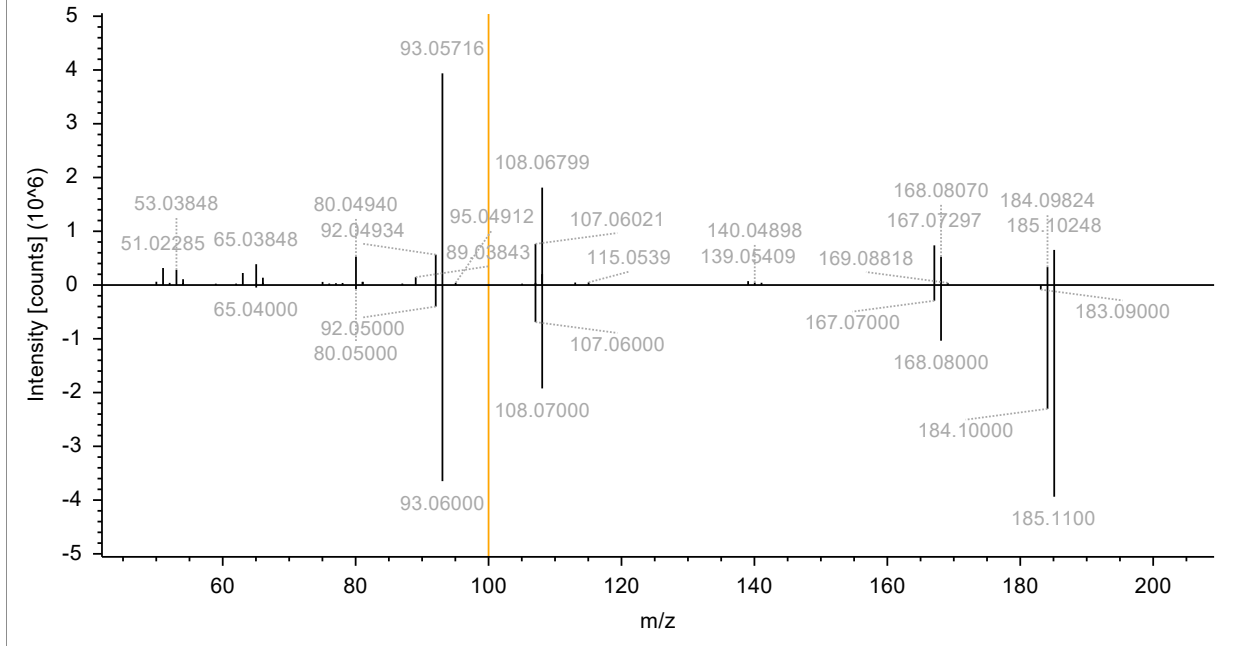
Phenyl-p-tolyl-amine (Match 94.5)

RAWFILE(top): 2023_10_26_Quant_Ext_T3_2_20231031045821 (F47) #12747, RT=17.123 min, MS2, FTMS (+), (HCD, DDA, +1)



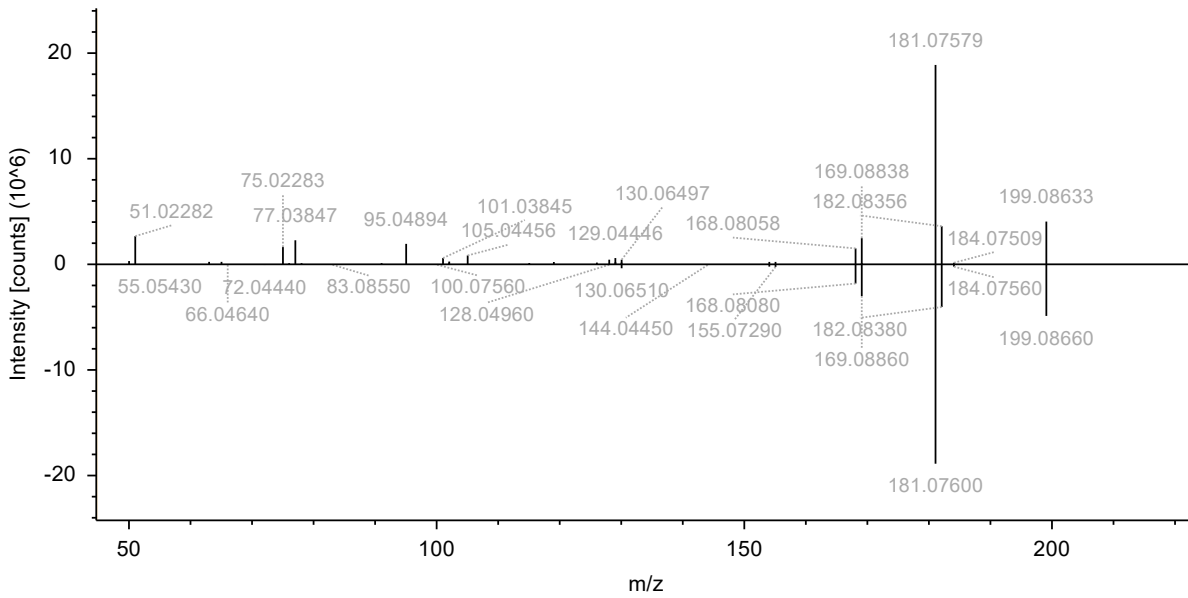
4-aminodiphenylamine (Match 91.1)

RAWFILE(top): 2023_10_26_Quant_Ext_T3_1_20231031042613 (F46) #13419, RT=18.014 min, MS2, FTMS (+), (HCD, DDA, +1)



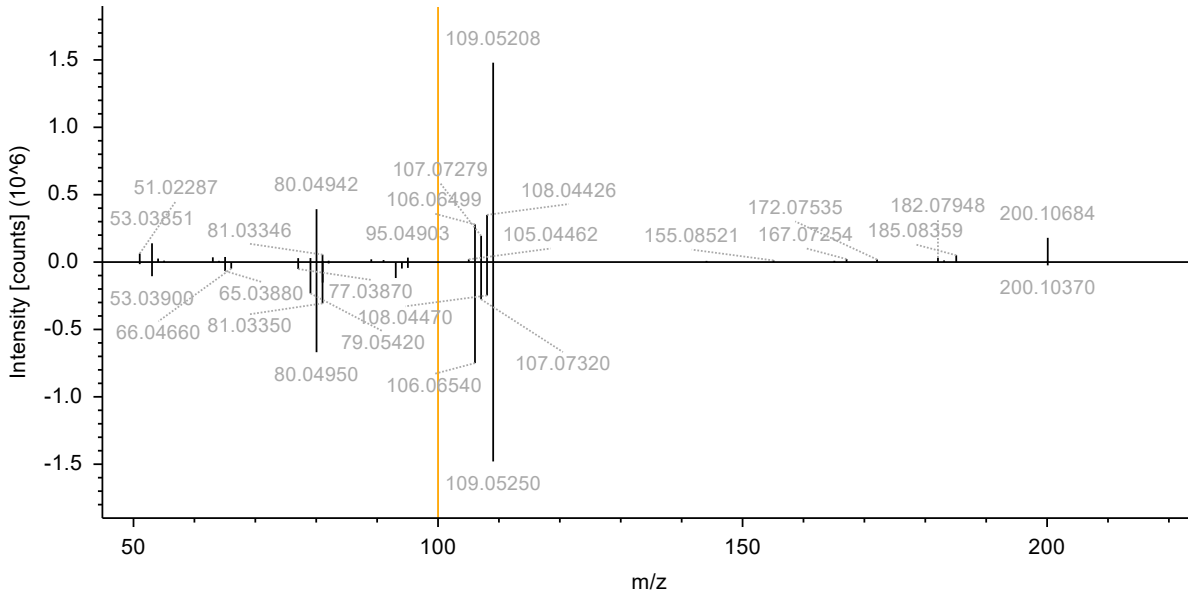
4-nitrosodiphenylamine (Match 90.4)

RAWFILE(top): 2023_10_26_Quant_Ext_T1_1_20231031011345 (F40) #9829, RT=13.251 min, MS2, FTMS (+), (HCD, DDA, 1+1)



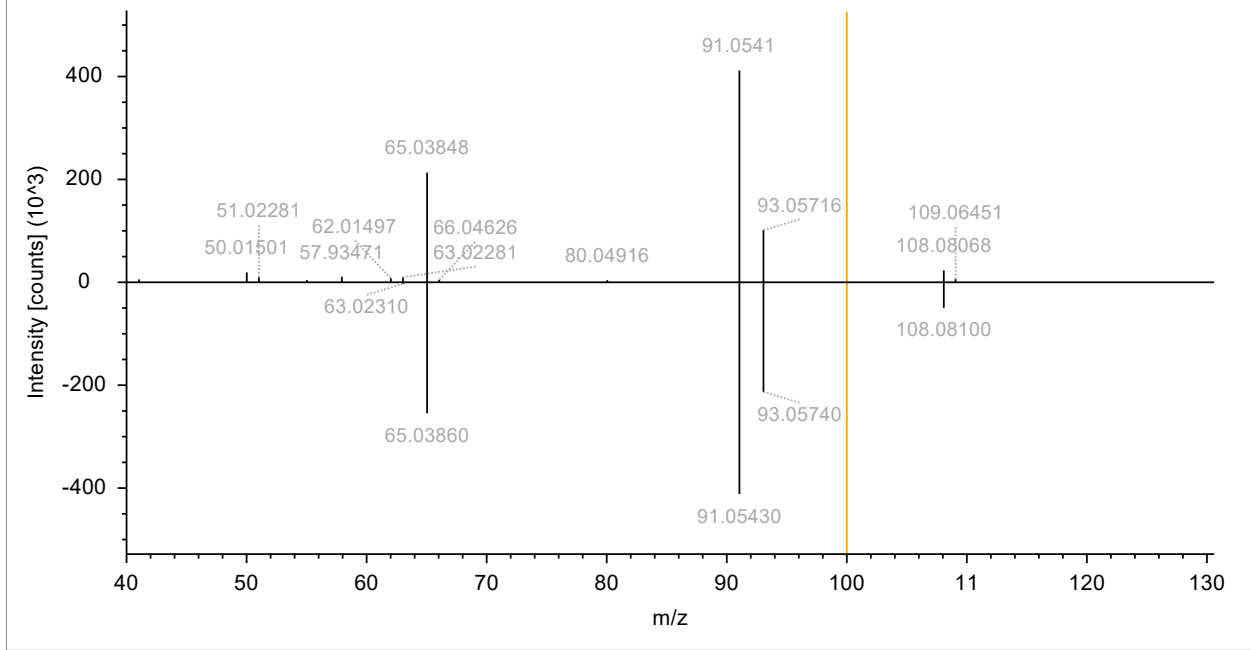
4-(4-methylanilino)phenol (Match 89.4)

RAWFILE(top): 2023_10_26_Quant_Ext_C11_1_20231030220118 (F31) #9930, RT=13.399 min, MS2, FTMS (+), (HCD, DDA, 1+1)



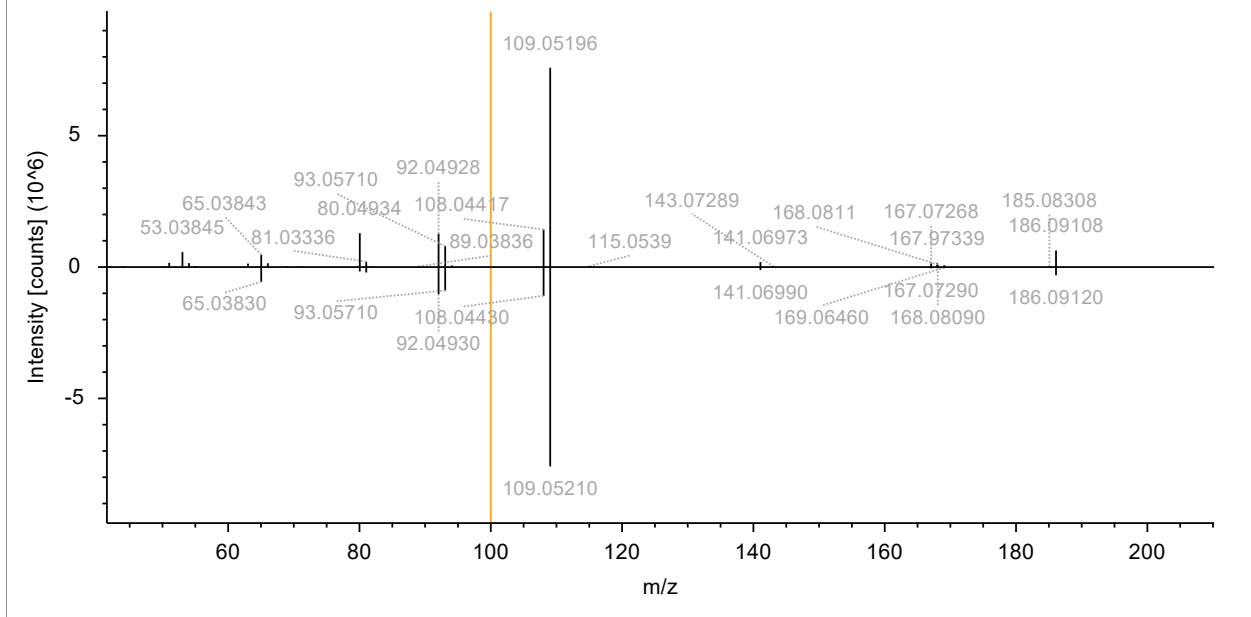
3-methylaniline (Match 97.7)

RAWFILE(top): 2023_10_26_Quant_Ext_T2_2_20231031032203 (F44) #1493, RT=2.049 min, MS2, FTMS (+), (HCD, DDA, 10+1)



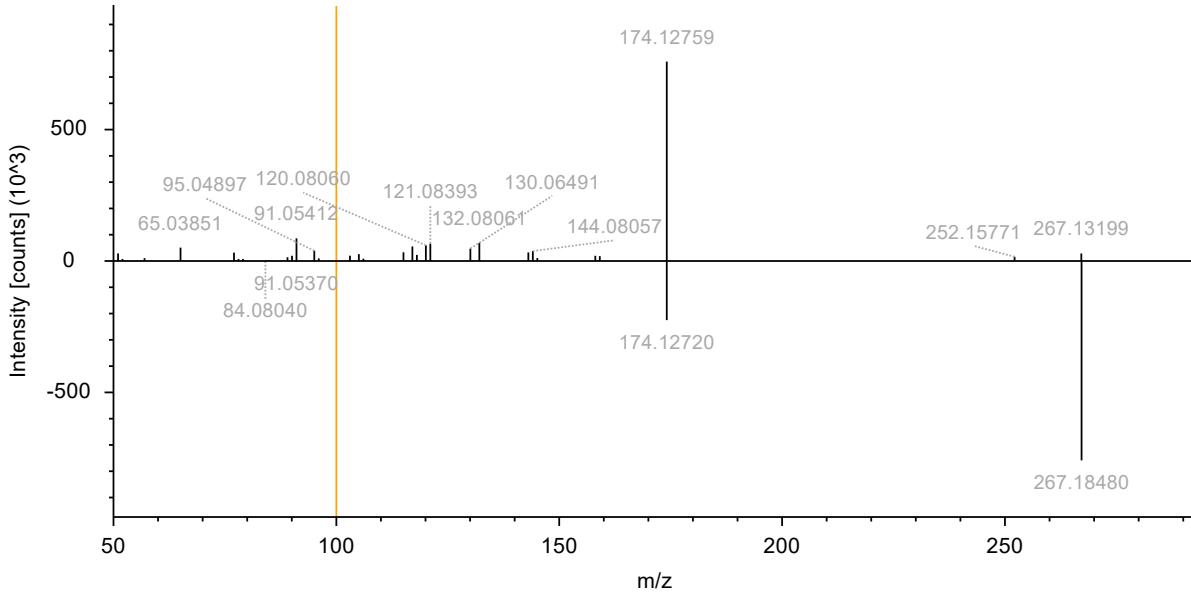
4-anilinophenol (Match 93.5)

RAWFILE(top): 2023_10_26_Quant_Ext_T1_2_20231031014550 (F41) #8596, RT=11.620 min, MS2, FTMS (+), (HCD, DDA, 10+1)



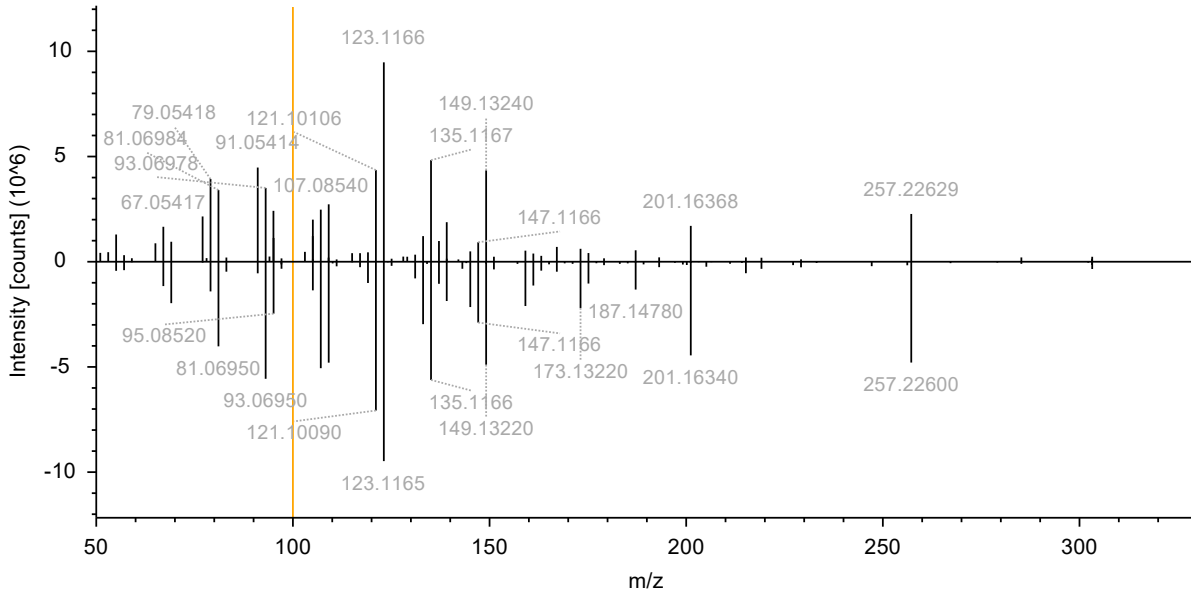
1-Benzyl-N-phenyl-4-piperidinamine (Match 87.3)

RAWFILE(top): 2023_10_26_Quant_Ext_T3_3_20231031053030 (F48) #6767, RT=9.147 min, MS2, FTMS (+), (HCD, DDA, 2f +1)



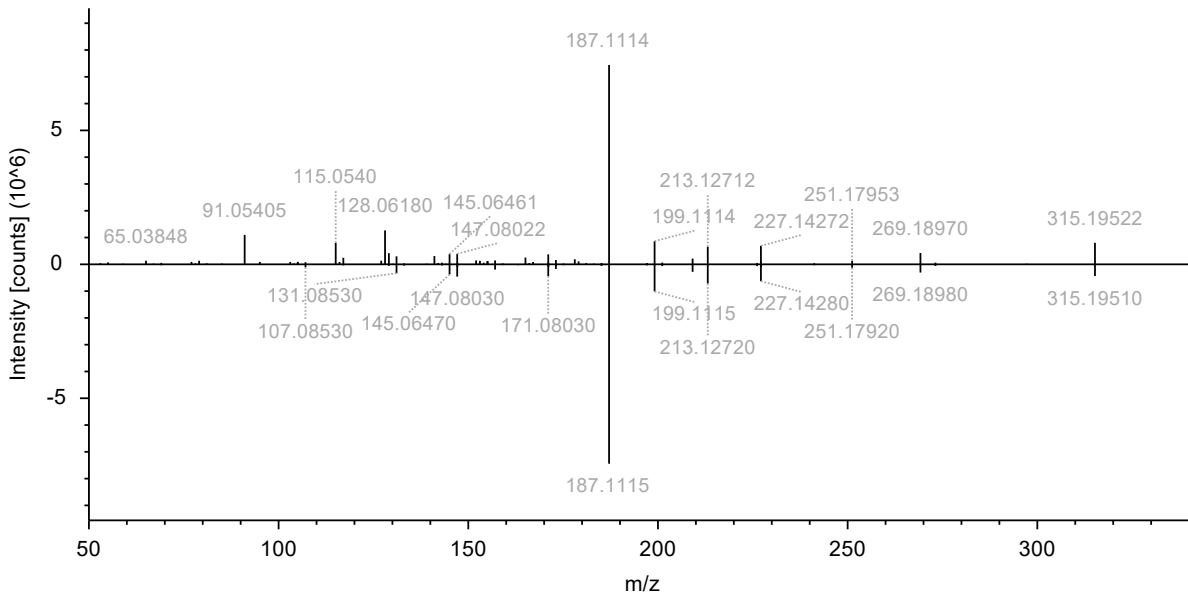
(-)-abietic acid (Match 87.6)

RAWFILE(top): 2023_10_26_Quant_Ext_C8_3_20231030181646 (F24) #17278, RT=23.163 min, MS2, FTMS (+), (HCD, DDA, +1)



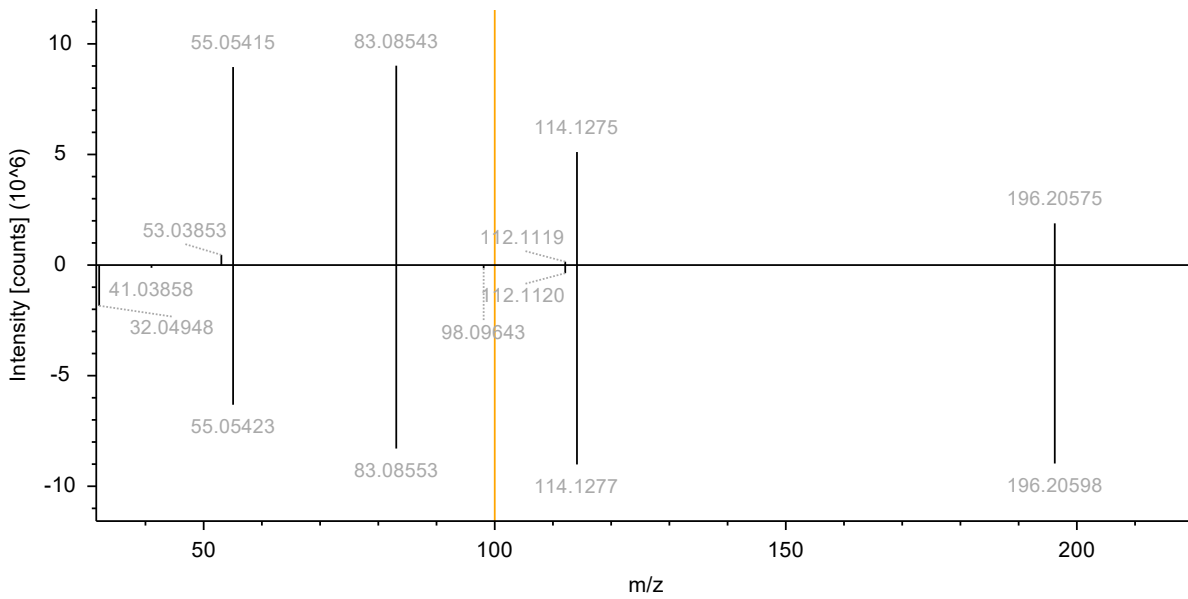
7-oxoabieta-8,11,13-trien-18-oic acid (Match 85.2)

RAWFILE(top): 2023_10_26_Quant_Ext_C9_3_20231030195259 (F27) #14456, RT=19.467 min, MS2, FTMS (+), (HCD, DDA, +1)



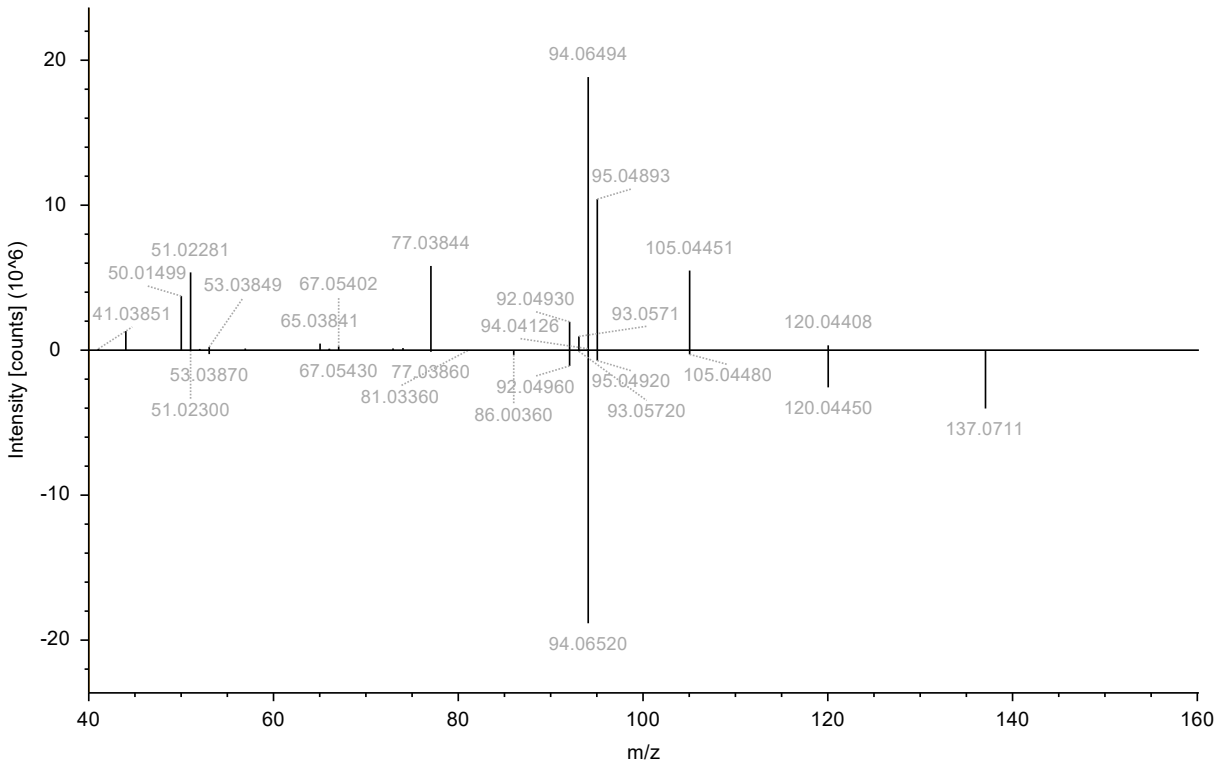
N-cyclohexyl-N-methylcyclohexanamine (Match 89.3)

RAWFILE(top): 2023_10_26_Quant_Ext_C11_1_20231030220118 (F31) #5745, RT=7.777 min, MS2, FTMS (+), (HCD, DDA, +1)



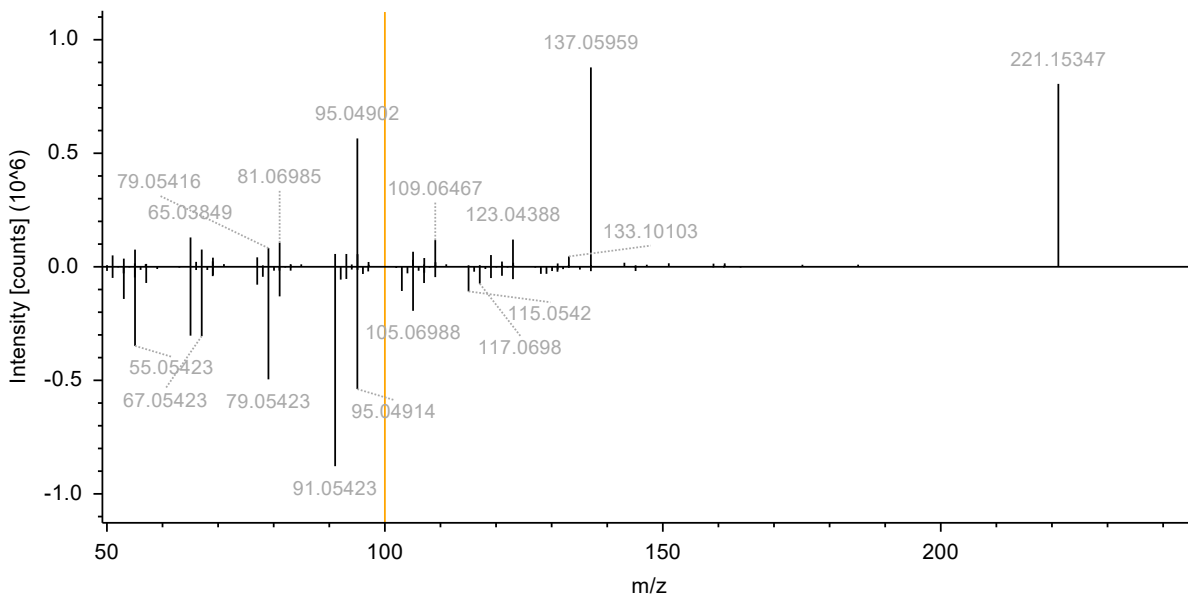
1-phenylurea (Match 80.5)

RAWFILE(top): 2023_10_26_Quant_Ext_T1_2_20231031014550 (F41) #3484, RT=4.730 min, MS2, FTMS (+), (HCD, DDA, 137.0706@+1)



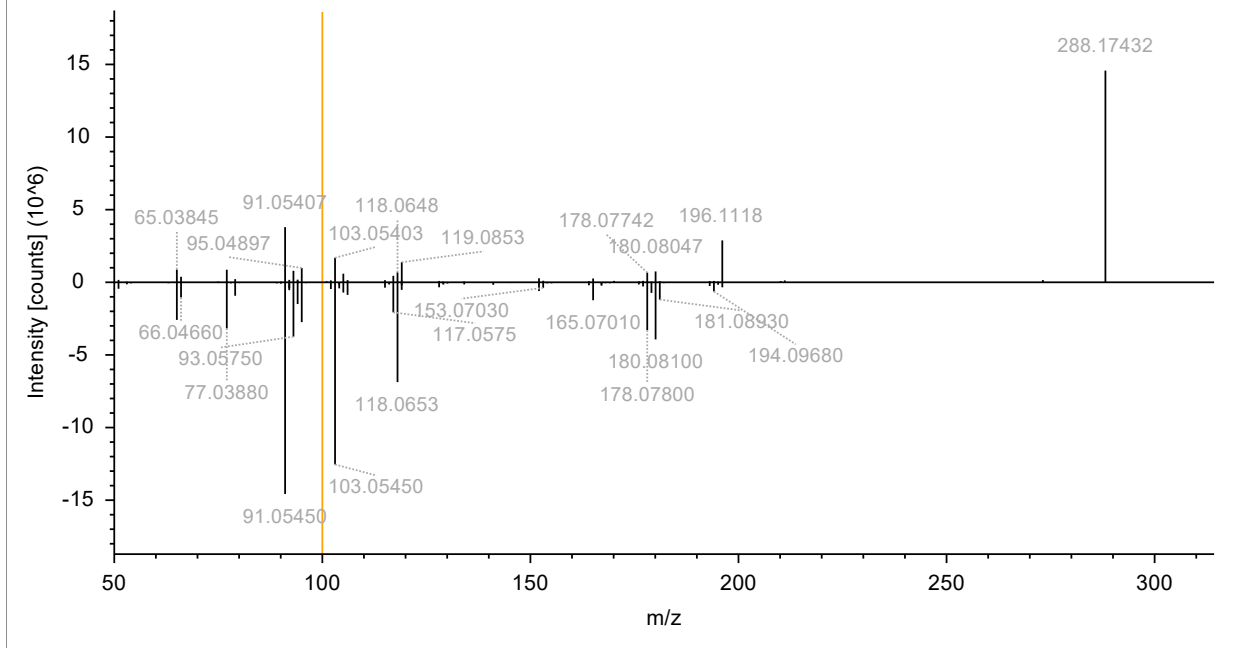
2,6-di-tert-butyl-1,4-benzoquinone (Match 77.1)

RAWFILE(top): 2023_10_26_Quant_Ext_T2_3_20231031035408 (F45) #14815, RT=19.863 min, MS2, FTMS (+), (HCD, DDA, +1)



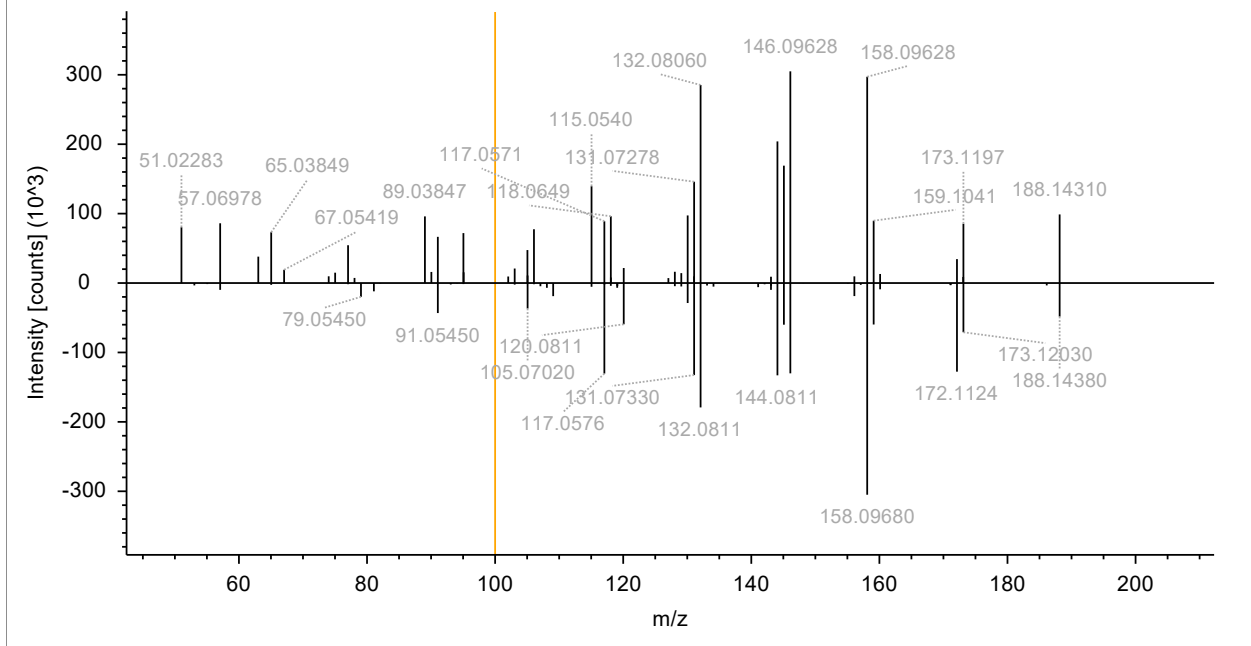
N-Phenyl-4-(2-phenyl-2-propanyl)aniline (Match 87.1)

RAWFILE(top): 2023_10_26_Quant_Ext_C10_1_20231030202504 (F28) #15933, RT=21.403 min, MS2, FTMS (+), (HCD, DD/ +1)



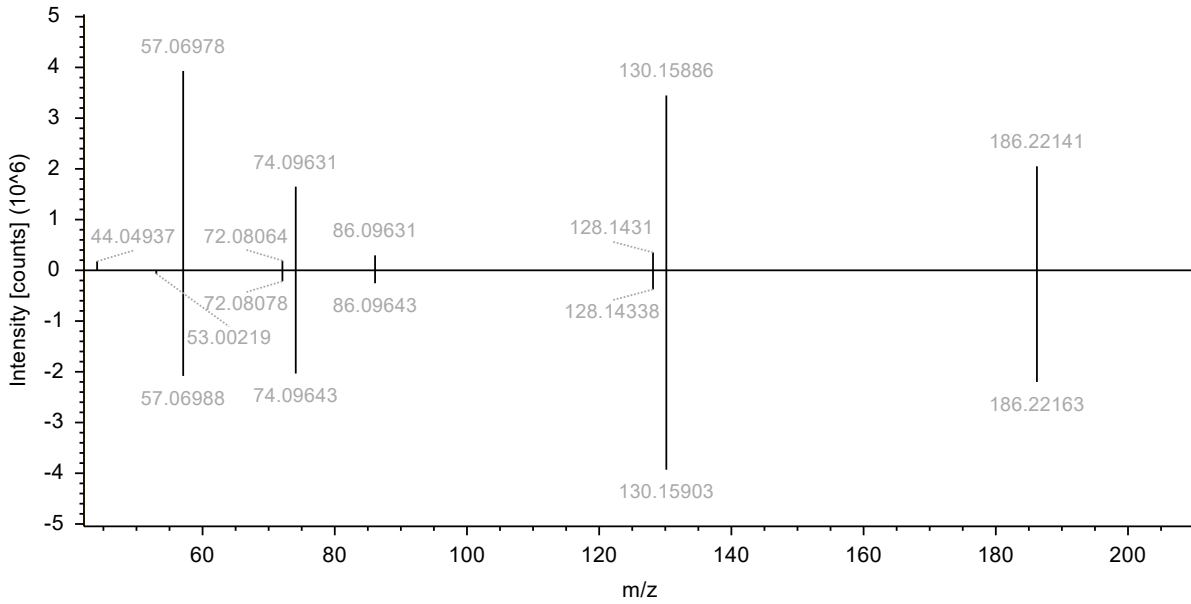
1,2-dihydro-2,2,4,7-tetramethylquinoline (Match 84.5)

RAWFILE(top): 2023_10_26_Quant_Ext_T3_3_20231031053030 (F48) #9822, RT=13.223 min, MS2, FTMS (+), (HCD, DDA, 1 +1)



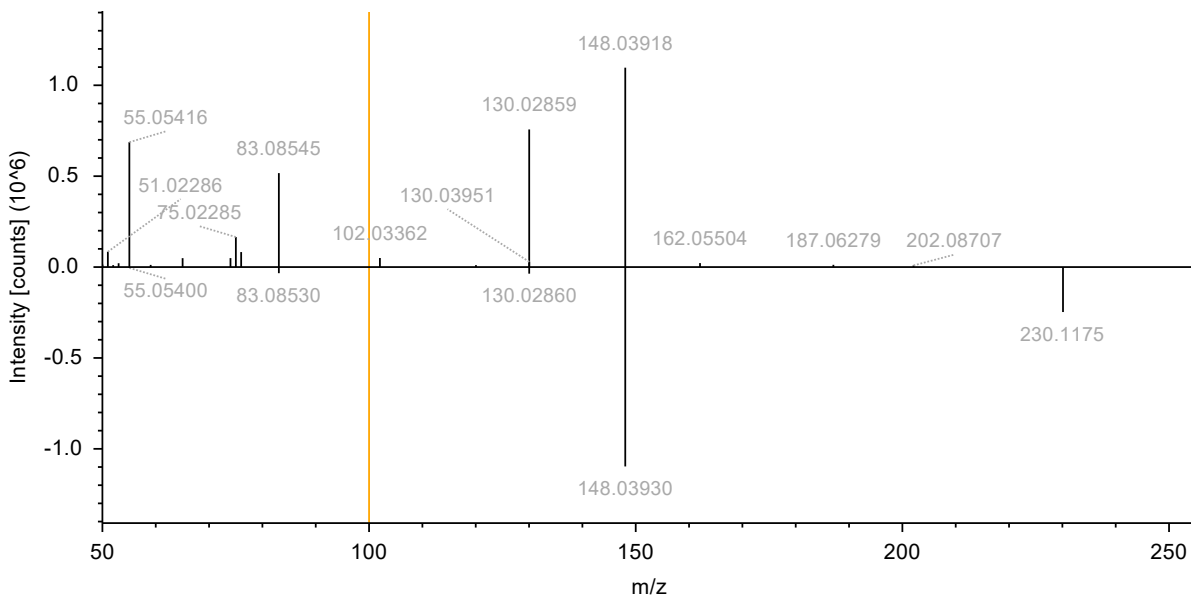
Tributylamine (Match 97.5)

RAWFILE(top): 2023_10_26_Quant_Ext_T3_2_20231031045821 (F47) #6276, RT=8.479 min, MS2, FTMS (+), (HCD, DDA, 18+1)



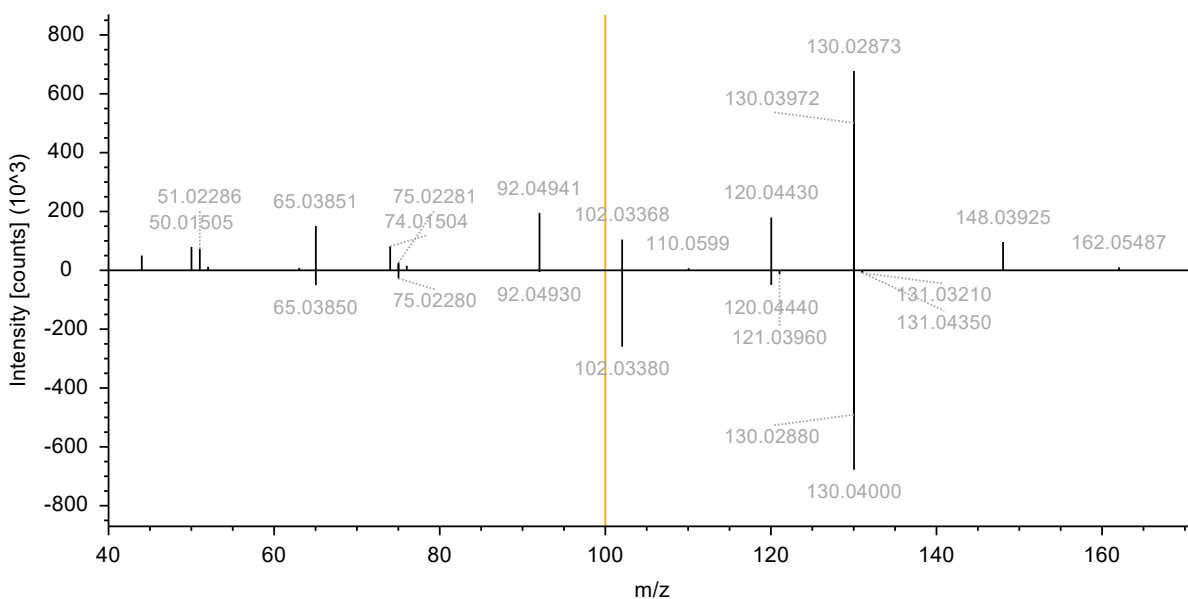
N-cyclohexylphthalimide (Match 94.1)

RAWFILE(top): 2023_10_26_Quant_Ext_T3_2_20231031045821 (F47) #7306, RT=9.861 min, MS2, FTMS (+), (HCD, DDA, 23+1)



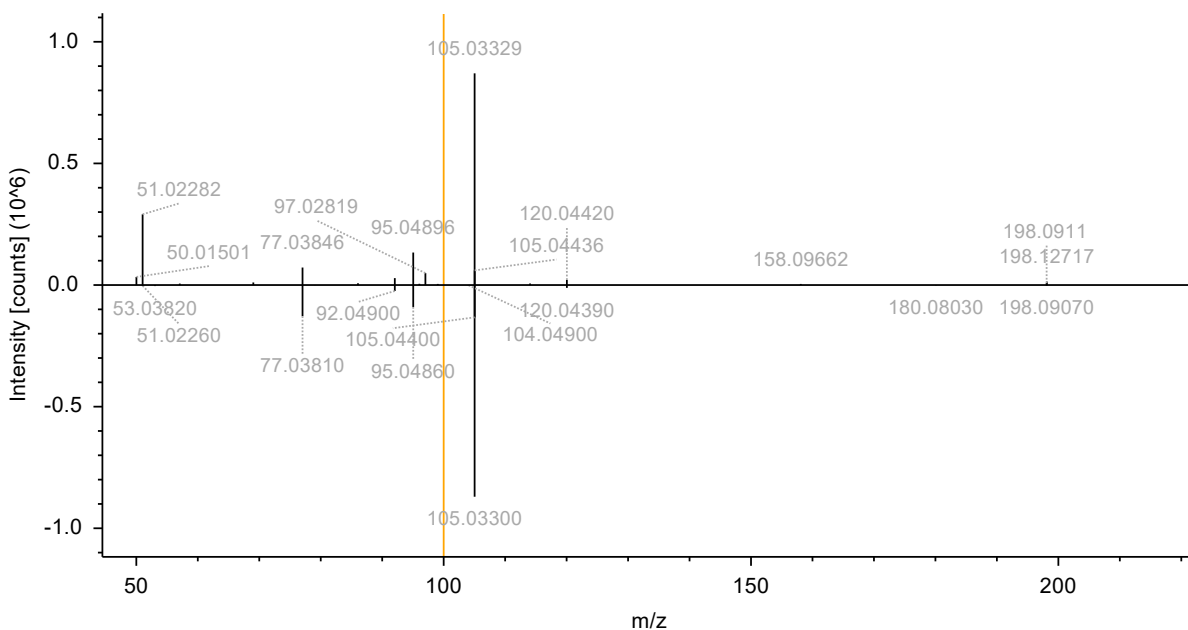
Phthalimide (Match 88.4)

RAWFILE(top): 2023_10_26_Quant_Ext_T3_2_20231031045821 (F47) #3632, RT=4.915 min, MS2, FTMS (+), (HCD, DDA, 14+1)



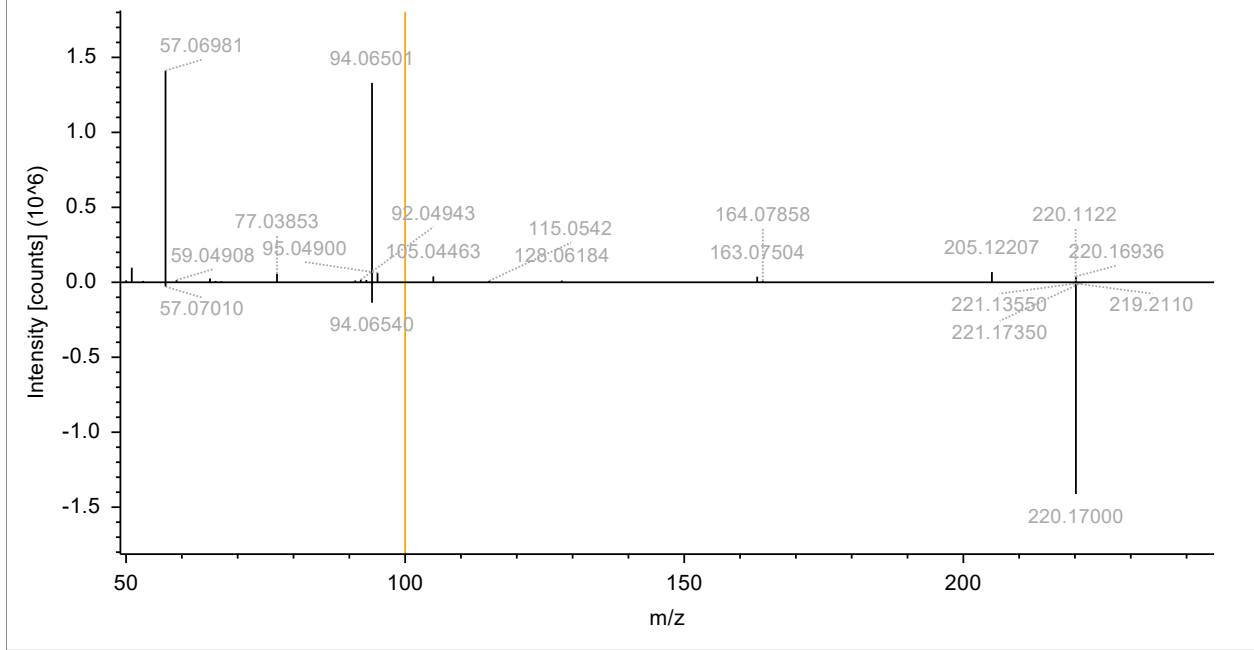
Benzanilide (Match 85.9)

RAWFILE(top): 2023_10_26_Quant_Ext_T2_1_20231031024959 (F43) #8838, RT=11.912 min, MS2, FTMS (+), (HCD, DDA, 14+1)



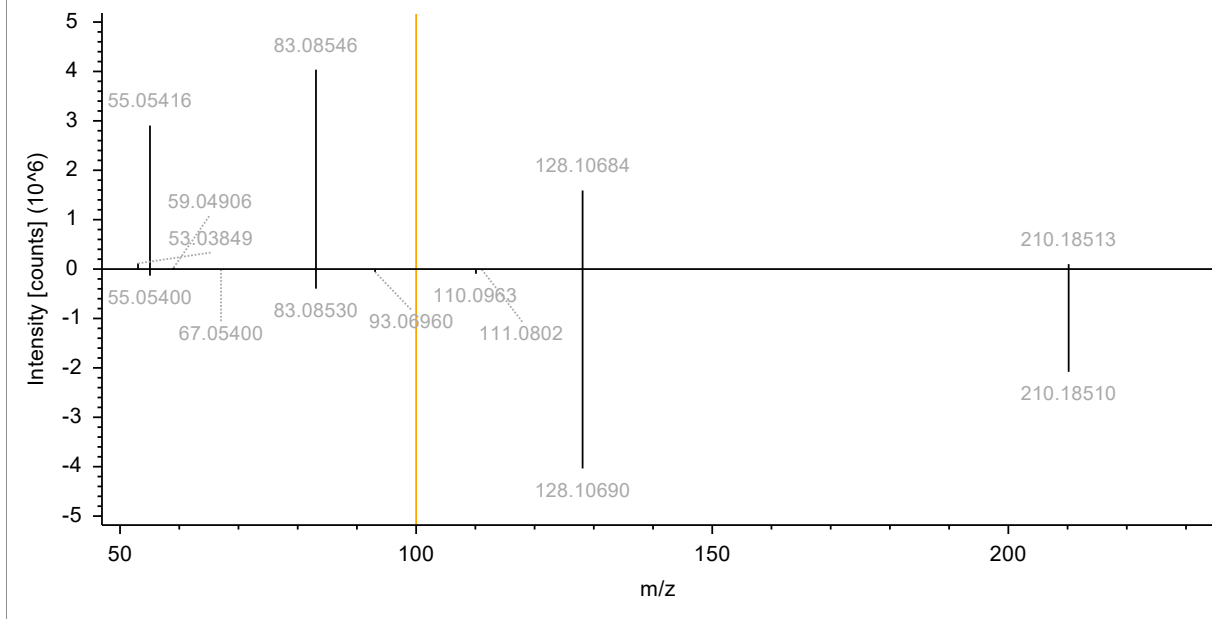
2-ethyl-N-phenylhexanamide (Match 89.6)

RAWFILE(top): 2023_10_26_Quant_Ext_T3_3_20231031053030 (F48) #11722, RT=15.748 min, MS2, FTMS (+), (HCD, DDA, +1)



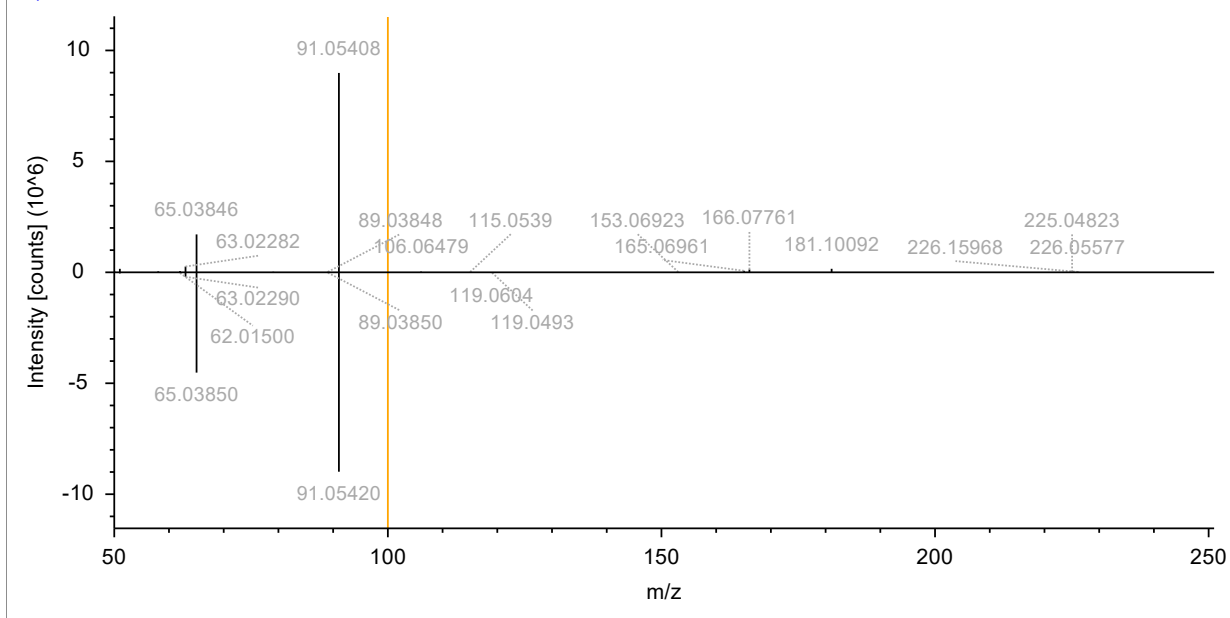
N-Cyclohexylcyclohexanecarboxamide (Match 89.4)

RAWFILE(top): 2023_10_26_Quant_Ext_C11_3_20231030230527 (F33) #12931, RT=17.424 min, MS2, FTMS (+), (HCD, DDA, +1)



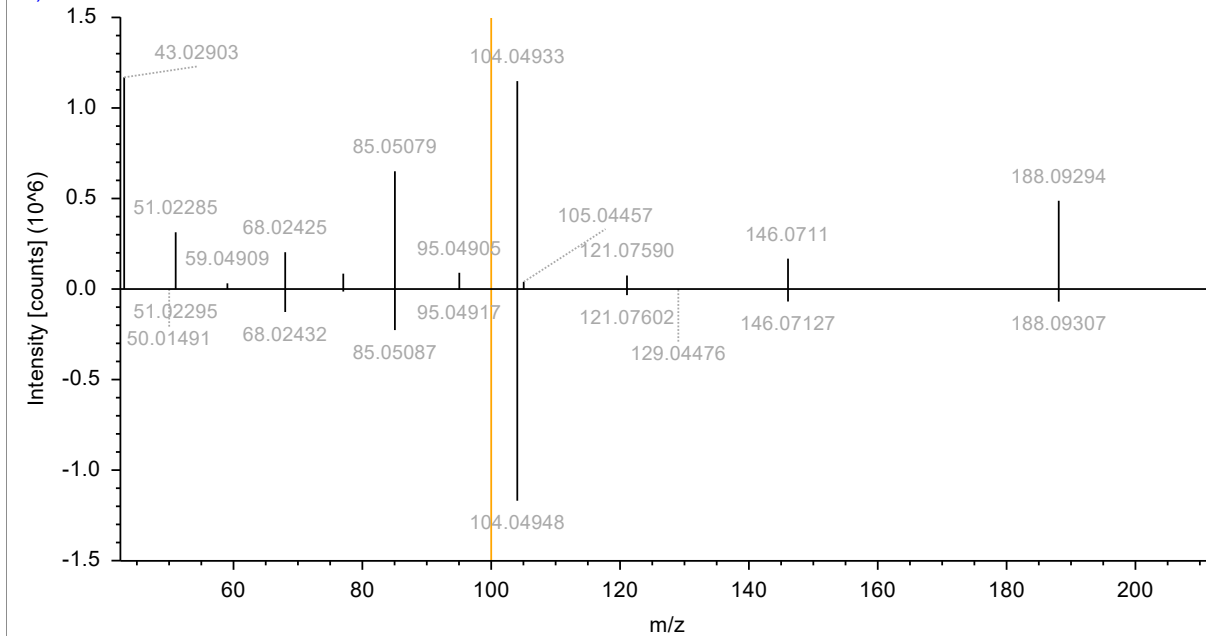
N-benzyl-2-methylbenzamide (Match 99.0)

RAWFILE(top): 2023_10_26_Quant_Ext_T2_2_20231031032203 (F44) #11045, RT=14.856 min, MS2, FTMS (+), (HCD, DDA, +1)



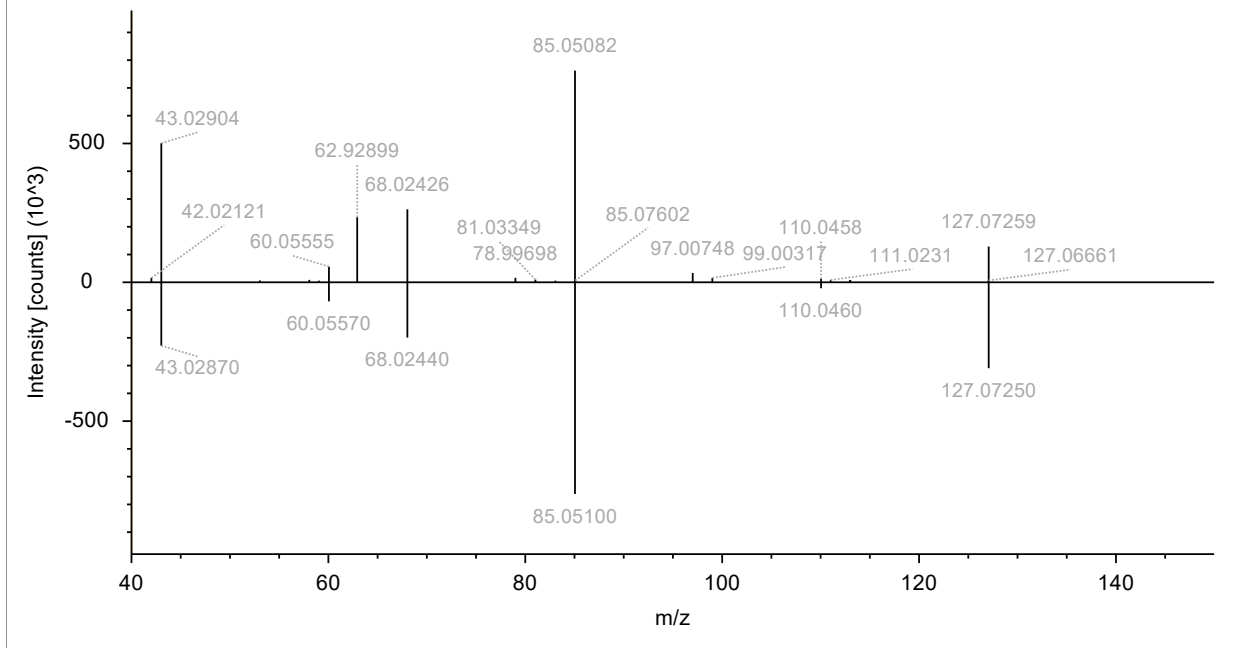
Benzoguanamine (Match 73.0)

RAWFILE(top): 2023_10_26_Quant_Ext_C5_1_20231030052657 (F13) #3903, RT=5.295 min, MS2, FTMS (+), (HCD, DDA, 18 +1)



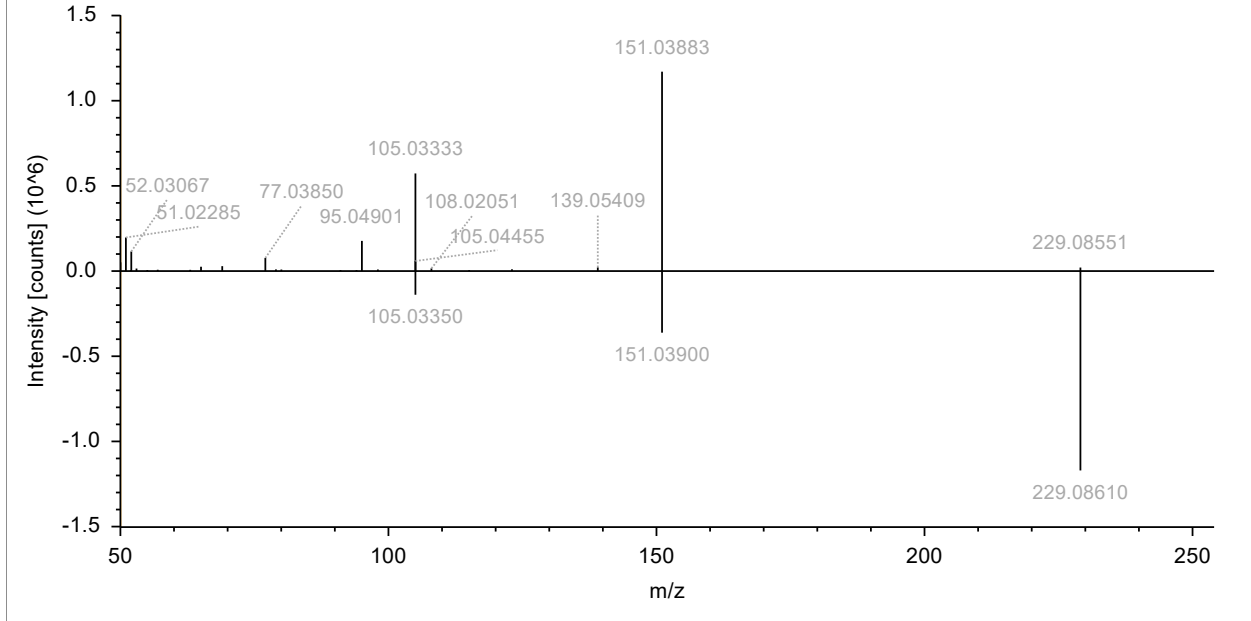
Melamine (Match 90.5)

RAWFILE(top): 2023_10_26_Quant_Ext_C8_3_20231030181646 (F24) #369, RT=0.541 min, MS2, FTMS (+), (HCD, DDA, 127+1)



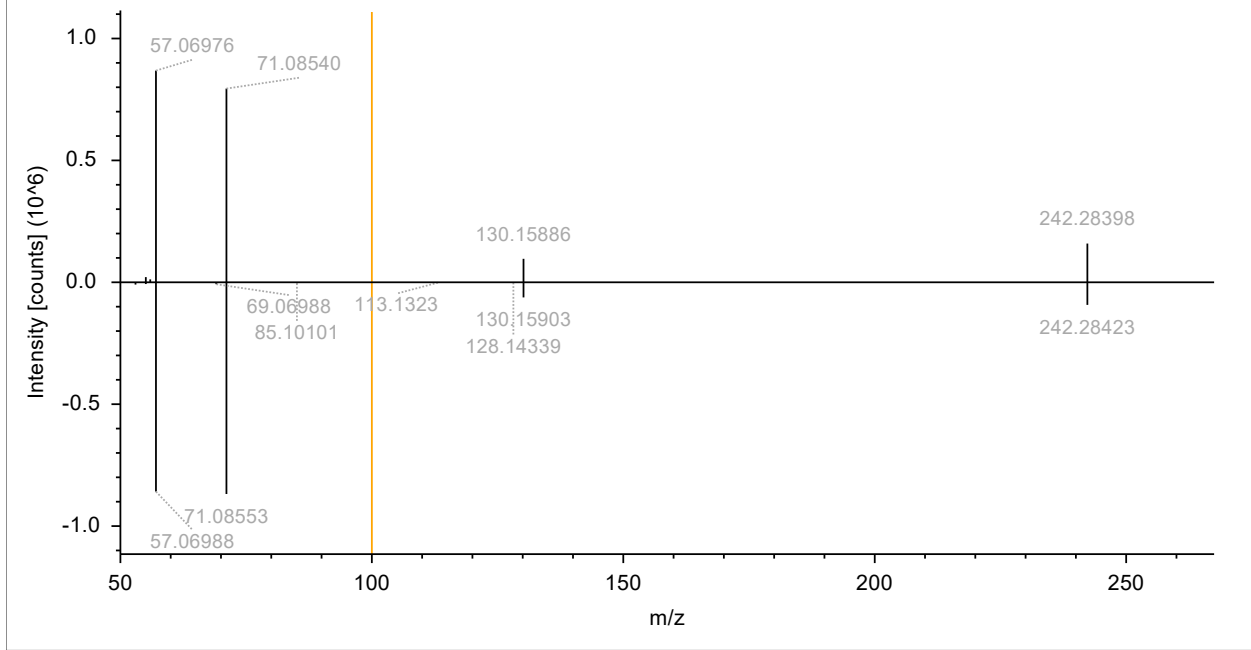
Benzophenone-3 (Match 91.8)

RAWFILE(top): 2023_10_26_Quant_Ext_C2_1_20231030003815 (F4) #12389, RT=16.673 min, MS2, FTMS (+), (HCD, DDA, 229+1)



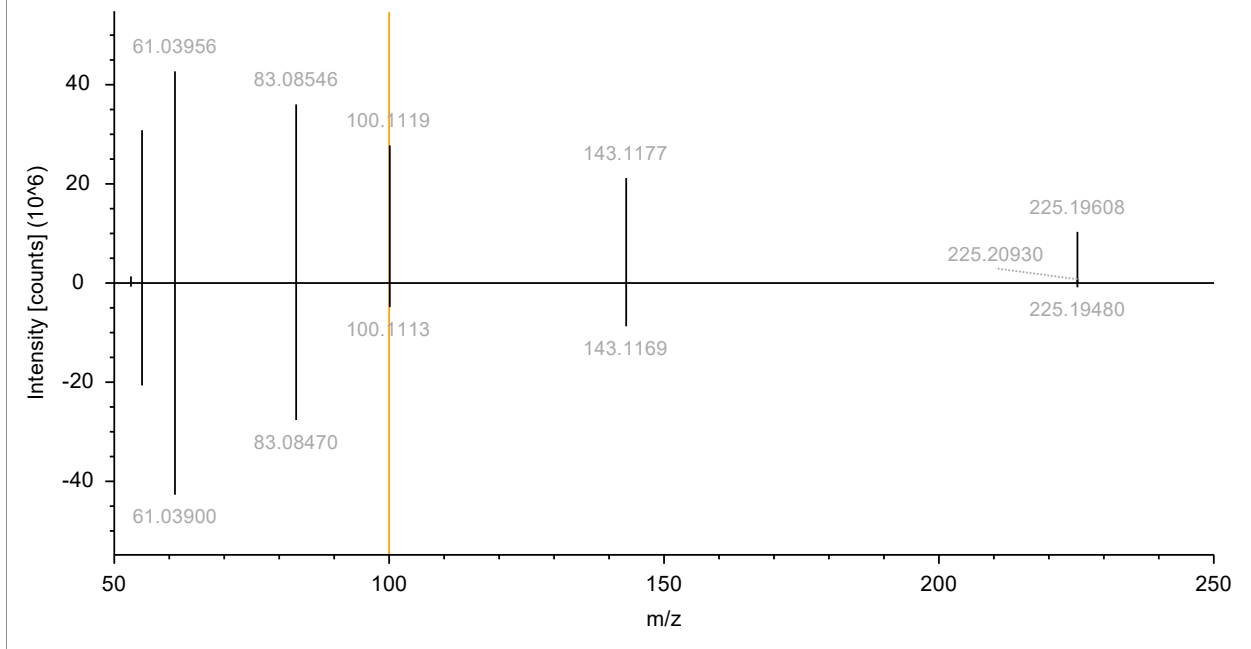
Bis(2-ethylhexyl) amine (Match 93.3)

RAWFILE(top): 2023_10_26_Quant_Ext_C11_1_20231030220118 (F31) #11212, RT=15.130 min, MS2, FTMS (+), (HCD, DD/ +1)



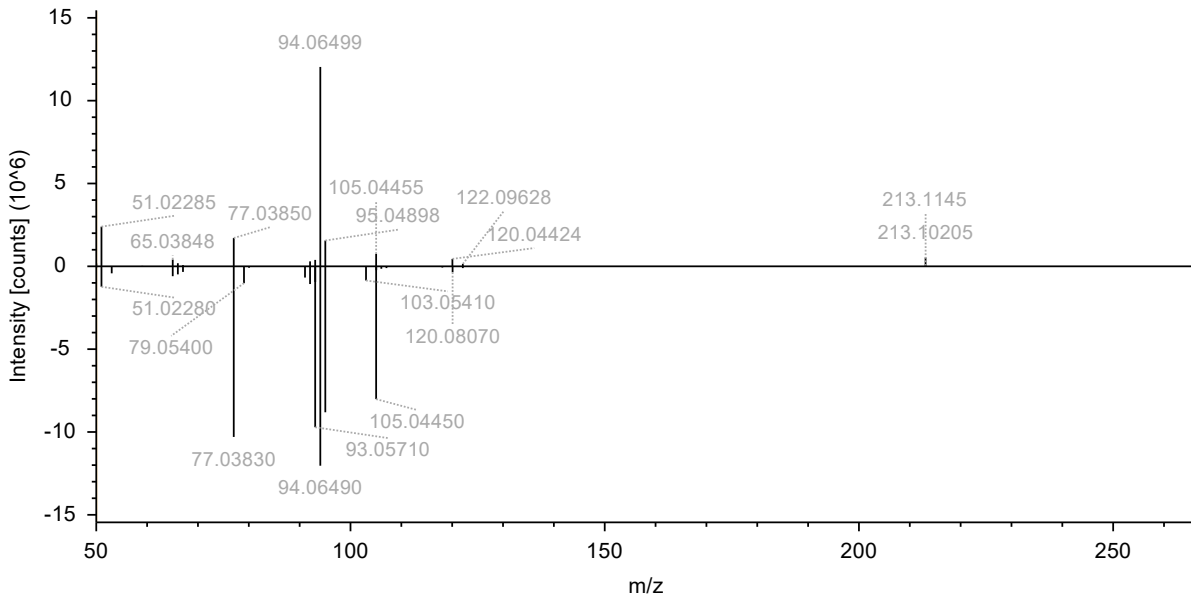
1,3-dicyclohexylurea (Match 99.1)

RAWFILE(top): 2023_10_26_Quant_Ext_T1_3_20231031021754 (F42) #11103, RT=14.953 min, MS2, FTMS (+), (HCD, DDA, +1)



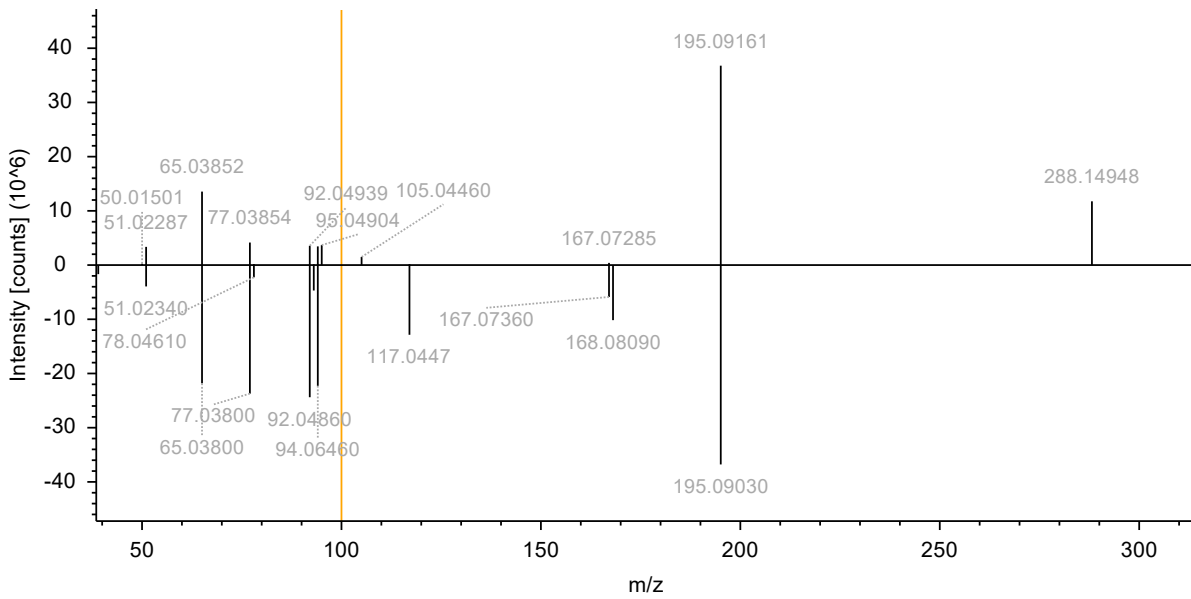
1-(2-ethylphenyl)-3-phenylurea (Match 88.5)

RAWFILE(top): 2023_10_26_Quant_Ext_T3_3_20231031053030 (F48) #6349, RT=8.585 min, MS2, FTMS (+), (HCD, DDA, 24 +1)



Triphenylguanidine (Match 81.1)

RAWFILE(top): 2023_10_26_Quant_Ext_T3_1_20231031042613 (F46) #7695, RT=10.382 min, MS2, FTMS (+), (HCD, DDA, 2 +1)



1,1-diethyl-3-phenylurea (Match 85.5)

RAWFILE(top): 2023_10_26_Quant_Ext_T1_2_20231031014550 (F41) #8943, RT=12.083 min, MS2, FTMS (+), (HCD, DDA, 1+1)

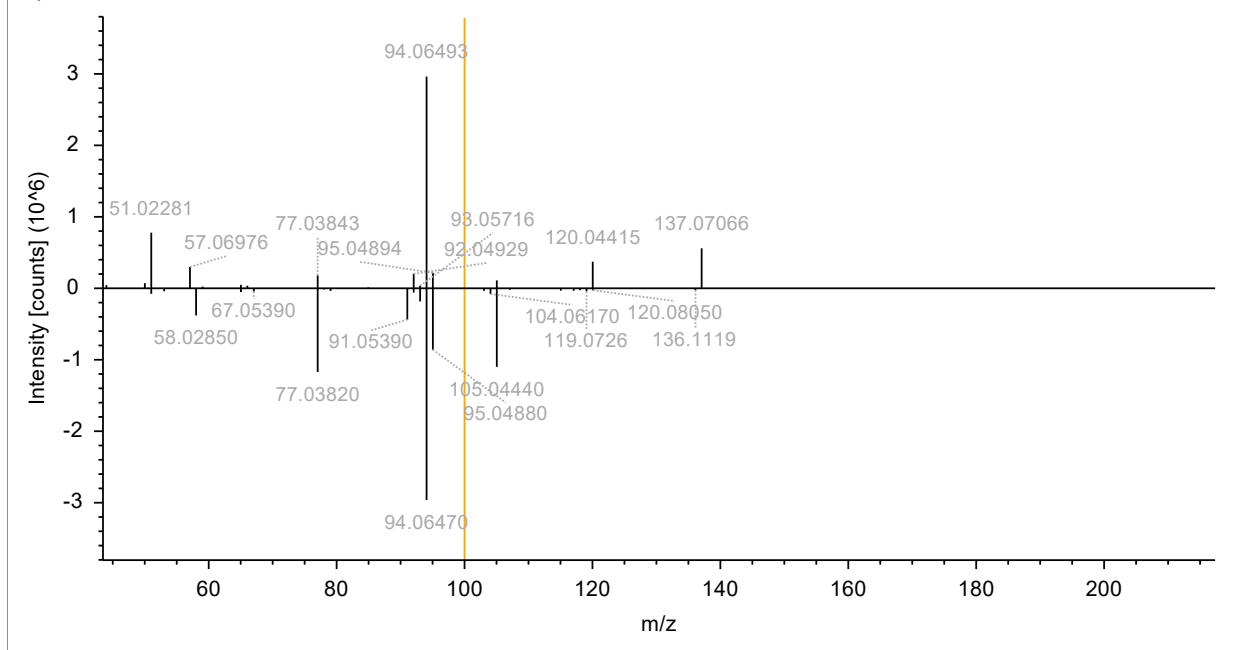
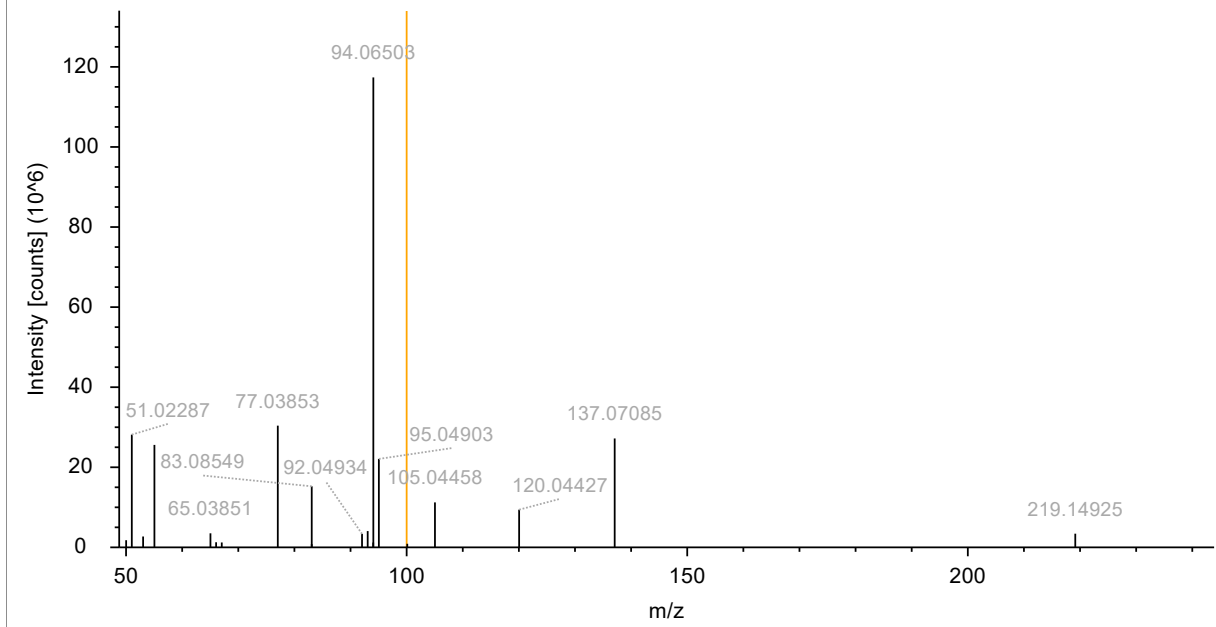


Figure S9. Comparison between experimental and mzVault library MS/MS spectra in CD 3.3.

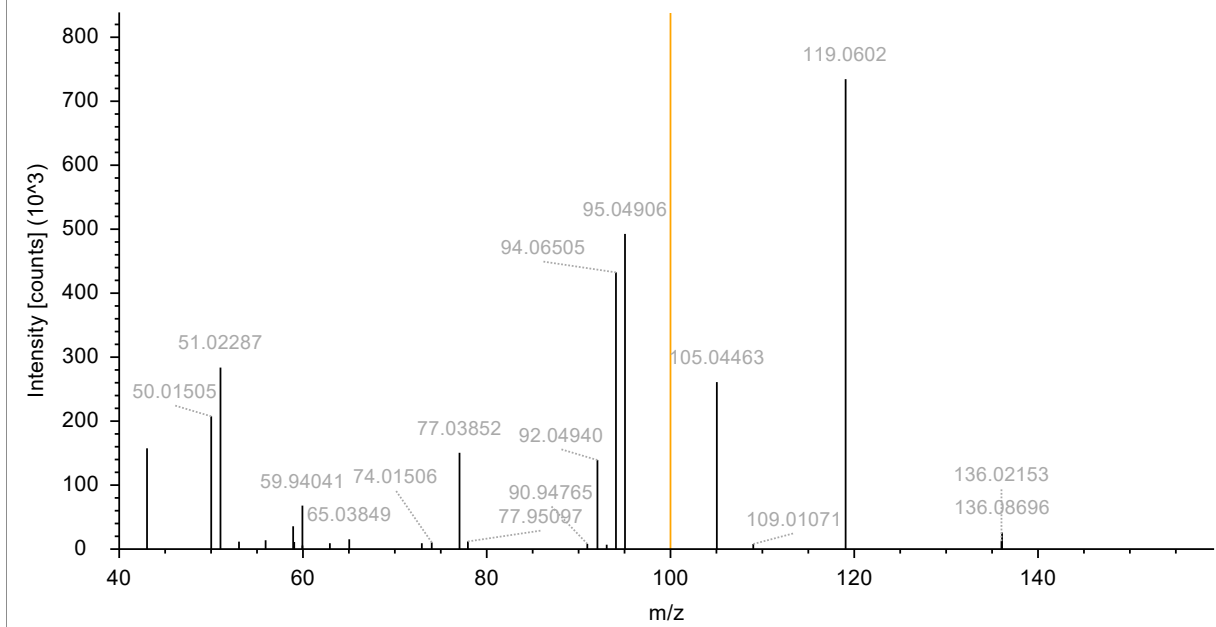
1-cyclohexyl-3-phenylurea

2023_10_26_Quant_Ext_T3_1_20231031042613 (F46) #10310, RT=13.879 min, MS2, FTMS (+), (HCD, DDA, 219.1489@(20;



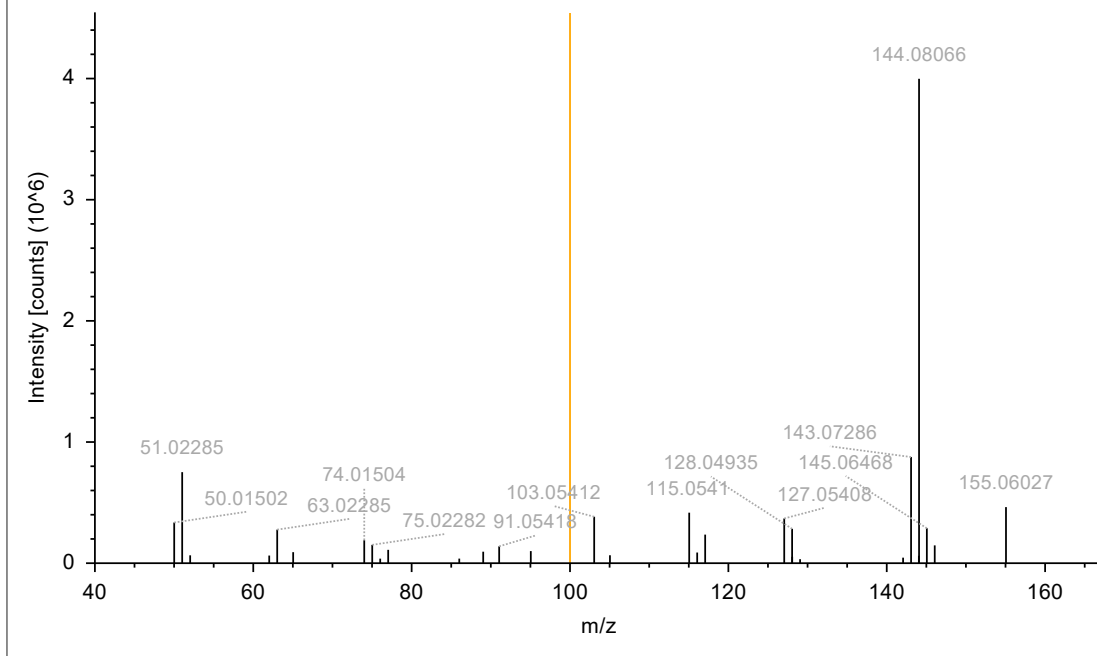
1-phenylguanidine

2023_10_26_Quant_Ext_T1_1_20231031011345 (F40) #1134, RT=1.569 min, MS2, FTMS (+), (HCD, DDA, 136.0868@(20;60



Naphthalen-2-amine

2023_10_26_Quant_Ext_T3_1_20231031042613 (F46) #13148, RT=17.655 min, MS2, FTMS (+), (HCD, DDA, 144.0)



N,N-dicyclohexyl-2-benzothiazolesulfenamide

2023_10_26_Quant_Ext_C11_1_20231030220118 (F31) #18419, RT=24.659 min, MS2, FTMS (+), (HCD, DDA, 347

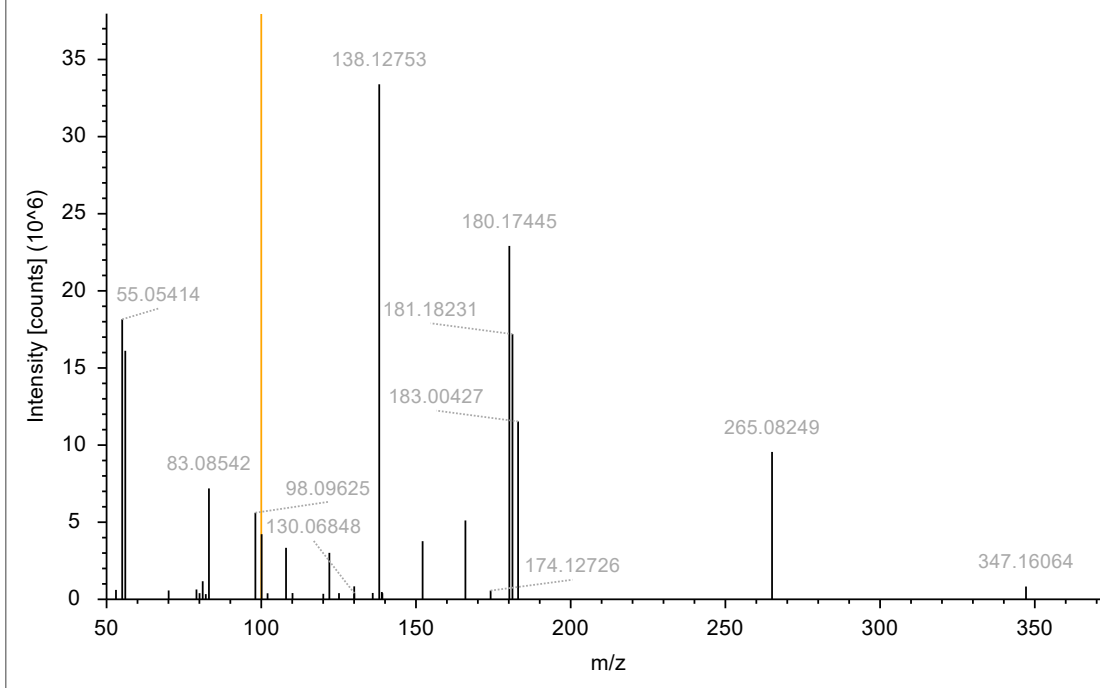
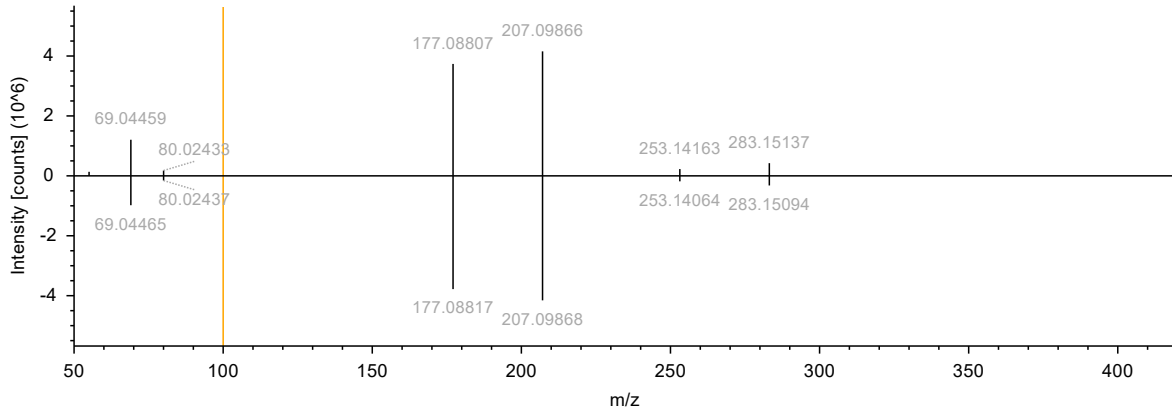


Figure S10. MS/MS Compounds identified from other sources (Level 2a).

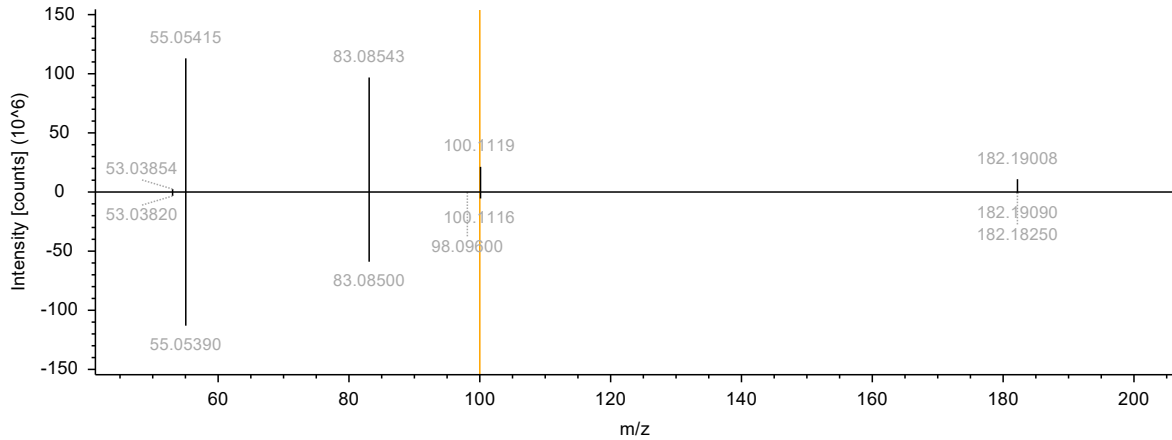
Hexa(methoxymethyl)melamine (Match 99.8)

RAWFILE(top): 2023_10_26_Quant_Ext_T1_1_20231031011345 (F40) #9540, RT=12.864 min, MS2, FTMS (+), (HCD, DDA, 391.2292@(20;60), +1)



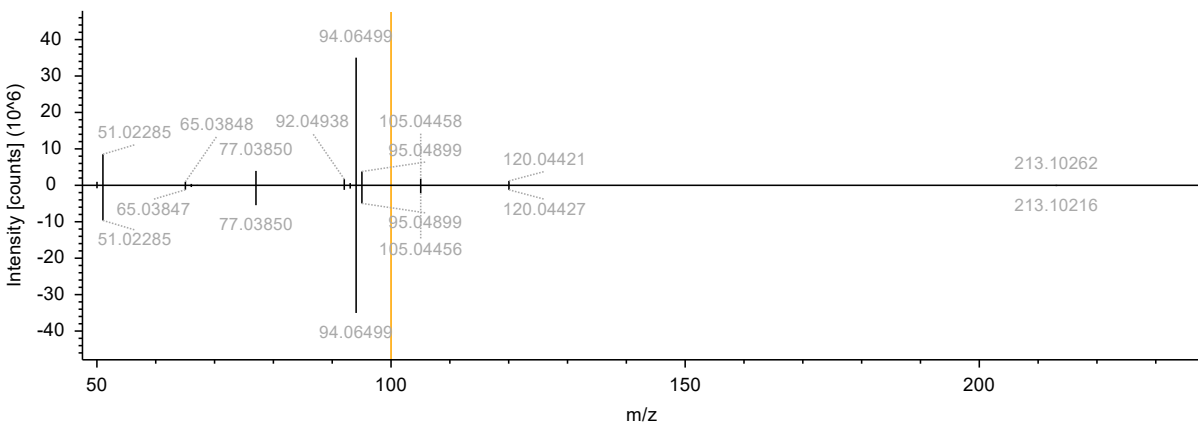
Dicyclohexylamine (Match 99.6)

RAWFILE(top): 2023_10_26_Quant_Ext_C11_1_20231030220118 (F31) #5993, RT=8.110 min, MS2, FTMS (+), (HCD, DDA, 182.1900@(20;60), +1)



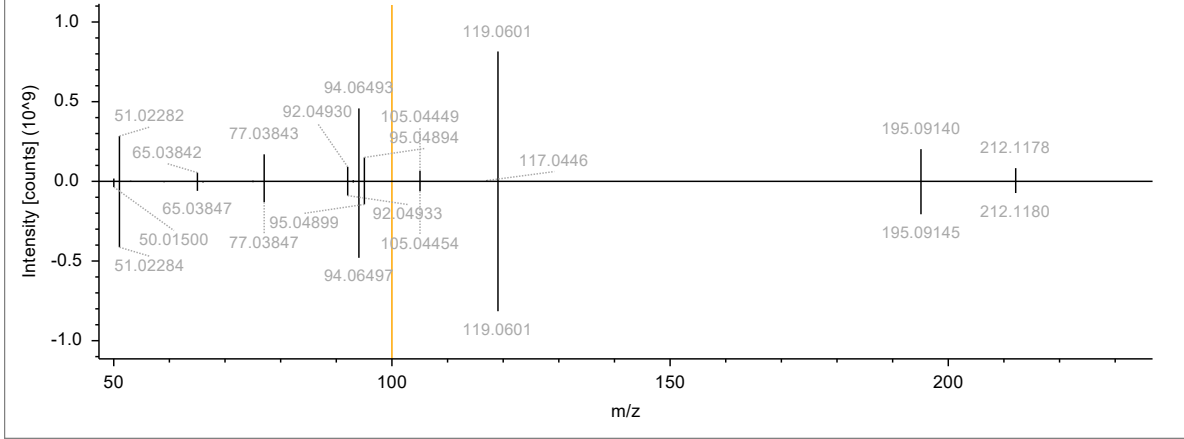
1,3-diphenylurea (Match 99.5)

RAWFILE(top): 2023_10_26_Quant_Ext_T1_1_20231031011345 (F40) #9484, RT=12.790 min, MS2, FTMS (+), (HCD, DDA, 213.1019@(20;60), +1)



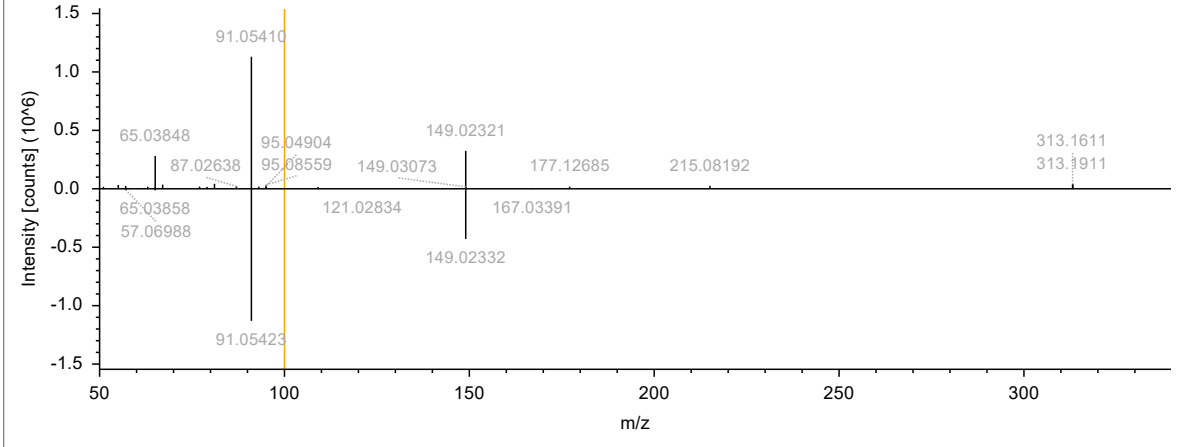
1,3-diphenylguanidine (Match 99.3)

RAWFILE(top): 2023_10_26_Quant_Ext_T1_2_20231031014550 (F41) #4737, RT=6.425 min, MS2, FTMS (+), (HCD, DDA, 212.1178@(20;60), +1)



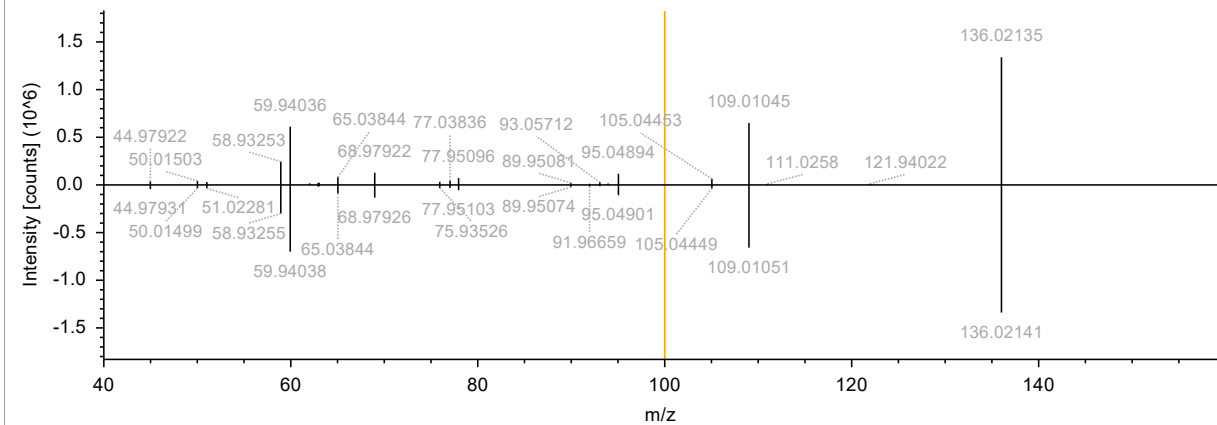
Benzyl butyl phthalate (Match 99.2)

RAWFILE(top): 2023_10_26_Quant_Ext_T1_3_20231031021754 (F42) #14293, RT=19.194 min, MS2, FTMS (+), (HCD, DDA, 313.1433@(20;60), +1)



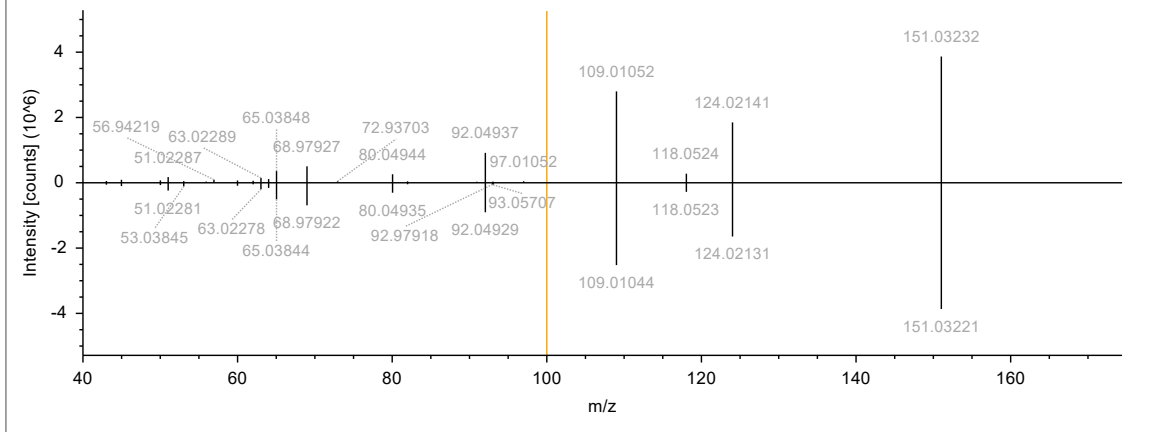
Benzothiazole (Match 98.0)

RAWFILE(top): 2023_10_26_Quant_Ext_T3_3_20231031053030 (F48) #7330, RT=9.901 min, MS2, FTMS (+), (HCD, DDA, 136.0215@(20;60), +1)



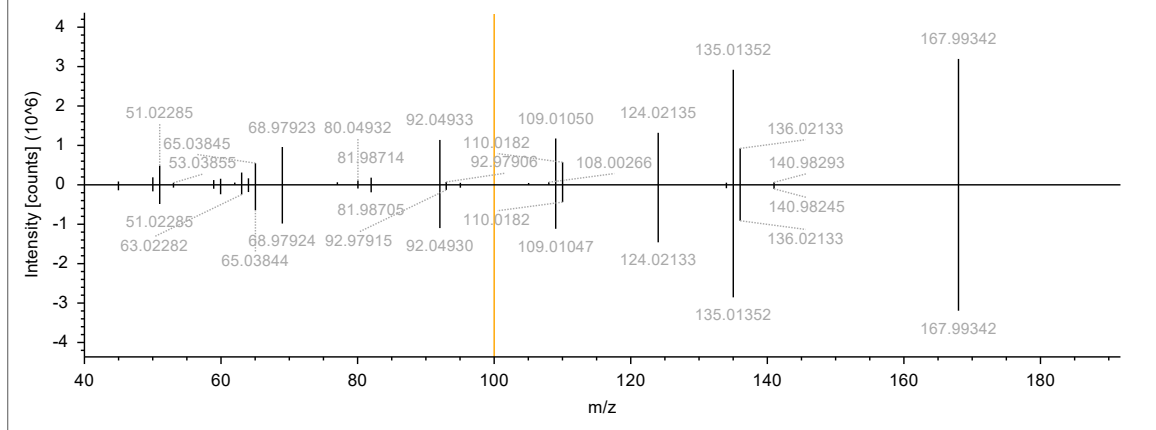
2-aminobenzothiazole (Match 98.0)

RAWFILE(top): 2023_10_26_Quant_Ext_C8_3_20231030181646 (F24) #3111, RT=4.227 min, MS2, FTMS (+), (HCD, DDA, 151.0323@(20;60, +1)



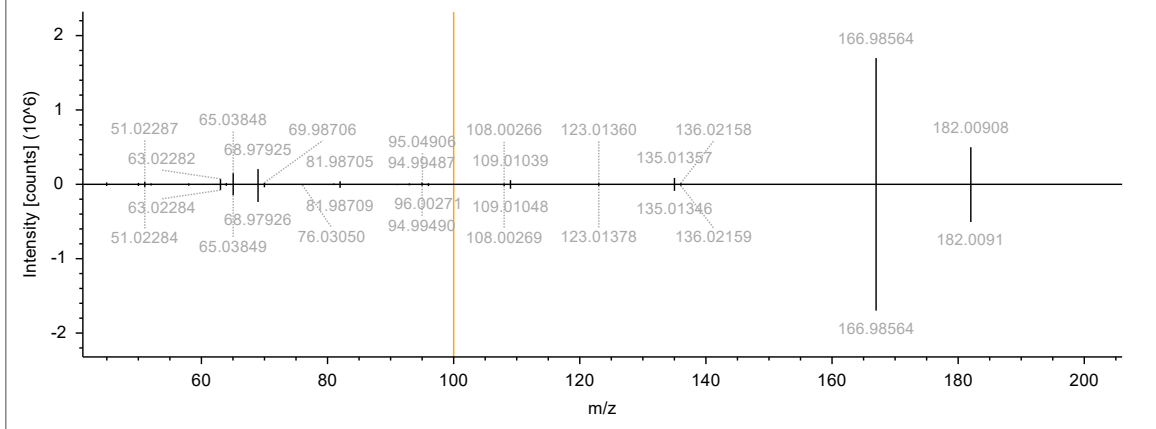
2-Mercaptobenzothiazole (Match 97.9)

RAWFILE(top): 2023_10_26_Quant_Ext_T3_3_20231031053030 (F48) #7782, RT=10.504 min, MS2, FTMS (+), (HCD, DDA, 167.9933@(20;60, +1)



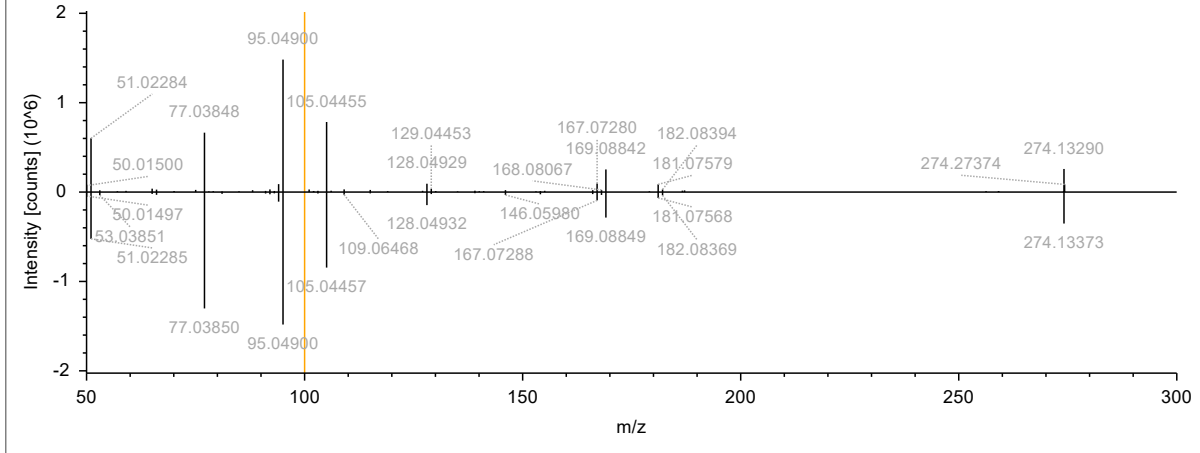
2-(methylthio)benzothiazole (Match 96.7)

RAWFILE(top): 2023_10_26_Quant_Ext_C7_1_20231030153623 (F19) #10873, RT=14.678 min, MS2, FTMS (+), (HCD, DDA, 182.0090@(20;60, +1)



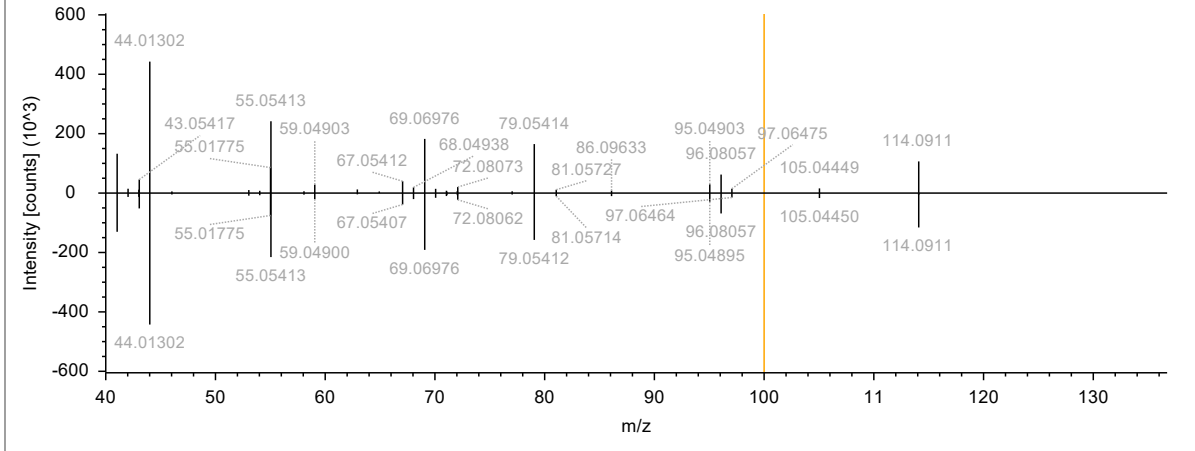
4-phenylazodiphenylamine (Match 96.3)

RAWFILE(top): 2023_10_26_Quant_Ext_C11_2_20231030223322 (F32) #15124, RT=20.309 min, MS2, FTMS (+), (HCD, DDA, 274.1337@(20;6+1)



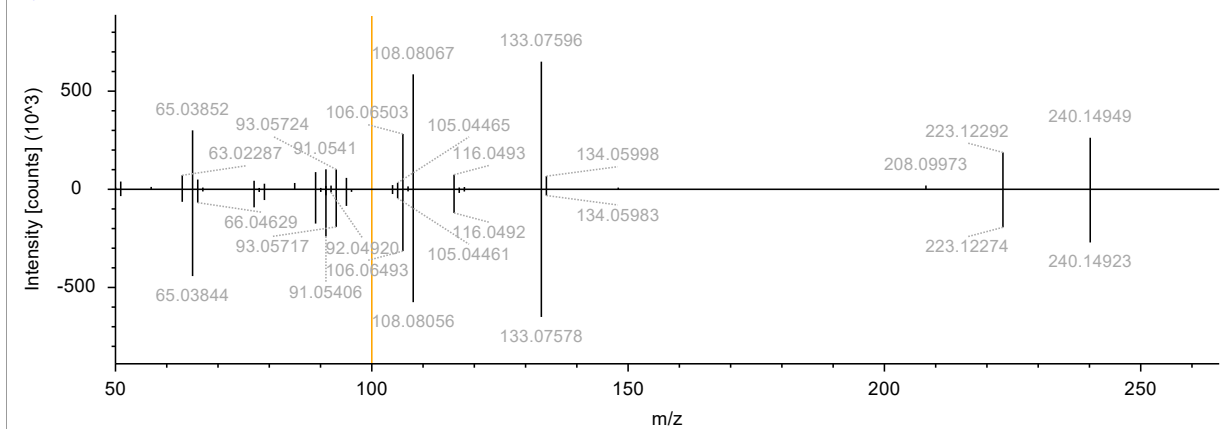
Caprolactam (Match 96.2)

RAWFILE(top): 2023_10_26_Quant_Ext_C11_2_20231030223322 (F32) #3309, RT=4.500 min, MS2, FTMS (+), (HCD, DDA, 114.0912@(20;60,+1)



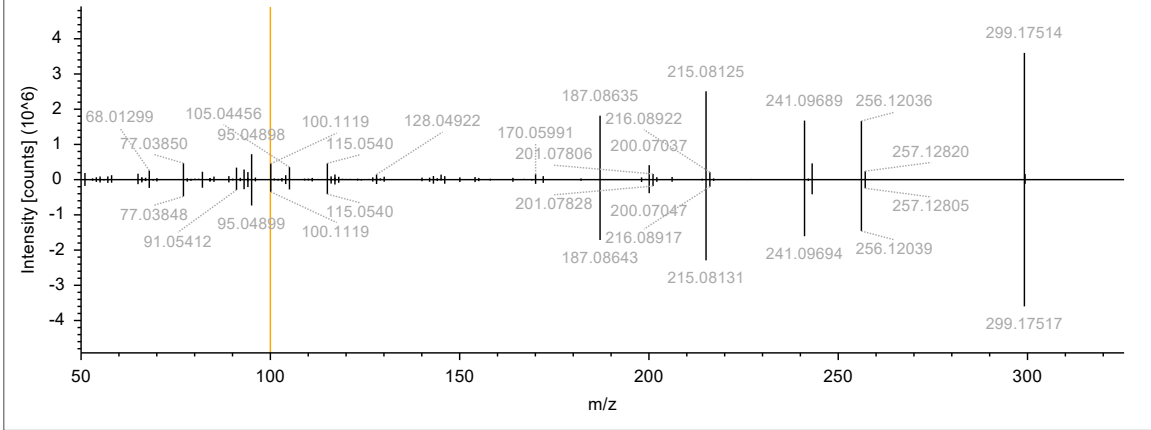
1,3-di-o-tolylguanidine (Match 95.6)

RAWFILE(top): 2023_10_26_Quant_Ext_C11_3_20231030230527 (F33) #6005, RT=8.125 min, MS2, FTMS (+), (HCD, DDA, 240.1493@(20;60,+1)



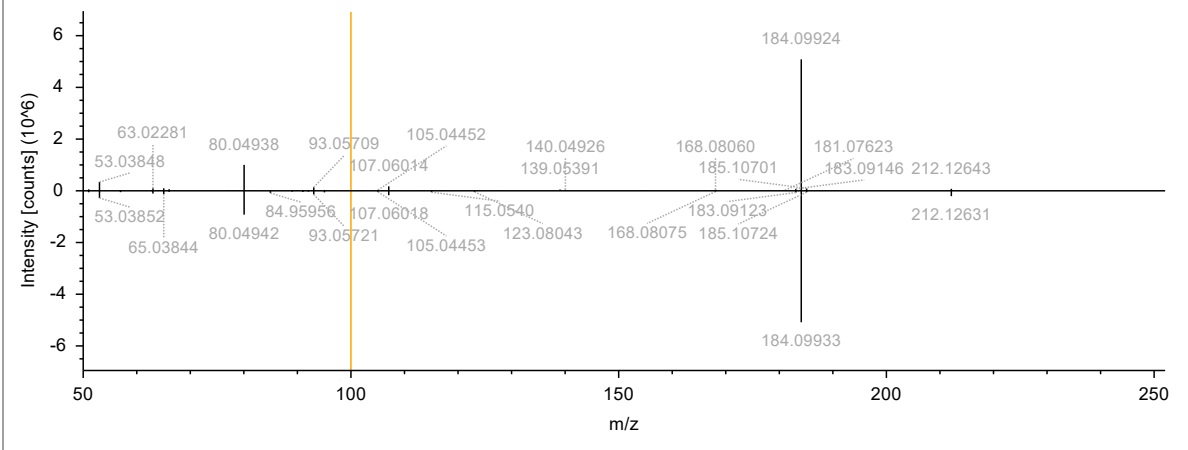
6PPD-quinone (Match 95.3)

RAWFILE(top): 2023_10_26_Quant_Ext_C11_2_20231030223322 (F32) #13362, RT=17.983 min, MS2, FTMS (+), (HCD, DDA, 299.1750@(20;6 +1)



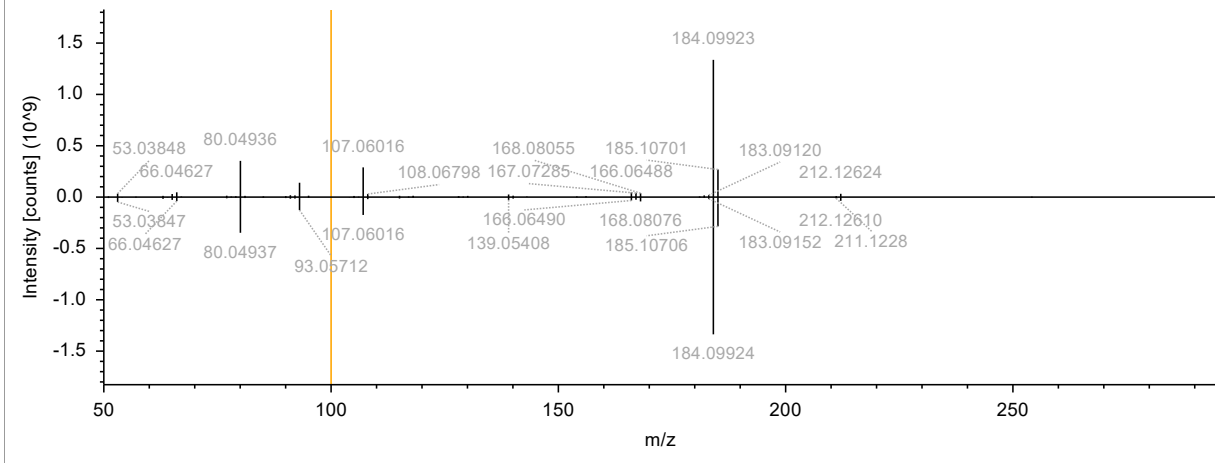
N-isopropyl-N'-phenyl-1,4-phenylenediamine (IPPD) (Match 93.2)

RAWFILE(top): 2023_10_26_Quant_Ext_C8_2_20231030174441 (F23) #7231, RT=9.737 min, MS2, FTMS (+), (HCD, DDA, 227.1542@(20;60, +1)



N-(1,3-dimethylbutyl)-N'-phenyl-p-phenylenediamine (6PPD) (Match 91.7)

RAWFILE(top): 2023_10_26_Quant_Ext_T3_3_20231031053030 (F48) #9602, RT=12.927 min, MS2, FTMS (+), (HCD, DDA, 269.2006@(20;60, +1)



2,2,4-trimethyl-1,2,3,4-tetrahydroquinoline (TMQ) (Match 84.9)

RAWFILE(top): 2023_10_26_Quant_Ext_T3_3_20231031053030 (F48) #6563, RT=8.874 min, MS2, FTMS (+), (HCD, DDA, 176.1431@(20;60), +1)

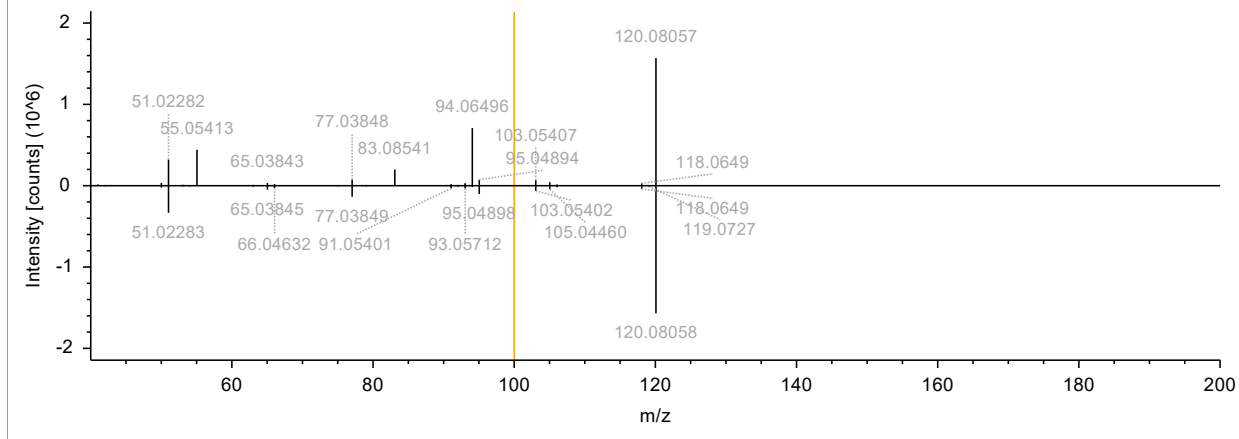
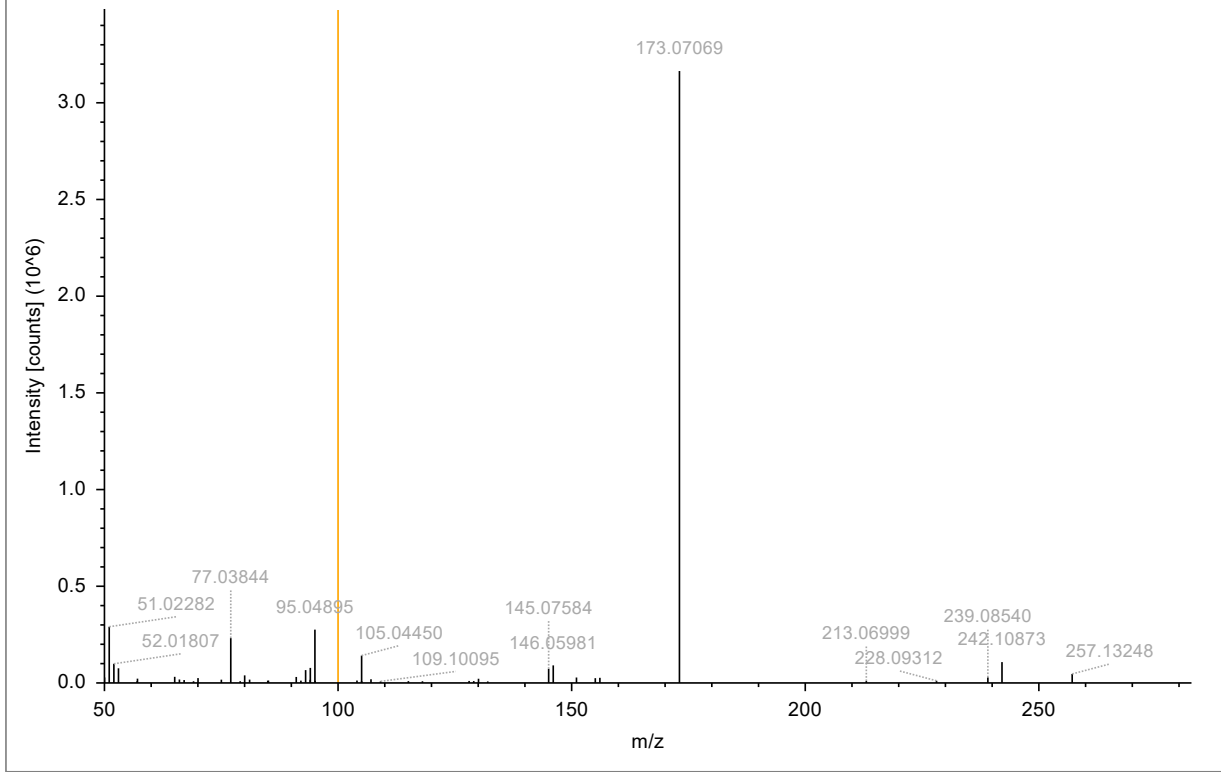


Figure S11. Comparison between experimental and in-house standard (Level 1).

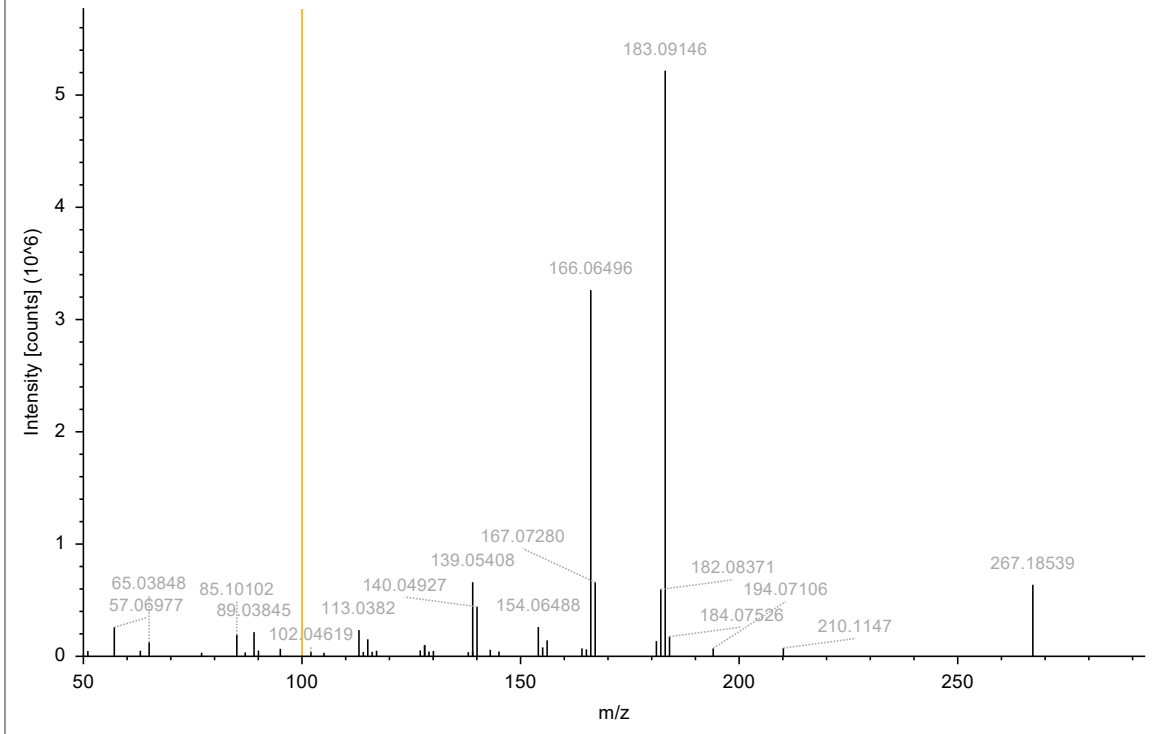
TP 256

2023_10_26_Quant_Ext_C11_2_20231030223322 (F32) #14642, RT=19.675 min, MS2, FTMS (+), (HCD, DDA, 257.1646@(20;60),



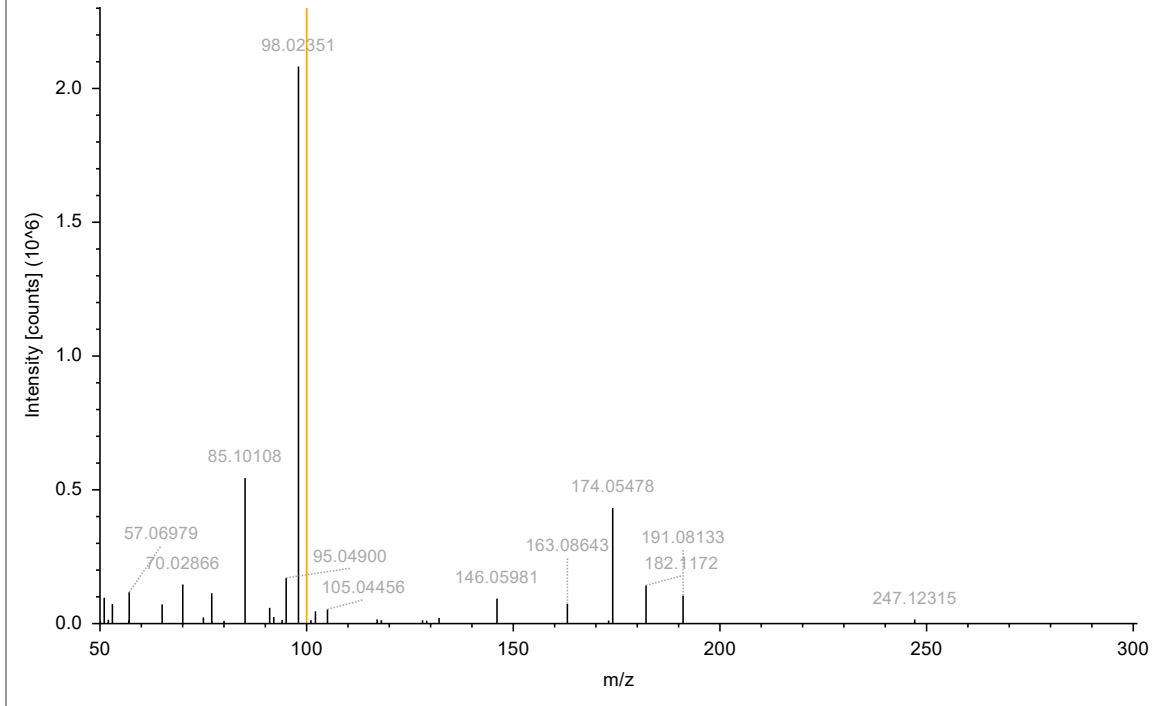
6QDI

2023_10_26_Quant_Ext_T3_2_20231031045821 (F47) #13394, RT=17.981 min, MS2, FTMS (+), (HCD, DDA, 267.1853@(20;60),



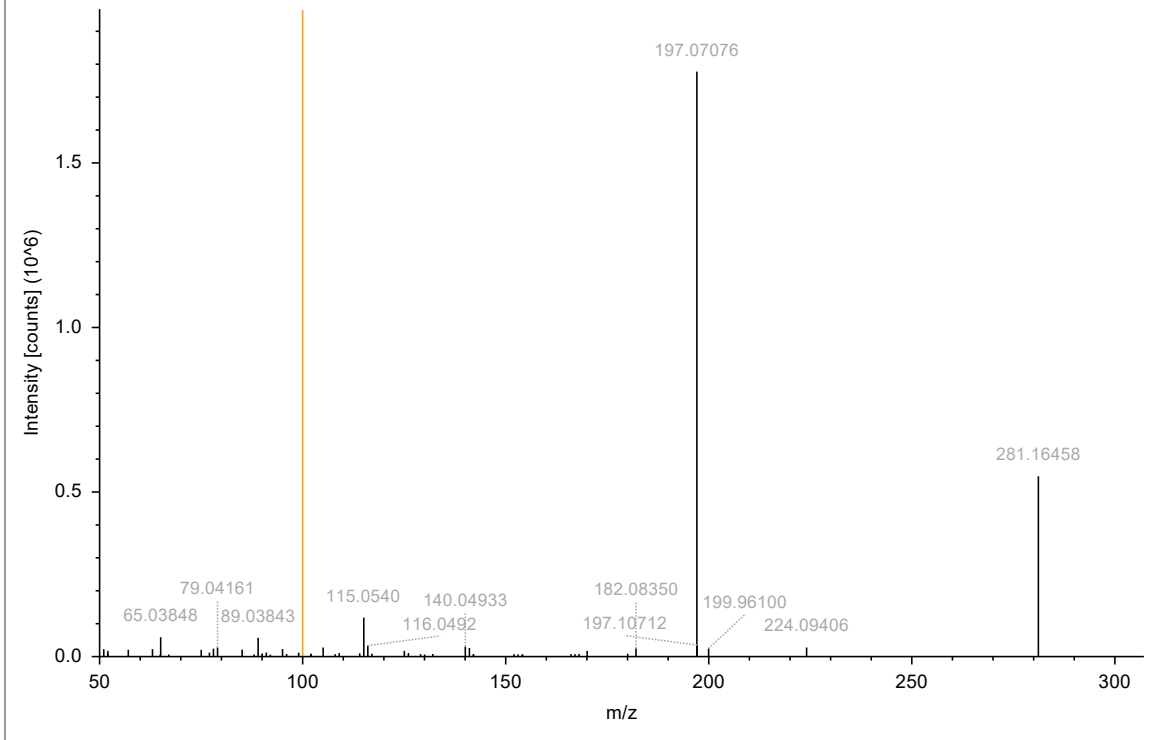
TP 274

2023_10_26_Quant_Ext_C8_2_20231030174441 (F23) #12783, RT=17.245 min, MS2, FTMS (+), (HCD, DDA, 275.1750@(20;60),



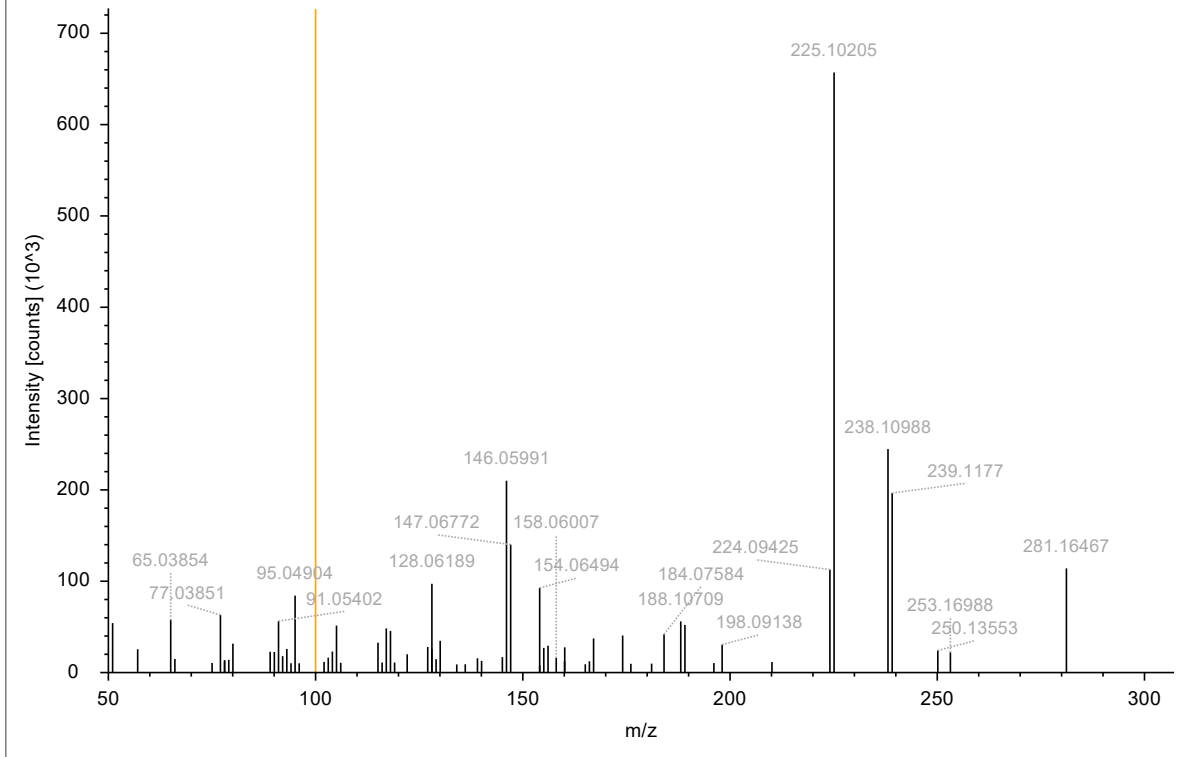
TP280a

2023_10_26_Quant_Ext_C11_1_20231030220118 (F31) #8460, RT=11.398 min, MS2, FTMS (+), (HCD, DDA, 281.1644@(20;60),



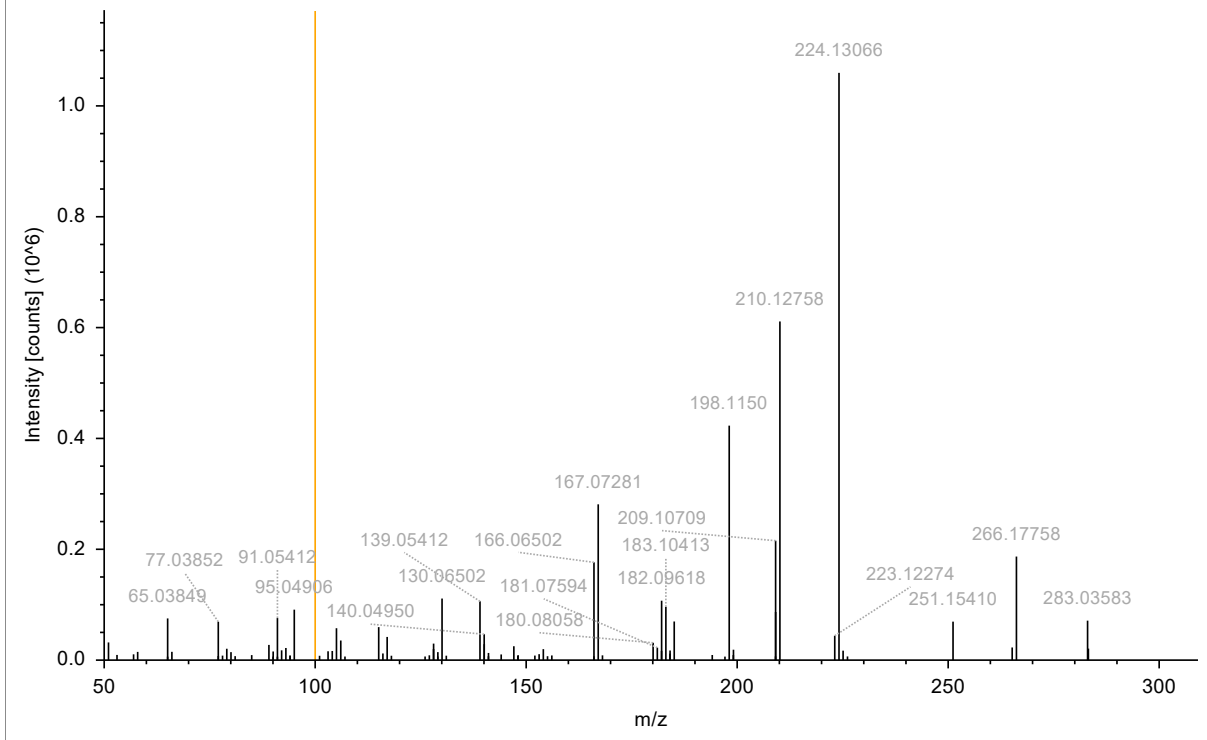
TP280b

2023_10_26_Quant_Ext_C11_3_20231030230527 (F33) #13139, RT=17.699 min, MS2, FTMS (+), (HCD, DDA, 281.1643@(20;60),



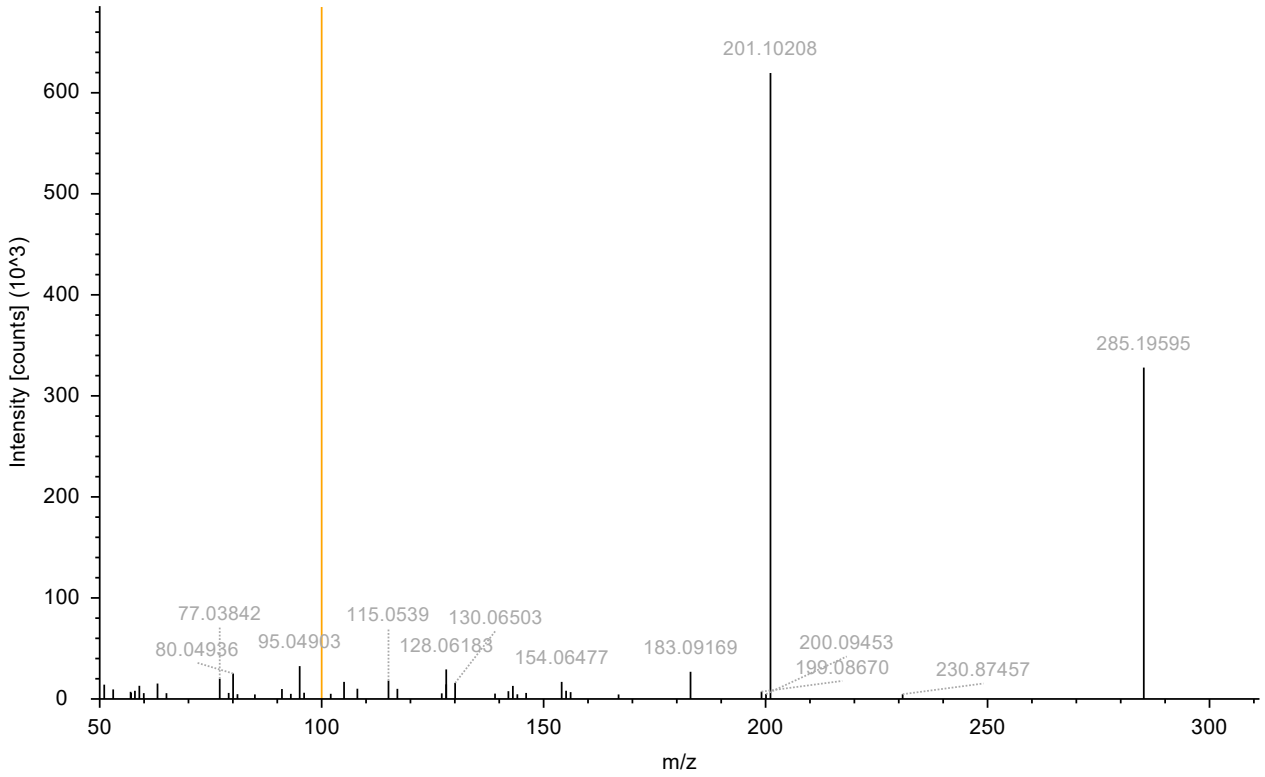
TP282b

2023_10_26_Quant_Ext_T3_1_20231031042613 (F46) #11269, RT=15.156 min, MS2, FTMS (+), (HCD, DDA, 283.1802@(20;60),



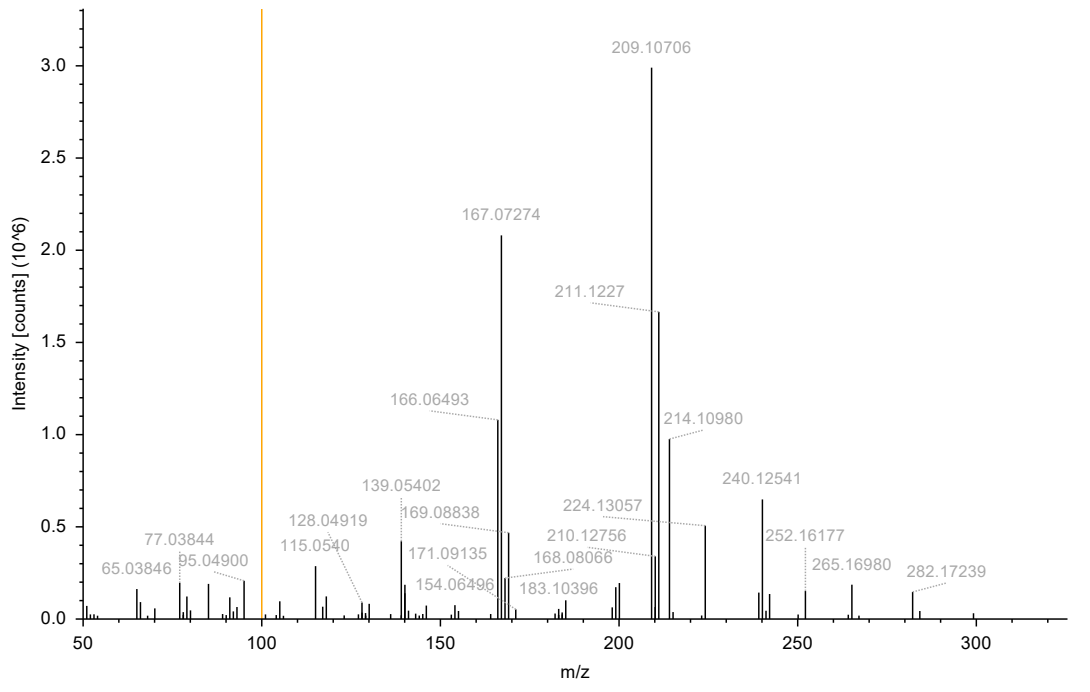
TP284a

2023_10_26_Quant_Ext_C11_3_20231030230527 (F33) #12047, RT=16.247 min, MS2, FTMS (+), (HCD, DDA, 285.1958@(20;60),



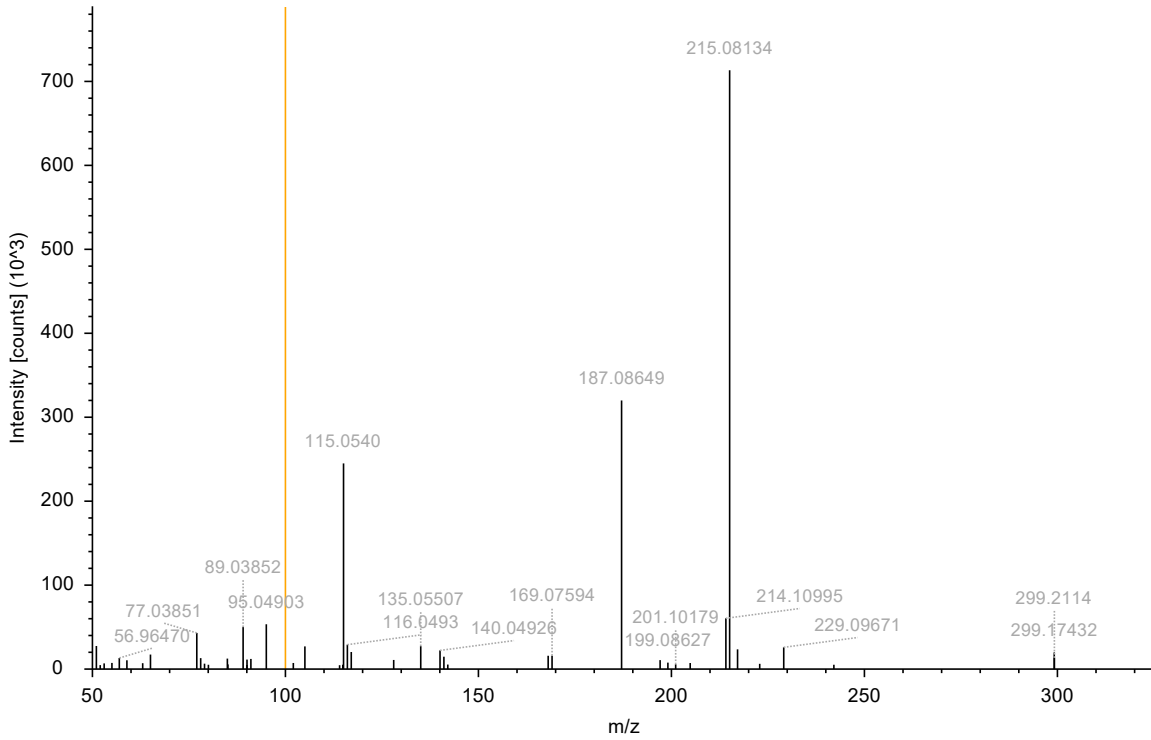
TP298b

2023_10_26_Quant_Ext_T1_1_20231031011345 (F40) #10003, RT=13.483 min, MS2, FTMS (+), (HCD, DDA, 299.1750@(20;60),



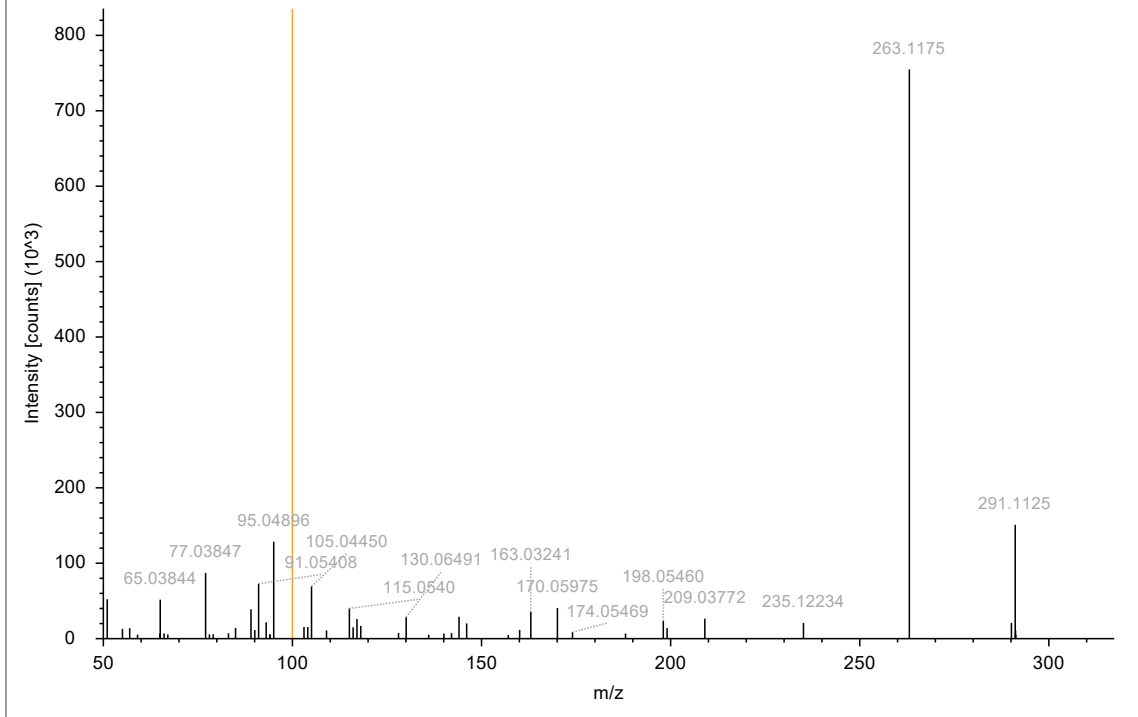
TP298c

2023_10_26_Quant_Ext_T2_2_20231031032203 (F44) #8774, RT=11.836 min, MS2, FTMS (+), (HCD, DDA, 299.1747@(20;60),



DPPD-quinone

2023_10_26_Quant_Ext_T1_2_20231031014550 (F41) #12112, RT=16.287 min, MS2, FTMS (+), (HCD, DDA, 291.1124@(20;60),



DTPD-quinone

2023_10_26_Quant_Ext_T1_2_20231031014550 (F41) #13162, RT=17.680 min, MS2, FTMS (+), (HCD, DDA, 319.1436@(20;60),

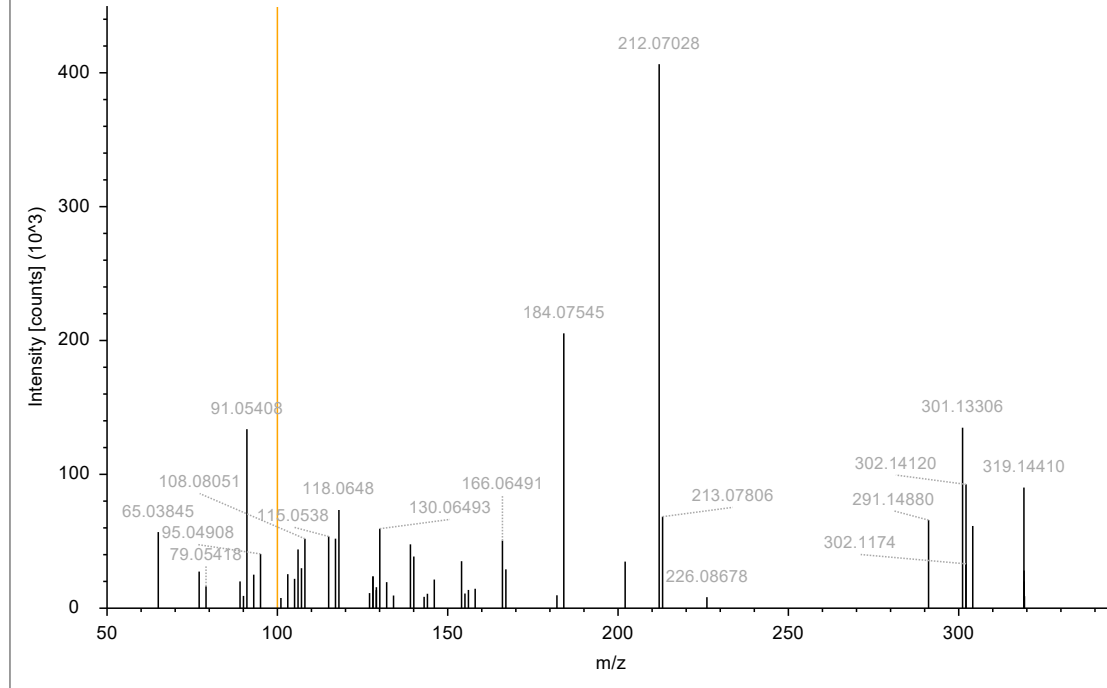


Figure S12. MS/MS of PPD transformation products in extractables.

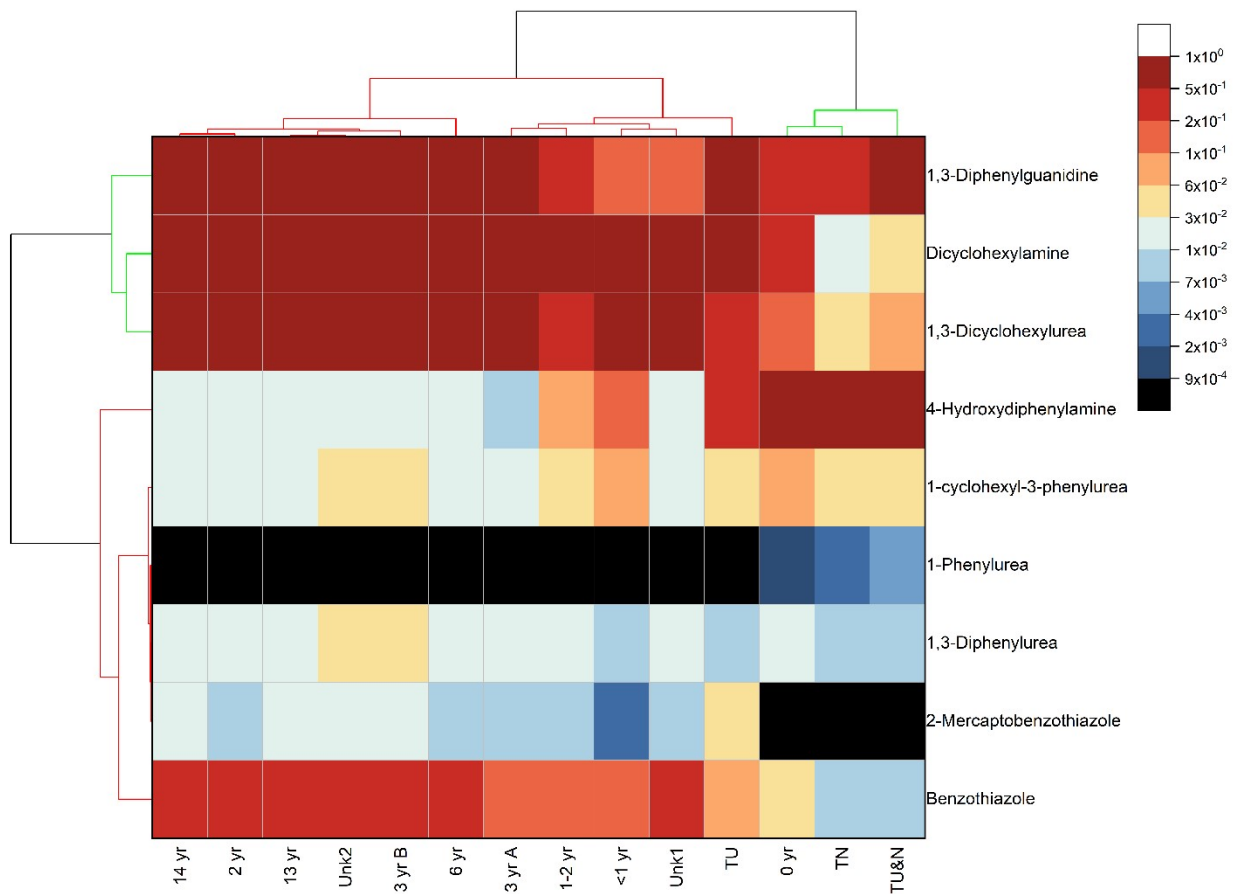


Figure S13. Hierarchical clustering of tire and turf crumb rubber leachables in positive ion mode.